UNIVERSIDADE DA BEIRA INTERIOR

Ciências

Thermodynamic study of protein adsorption mechanism on a salt-tolerant anion-exchange support

João Miguel Barata Duarte

Dissertação para obtenção do Grau de Mestre em

Biotecnologia

(2º ciclo de estudos)

Orientador: Prof. Doutora Ana Cristina Mendes Dias Cabral

Co-orientador: Mestre Francisco Soares Marques

Covilhã, outubro de 2017

Ao Américo

"Não sou nada.

Nunca serei nada.

Não posso querer ser nada.

À parte isso, tenho em mim todos os sonhos do mundo."

Tabacaria - 15/1/1928

Álvaro de Campos (Heterónimo de Fernando Pessoa)

Acknowledgments

Inicialmente gostaria de agradecer à Professora Ana Cristina Dias-Cabral por me ter dado a oportunidade de integrar o seu grupo de investigação, pelo seu suporte e orientação neste trabalho e pela sua contagiante paixão pela ciência que me fez ter uma visão completamente diferente do mundo molecular que nos rodeia.

Não menos importante, foi o incansável apoio do meu co-orientador Francisco Marques, que me ajudou a superar as dificuldades encontradas ao longo deste percurso, sempre com uma perspetiva rigorosa, curiosa, critica e ambiciosa sobre este trabalho. "*Scientia potentia est*".

Também agradecer à UBI, em especial ao centro de investigação CICS-UBI e às grandes amizades aqui criadas ou fortalecidas. João C., Gregory, Gonçalo, Sara, Filipa P., Rita, Filipa F., Patrícia, e aos meus companheiros Boga e Mário.

Não queria deixar de lembrar aqueles que de forma incondicional fizeram sempre parte da minha vida, fazendo de mim o que hoje sou: Pedro, Telmo, António, Paulo A., Fábio, Ivo, Ana, João S., Raquel, Paulo B. e Norberto.

Um agradecimento especial à minha querida Tânia, por todo o seu amor e apoio mesmo nos momentos mais difíceis.

E claro, à minha família, especialmente à mãe e ao pai, à minha irmã e à minha afilhada Maria Luísa, e por fim, aos avós, que sempre sonharam com este momento.

Só foi possível graças a todos vós…

Bem-hajam.

Resumo Alargado

Nas últimas décadas, o crescente interesse na aplicação de produtos biológicos, nas mais diversas áreas, veio revolucionar as indústrias de biotransformação, cosmética, diagnóstico, investigação e desenvolvimento, alimentar e farmacêutica. No caso da indústria farmacêutica, é crucial a obtenção de produtos em elevada quantidade, para poderem ser disponibilizados a todos os pacientes e com elevados níveis de pureza e homogeneidade de forma a assegurar uma boa resposta terapêutica e a segurança dos doentes.

Com o desenvolvimento da tecnologia recombinante e dos processos de fermentação, é já possivel obter rendimentos elevados durante o processo de "upstream" de biofármacos, redirecionando o foco das empresas em mitigar antes os custos associados ao processo de "downstream", que para garantir a qualidade do produto engloba sempre nas suas etapas, passos de separação e de purificação, reconhecidos como os mais caros. Assim, a redução de custos pode ser conseguida aumentando o rendimento (quantidade de produto obtido por unidade de tempo) destes passos ou reduzindo o número dos mesmos na obtenção dos biofármacos com os níveis de pureza desejados.

Devido à sua elevada eficiência e capacidade de adsorção para diferentes tipos de biomoléculas, as cromatografias de afinidade, de troca iónica e de interação hidrofóbica têm sido das técnicas mais utilizadas nas das etapas de separação e purificação. No entanto, com o intuito de ultrapassar algumas das desvantagens associadas aos ligandos convencionais, recentemente, as equipas de investigação e desenvolvimento de suportes cromatográficos têm vindo a investir no design de novos ligandos, capazes de conjugar múltiplas interações. Um bom exemplo é a cromatografia de troca aniónica tolerante a sal, que permite obter as vantagens inerentes aos suportes de troca iónica (elevada versatilidade e elevadas capacidades de ligação sem comprometer a estrutura das biomoléculas), mas superando a grande desvantagem da necessidade de diluir ou diafiltrar as amostras a processar, de forma a baixar a condutividade dos meios. Está já descrito na literatura que o uso de poliaminas (aminas primárias e secundárias) como ligando, em detrimento de aminas quaternárias (ligando Q), é uma das explicações para as propriedades de tolerância ao sal devido à combinação de interações eletrostáticas com pontes de hidrogénio. A possibilidade destes ligandos em manter a adsorção de uma amostra em condições de condutividades superiores a 30mS.cm^{-1}, faz com estes novos suportes possam ser usados tanto nos passos de captura, fazendo um processamento direto de amostras biológicas, como nos passos de polimento devido à elevada resolução obtida na separação de agregados ou formas diméricas. Contudo, o aumento da complexidade destas novas alternativas faz aumentar drasticamente a dificuldade em compreender os mecanismos de interação envolvidos no processo de adsorção. A compreensão destes mecanismos, é crucial para o desenvolvimento de futuros suportes, simulações moleculares e ainda na transposição de uma escala laboratorial para uma escala industrial.

A análise dos eventos termodinâmicos dos processos de adsorção através da Microcalorimetria de Fluxo (FMC) tem vindo a provar ser uma importante ferramenta na obtenção de uma melhor compreensão das forças motrizes, dos mecanismos e das cinéticas envolvidas no processo de adsorção de biomoléculas em diferentes sistemas cromatográficos. O FMC é uma técnica em que o modo de funcionamento é muito semelhante ao de um sistema cromatográfico, mas com a particularidade de ter acoplado à coluna dois termístores que permitem medir *in situ* variações de energia causadas pela adsorção das biomoléculas ao suporte. Assim, recorrendo ao uso da técnica de FMC, o objetivo deste trabalho foca-se na compreensão da influência de fatores como o pH e a concentração de sal no mecanismo de adsorção da albumina bovina sérica (BSA), a suportes de cromatografia de troca aniónica tolerante a sal. A fim de complementar e interpretar os resultados obtidos por FMC, foram ainda obtidas as isotérmicas de adsorção e realizados estudos de retenção. Estes estudos foram associados com diferentes modelos teóricos, nomeadamente: a teoria de "*Langmuir*", o modelo de "*Stoichiometric displacement" (SD)*, o modelo de Yamamoto, o modelo de "*Steric Mass Action" (SMA)* e a análise de "*Preferential interaction" (análise de Perkins)*.

Os resultados obtidos por microcalorimetria de fluxo demonstraram que as forças motrizes do processo de adsorção em suportes tolerantes a sal são diferentes das dos suportes puramente iónicos, como o Toyopearl DEAE 650M, Toyopearl GigaCap Q-650M e TSKgel SuperQ 5PW. Nestes, como previamente demonstrado pelo nosso grupo de investigação[1], revelou-se a presença de um evento endotérmico inicial relacionado com o processo de dessolvatação, seguido de um evento exotérmico associado à interação entre a proteína e o suporte. No caso do suporte tolerante a sal, na ausência e na presença de sal, observou-se sempre um único pico exotérmico a pH 8,0 e o aparecimento de dois picos exotérmicos a pH 6,0, onde o segundo pico ocorre após a amostra que contém proteína ser totalmente substituída pela solução tampão no interior da coluna. Este "*timing*" leva-nos a crer que existe adsorção secundária da proteína após a criação de novos locais de ligação resultantes de reorganização da mesma à superfície do suporte. A pH 8,0 não se observa este segundo evento, indicando que a adsorção inicial da proteína é forte e favorável o suficiente para não sofrer quaisquer alterações. Esta conformação preferencial a pH 8,0 pode estar relacionada a formação de pontes de hidrogénio para alem das interações electroestáticas. Apesar de o fornecedor da resina Toyopearl NH2-750F referir que o pKa do ligando é de 8,5, está bem descrito na literatura[2] que o pKa de cada grupo de amina é influenciado pela sua posição no ligando e pelo tamanho da cadeia alifática. *Blagbrough et al.*[2] refere ainda que poliaminas como a espermina (pK_a=11,1) apenas a pH ligeiramente abaixo de 6,8 é que possui uma protonação completa de todas as aminas. Traspondo estes conceitos para o nosso trabalho, é plausível que a pH 6,0 todas as aminas já estejam protonadas fazendo com que as forças motrizes de adsorção sejam maioritariamente eletrostáticas enquanto que a pH 8,0, existam ainda aminas não protonadas que ficam disponíveis para estabelecer pontes de hidrogénio. Estas múltiplas interações podem requerer uma conformação preferencial da

proteína-ligando impedindo posteriores reorganizações e conferindo uma elevada tolerância ao sal.

Com o aumento da concentração de sal observam-se também diferenças significativas nas áreas dos picos. A pH 6,0, com o aumento da concentração de sal, verificou-se que a energia associada ao segundo evento aumenta, ao contrário do que se verifica no primeiro evento exotérmico, onde o aumento da concentração de sal provoca uma diminuição da energia libertada. O sal tem a propriedade de blindar as interações eletrostáticas e enfraquecer a interação durante o processo de adsorção, por isso, é intuitivo pensar que quanto maior a concentração de sal no meio, mais fraca será a interação inicial proteína-suporte (diminuição do primeiro pico exotérmico), possibilitando a reorganização da proteína à superfície e a formação de interações mais favoráveis (aumento do segundo evento exotérmico). Como esperado, a pH 8,0 os resultados demonstraram-se semelhantes aos observados a pH 6,0 para o primeiro evento exotérmico, observando-se a sua diminuição com o aumento da concentração de sal.

A aplicação dos modelos veio suportar as explicações avançadas pela interpretação dos resultados de FMC. A pH 8,0 a BSA possui uma maior pegada à superfície do ligando (*Steric mass action*), fazendo com que se estabeleça um maior número de pontos de interação proteína-suporte (*Stoichiometric Displacement* e modelo de *Yamamoto*), e consequentemente uma maior remoção de moléculas de água e iões à superfície (*análise de Perkins*). Isto indica-nos que a proteína adota uma conformação especifica e altamente estável devido ao à formação múltiplas interações (eletrostáticas e pontes de hidrogénio), que dificulta a disrupção da adsorção por parte do sal, daí se ter observado uma maior tolerância ao sal a pH 8,0 do que a pH 6,0 (com base nas isotérmicas de adsorção, observa-se uma redução mais acentuada da capacidade máxima a pH 6,0 do que a pH 8,0 com o aumento da concentração e sal). Estes resultados também são claros quando se observa a diferença dos valores energéticos da adsorção primária, sendo claramente superiores a pH 8,0 devido ao maior número de locais de interação.

Por fim, nas injeções a pH 8,0, mas perto do limite de saturação da coluna, foi observado a presença de um segundo evento exotérmico semelhante aos obtidos a pH 6,0. Estes resultados reforçam ainda mais a teoria de que a pegada da BSA à superfície é superior a pH 8,0, isto porque quando um número muito elevado de moléculas de BSA entram em contacto com o suporte, a competição pelos locais de ligação torna-se mais significativa e nem todas as moléculas conseguem adotar a posição de interação preferencial com o suporte, ficando então sujeitas a sofrer fenómenos semelhantes aos descritos a pH 6,0.

Todos estes resultados confirmam que, para uma visão mais consistente dos mecanismos de adsorção, a utilização da microcalorimetria de fluxo mostra-se de grande interesse no estudo sistemático dos diferentes suportes cromatográficos. Para além disso, também a modelação associada a estudos de estrutura molecular demonstraram ser ferramentas importantes para a

elucidação do complexo processo que é a adsorção de proteínas. Modelações teóricas, semi-empíricas e simulações computacionais relacionadas com o mecanismo de adsorção, especialmente de moléculas com alto peso molecular, procuram contabilizar estes eventos entalpicos sempre com o objetivo final de desenvolver não só processos cromatográficos mais rápidos, eficazes e com melhores rendimentos, como também simplificar e diminuir os custos associados à produção biotecnológica de biomoléculas com interesse farmacêutico.

Palavras-chave

Cromatografia tolerante a sal; Microcalorimetria de fluxo; Isotérmicas de adsorção; Modelo de *Stoichiometric displacement;* Modelo de *Yamamoto;* Modelo de *Steric mass action;* Análise de *Preferential interaction; BSA.*

Abstract

Ion exchange chromatography is one of the most used methods in downstream processing for protein purification due to its usual high dynamic binding capacity (DBC) and versatility. However, when starting with high conductivity feedstocks (≥15mS.cm^{-1}), additional steps are required before loading, such as dilution and/or diafiltration, which increases process time and costs. Thus, there is a need of specifically designed resins for the direct processing of biological feedstocks or intermediate fractions without these extra steps. One example is the *Toyopearl NH2-750F* support, referred as a "salt tolerant chromatography" resin, used in this work. This resin can to maintain high DBC at conductivities greater than 30mS.cm^{-1}, making it ideal for protein initial capture step or even for polishing steps (antibody aggregates removal). However, its retention and separation mechanisms are still not fully understood.

Flow microcalorimetry may provide an improved understanding of the driving forces and mechanisms involved in the interaction process during biomolecules adsorption in chromatography due to its ability to measure adsorption enthalpy in the flow mode. Furthermore, adsorption isotherms and retention studies using the Stoichiometric Displacement model, the Steric Mass Action model, Yamamoto's approach and the Preferential Interaction analysis may also successfully elucidate biomolecule adsorption onto a chromatographic resin. Using all the upmentioned tools, this work aims to elucidate how the salt concentration, pH and protein surface concentration affect the adsorption mechanism of BSA, as a model protein, onto a salt tolerant anion exchange support (*Toyopearl NH2-750F)*.

FMC results show that under all the studied conditions, the adsorptive process is enthalpically driven. At pH 8.0, a single exothermic event was observed, with higher enthalpic values when compared to pH 6.0, probably due to the establishment of higher number of binding points demonstrated by the Stoichiometric Displacement model and the Yamamoto's approach. Nevertheless, at pH 6.0, a second chronological event occurs during BSA adsorption, leading us to believe that the protein is organizing itself on the support surface, resulting in secondary adsorption and/or surface transport phenomena. This specific adsorption (a single exothermic event) at pH 8.0 may be related to the establishment of hydrogen bonding in addition to the electrostatic interactions. Contrary to what occurs at pH 6.0, at pH 8.0 not all the ligand amines are protonated, being available to establish hydrogen bonding that requires a specific footprint on the support surface and consequently, a greater ability to sustain the adsorption at high salt concentrations.

Additionally, the presence of salt also promotes changes in the peak areas. As expected, salt shield the protein and ligand surface, weakening the electrostatic attractive forces, which led to a decrease of the first exothermic signal at pH 6.0 and a decrease of the single exothermic event at pH 8.0. On the other hand, the second exothermic peak at pH 6.0, increases with the

increase of salt concentration, thus, as weaker is the initial adsorption (due to the increasing of salt concentration); greater will be the amount of BSA molecules that suffer secondary adsorption events.

All these results may be used for model development, computer molecular simulations, and theoretical approaches development, confirming that FMC is a powerful technique to further elucidate the complexity of protein adsorption during a chromatographic process.

Keywords

Salt-tolerant chromatography; Flow microcalorimetry; Adsorption Isotherms; Stoichiometric displacement model; Yamamoto's approach; Steric mass action model; Preferential interaction analysis.

Table of Contents

Figures

Tables

Chapter I. Introduction

1.1.Protein therapeutics

1.1.1 Protein as a biopharmaceutical molecule

In the last decades, applications of biological products increased in a significant way, providing the revolution of many kinds of industries like biotransformation, cosmetics, diagnostics, research and development, food and pharmaceuticals. According to the intended application, different degrees of purity are required, some of those biological products can be used as a crude extract with no purification or lightly refined, while others, as biopharmaceuticals, the high purity level, and homogeneity is a pivotal parameter to ensure a good therapeutic response and the patient safety[3]. These levels are subject to legislation by regulatory authorities, such the U.S. Food and Drug Administration (FDA), the European Agency for the Evaluation of Medical Products (EMEA) and World Health Organization (WHO), providing an international control to standardize and ensure the quality and safety of the bioproducts[3–5].

In comparison with small molecules, proteins have great advantages:

- The specific structure and functions of proteins allow an effective mechanism of action and targeted drug delivery, being well tolerated by the body and are less likely to elicit immune responses[6,5].

- Regulatory agencies, like FDA, have a minor approval time for therapeutic proteins when compared to chemical drugs[7]. Currently, these agencies provide a priority review to therapeutics drugs that address unmet needs or rare diseases.

- The protein market is continuing to trend upward[8]. In 2013, therapeutic proteins were on the top ten pharmaceuticals sold in the United States and seventh in the worldwide market [4]. Documents published by *MarketsandMarkets*® (a global market research and consulting firm) indicated that the protein therapeutic market is poised to reach US$ 208 Billion by 2020 from $85 billion in 2010 (mainly due to the market of monoclonal antibodies and insulin)[9,10].

1.1.2. Proteins structure and proprieties

Proteins are highly structured amphoteric biopolymers composed of amino acids as building blocks and usually have a compact structure. However, depending on the environment, interphase conditions, and binding of substrates, they can be flexible enough to change their conformation[3,11-13]. In our body, proteins perform different vital functions that can be divided into three major categories: molecular function (catalyze biochemical reactions), biological process (transport molecules in the bloodstream, within a cell or from one organ to another) and as a cellular component (receptors and channels in membranes; intracellular and extracellular scaffold supports)[4,6].

At the turn of the century, proteomics has become an emerging scientific research area with the aim of discovering protein composition, structure, and its own unique activity patterns. Due to the complex and diverse structure of proteins, proteomic researchers estimate that functionally distinct proteins may exceed the 100,000, which presents an immense challenge to understand the protein diseases mechanism caused by mutations, abnormalities or abnormal concentration levels. On the other hand, these numerous functional varieties, open doors for modern medicine to develop more safe, efficient and consistent therapeutic strategies[4].

In order to understand the complexity of proteins, *Figure 1* shows its structural organization divided into four different levels[3,11,12].

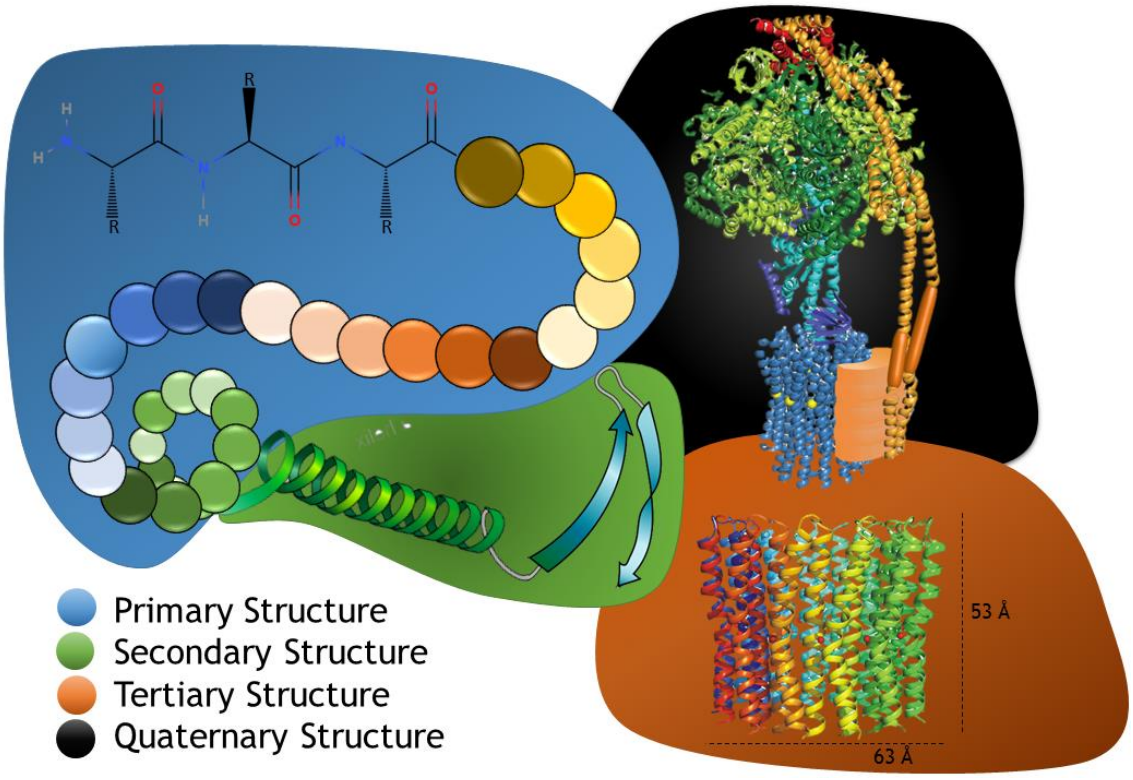

Figure 1 - Representation of ATP synthase structure subdivided into four distinct levels; Blue: primary Structure; Green: Secondary structure; Orange: Tertiary Structure; Black: Quaternary Structure. Adapted from [14]

Primary Structure of proteins is determined by the order in which the amino acids are arranged in the polypeptide chain.

Secondary Structure is defined by the folding of the amino acid sequence in a three-dimensional form called α – helices, ß –sheets and loops.

Tertiary Structure refers to the geometric shape when the elements of the secondary structure (α - helices, ß - sheets, and loops) are folded together. The predominant intramolecular interactions responsible for the stability of this structure are hydrophobic interactions and disulfide bridges. These forces are responsible for exposing the polar (charged) residues on the surface and form a tightly packed core with the hydrophobic domains.

Quaternary Structure is established by the clustering of two or more polypeptide chain in a superstructure with a particular geometry usually essential to biological function. The clustering results in a globular or fibrous shape that is stabilized by hydrogen bonding, hydrophobic interactions, disulfide bonds and salt bridges.

Besides the amino acid sequence, most of eukaryotic proteins suffer post-translational modification (PTM) in Golgi bodies, which increase the structural and functional diversity of proteome. These modifications consists in the addition of functional groups (e.g. amino, carboxylate, phenolic, thiol, imidazole, guanidine) covalently bonded to a protein and the subsequent folding processes necessary for a protein to mature functionally[3,11,12]. One of the great problems triggered by the scale-up biotechnology production of proteins is the deficient PTM, i.e. the modifications are altered or incomplete, resulting in variation of biological activity, stability, and biophysical properties such as solubility, charge, hydrophobicity, and size[15].

1.2. Liquid chromatography (LC)

The biopharmaceutical industry searches to adopt a continuous bioprocess of biologics manufacturing respecting the good manufacturing practices (GMP). For that happen, companies need to have available proper technologies, which will reduce not only the capital expenses footprint, and product cost of goods, but will also increase the yield, productivity, flexibility, and purity levels[16]. Due to protein market expected booming[8,9], this is even truer for the protein bioindustry.

Protein biotechnological production process can be divided into two sequential steps. The upstream processing, which comprises the protein production, host selection and cell fermentation and, the downstream processing that is responsible for the harvest, lysis, separation and purification of the desired molecule[17]. The research and development in

upstream processes and the drastic improvement of DNA recombinant technologies provided an increase in biopharmaceuticals yield and productivity[10,17–19]. Of course, these changes have a profound impact on the demand for better downstream bioprocessing technologies. Special attention should be given to the separation and purification steps, considered the most expensive [3]. Due to its high efficiency and specificity when compared with other techniques, liquid chromatography is one of the principal techniques used to separate and purify chemical compounds or biopharmaceuticals from complex mixtures. This separation technique employs a fixed-bed of a solute-interacting material, known as the stationary phase and, a fluid phase that carries the solute, known as the mobile phase. The different solute affinities with the stationary phase cause the retention of molecules according to affinity degree with the chromatographic support (high-affinity biomolecules are retained while the mobile phase flows through the column with the lower affinity ones). The molecules retained in the support are subsequently recovered with the alteration of the protein/ligand biophysical proprieties or by a competitive adsorption[3,4,20,21]. Presently, *MarketsandMarkets*® estimate that the chromatography resin demand will upsurge 7.5% (Compound Annual Growth Rate (CAGR)) between 2016 and 2021, meaning a growing from USD 5.49 Billion in 2016 to USD 7.88 Billion by 2021, which makes clear the potential of doing research in this area.

Depending on the intended application, chromatography can be subdivided into two types: Preparative chromatography when the purpose is the purification with the subsequent recovery of the analyte and, analytical chromatography, when the purpose of the molecules separation is just for the analysis, quantification, identification, or study the protein's structure and function[22]. Several branches can be identified in liquid-solid chromatography, considering the type of stationary phase ligand nature (*Figure 2*):

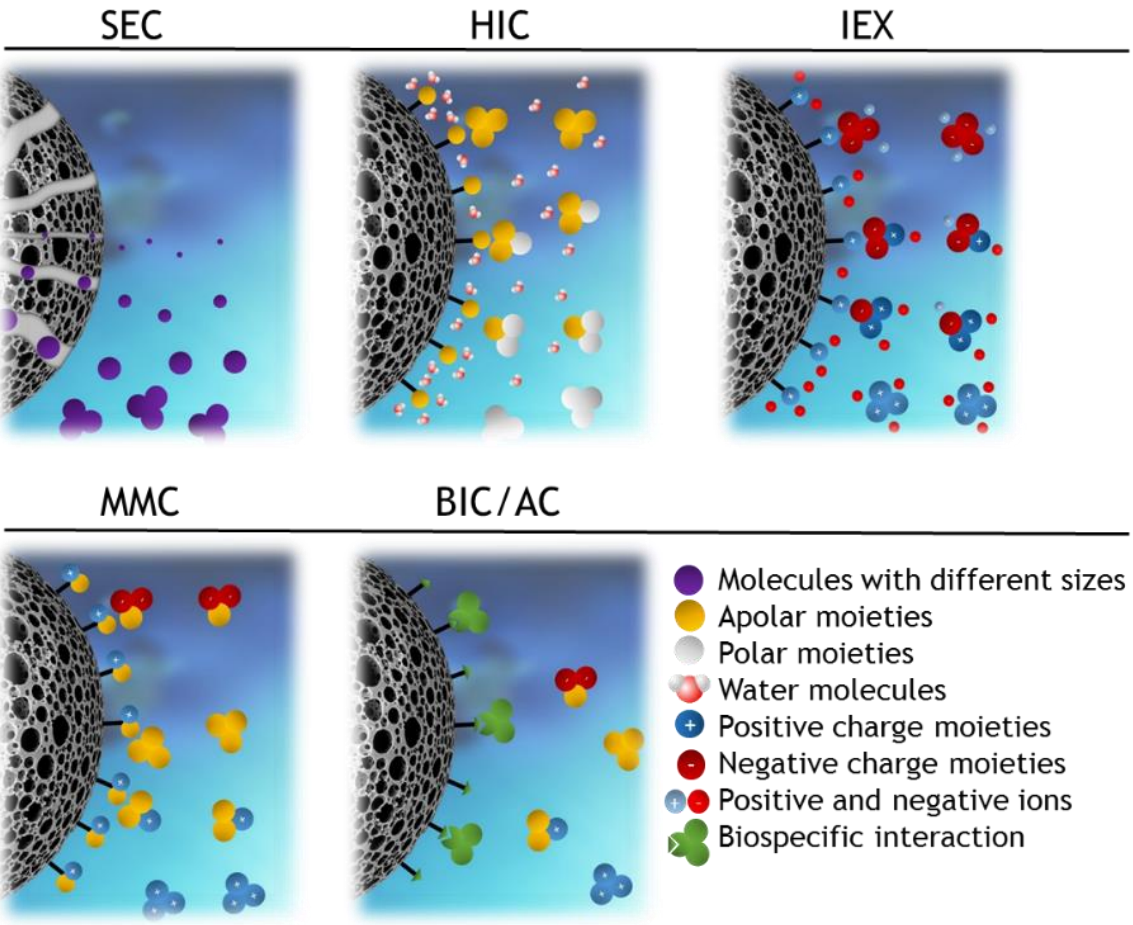

Figure 2 - LC molecule-stationary phase base interaction illustration. Respectively SEC, HIC, IEX, MMC and AC.[23]

1.2.1. Size-exclusion chromatography (SEC)

SEC or gel-filtration chromatography is based on the separation by the steric exclusion of proteins from the porous network of the chromatographic particles. This separation does not allow the adsorption between the analyte and the stationary phase, instead, the retention time of biomolecules is according to their molecular size and sometimes molecular weight. Smaller molecules have greater accessibility to smaller pores of the cross-linked bead, meaning a larger running path and, consequently, a greater retention time than the biggest ones. Larger molecules have less accessibility to smaller pores, resulting in a must faster flow through the column[15].

SEC is commonly used in capture step to partially purify the molecule of interest from the vast amount of impurities produced in the upstream process, and in the polishing step to remove the aggregates and unwanted isoforms[20].

The differences in hydrodynamic volume between proteins makes their SEC separation an entropy-controlled process, function of their molecular weight, molecular configuration (architecture), and molecular conformation (shape)[21].

Applicability:

- Separation of protein isomers, aggregates and protein mixtures.
- Protein desalting;
- Measuring the average molecular mass;
- Determination of hydrodynamic diameters.

1.2.2. Reverse-phase chromatography (RPC)

In reversed-phase chromatography, molecules are separated by their hydrophobicity level. The most common chromatographic operation mode used in RPC is the gradient elution using a specific ratio of a water – miscible organic solvent. Initially, the binding of protein hydrophobic moieties to a strong hydrophobic ligand is promoted due to the low percentage of organic solvent in the sample. After the adsorption, elution is promoted by adding organic modifiers such methanol, isopropanol, ethanol, and acetonitrile. Organic modifiers will give back to the mobile phase the affinity to protein, promoting its desorption. The greater the hydrophobicity of the protein, the higher it is its affinity for the stationary phase and consequently longer will be the retention time[20].

The adsorption driving forces in RPC are related to the decrease of free energy and heat capacity that is detected when a non-polar molecule is transferred from a polar environment to a non-polar one, resulting in an increase in entropy levels. This can be explained mainly by the water molecules reorganization described by the solvophobic theory and the preferential interaction theory[21].

RPC is a powerful technology used in analytical chromatography, however, the use of organic solvents in preparative chromatography is an obstacle for method approval by the regulatory agencies. Furthermore, not all proteins can have contact with these solvents, some of them can be irreversibly denatured due to the exposure of hydrophobic moieties present in the globular protein core[3].

1.2.3. Hydrophobic interaction chromatography (HIC)

To address the issue associated with organic solvents, HIC as RPC adsorbs the analyte based on its hydrophobicity levels, without using non-polar solvents that may promote biomolecule denaturation. Instead, the hydrophobic character of a protein is promoted by the high concentration of antichaotropic/kosmotropic salts[23]. These salts stabilize the water-water interaction, affecting not only the molar concentration of water but also, changing the hydration shell of the protein [3]. The salting out effect promotes the hydrophobic interaction forces between protein and ligand. After adsorption, elution is proceeded by decreasing salt concentration, which reduces, during the gradient, the hydrophobic interactions between the protein and the support.

1.2.4. Ion exchange chromatography (IEX)

IEX is one of the most widely used chromatography branches for the separation of proteins thanks to high binding capacities, versatility, resolving power and the ability to preserve biomolecules biological activity[24]. Due to polar amino acids charge, which is dictated by media pH, proteins can assume a superficial net charge useful to reversibly interact with the oppositely charged ligands immobilized on the support. The equilibrium of solid phase with free counter-ions is disturbed by the interaction with a charged protein, promoting *the exchange*. After the adsorption, the elution is promoted by increasing the concentration of salt ions. High ionic strength levels, generate a charge shielding of the protein and ligands surface, reducing electrostatic interaction[25].

Cation and anion exchangers are categorized as weak or strong depending on their ability to protonate. Due to their pk_a-values, strong ion-exchangers hold their charge at any practical pH (2 to 10) while the weak ones need a suitable working pH (*Table 1)*. To guarantee the opposite charge between the protein and the ligand, its common the use pH-values above or below the protein isoelectric point (PI) as well as the pK_a of the ligand. However, even at the protein isoelectric point, PI (when the net charge is zero), adsorption can occur due to the protein asymmetrical surface charge distribution (*Figure 3*). It is also important to note that post-translational modification has an important role in protein net charge because originates the micro-heterogeneity in protein surface[3].

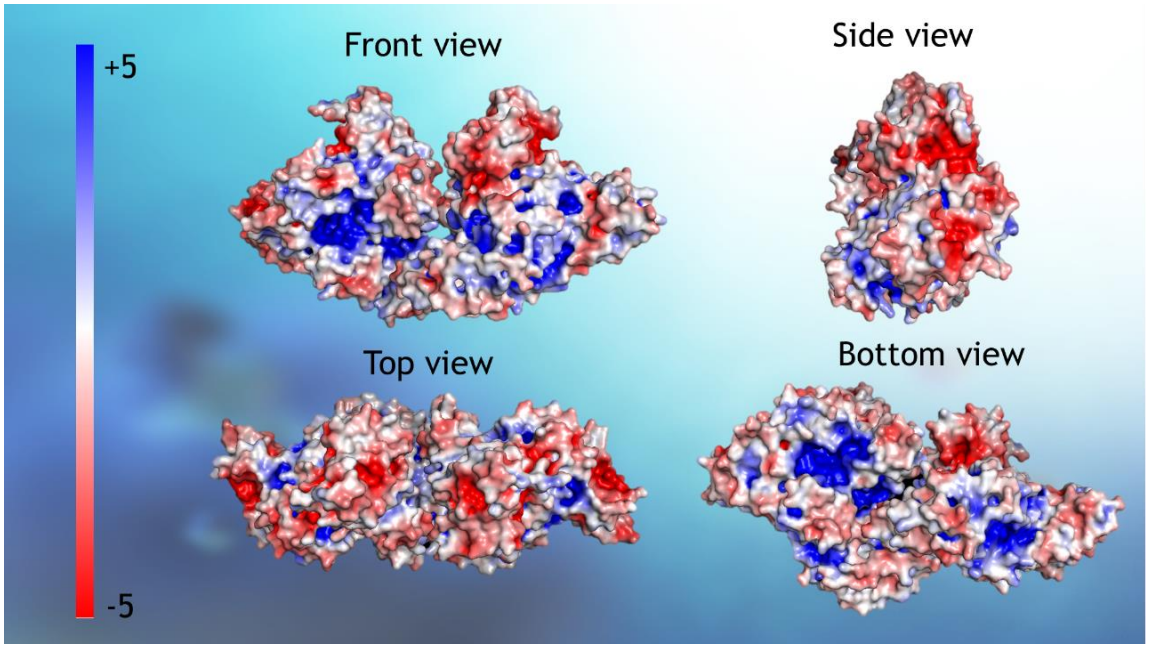

Figure 3 - Representation of the electrostatic potential distribution on BSA surface (pH 7.0), calculated from the Coulomb law using PyMOL plugin "APBS", ignoring solvent screening effect. For electrostatic potential, red is used for negative (-) and blue for positive (+). The protein structure was published by [26] and downloaded from Protein Data Bank.

Table 1 - Type, structure, pK_a and charge of IEX ligands on different values of solution pH. Adapted from[27].

Ion Exchanger type	Functional group on IE matrix			Charge Z of the functional groups
				pH of the solution
	Name	Structure		<2.0 | 2.0-2.5 | 2.5-3.0 | 3.0-5.0 | 5.0-7.0 | 7.0-10.0 | 10.0-11.0 | >11
Strong anion exchanger	Trimethyl aminomethyl (Q)	$-O-CH_2-N^+(CH_3)_3$	12.2	Z=+1 | Not stable
	Trimethyl aminoethyl (TMAE)	$-O-CH_2-CH_2-N^+(CH_3)_3$	> 13	Z=+1
	Diethyl-(2-hydroxypropyl) aminoethyl (QAE)	$-O-CH_2-CH_2-N^+(CH_2-CH_3)_2(CH_2-CHOH-CH_3)$	12.2	Z=+1
	Trimethylamino-hydroxypropyl (QA)	$-O-CH_2-CHOH-CH_2-N^+(CH_3)_3$	12.2	Z=+1
Weak anion exchanger	Dimethyl aminoethyl (DMAE)	$-O-CH_2-CH_2-NH^+(CH_3)_2$	~10	Z=+1 | 0<Z<1 | Z=0
	Diethyl aminoethyl (DEAE)	$-O-CH_2-CH_2-NH^+(CH_2-CH_3)_2$	6.0-9.0	Z=+1 | 0<Z<1 | Z=0
Weak cation exchanger	Carboxymethyl (CM)	$-O-CH_2-COO^-$	3.5-4.5	Z~0 | -1<Z<0 | Z=-1
Strong anion exchanger	Sulfopropyl (SP)	$-O-CH_2-CH_2-CH_2-SO_3^-$	2-2.5	Z~0 | Z=-1
	Sulfoethyl (SE)	$-O-CH_2-CH_2-SO_3^-$	2.0	Z=-1
	Sulfomethyl (S)	$-O-CH_2-SO_3^-$	2.0	Z=-1

1.2.5. Multimodal or mixed-mode chromatography (MMC)

More recently, the demand to avoid the drawbacks of the conventional methods boosted the research of more elegant alternatives that combine multiple interactions on the adsorption mechanism. Such strategies can be more selective and specific than HIC or IEC separately, however, MMC increase the complexity and the difficulty of understanding the adsorption process. This higher complexity of multimodal media normally requires process optimization studies in order to take full advantage of the potential of this technology[28].

Multimodal ligands interact with the target molecule through two or more different modes (e.g. electrostatic, hydrophobic and hydrogen bond interactions) at the same time, or as a single one, selecting the conditions that minimize or modify one interaction that normally occurs, acting as the "single-mode" chromatography. Depending on adsorption main driving forces, elution is usually performed with alteration of pH, salt concentration or adding molecules that compete for the same resin binding site with the protein[28–31].

Three different strategies are applied to design of multimodal chromatography resins (*Figure 4*):

- The stochastic approach, where two or more ligands with different proprieties are linked independently on the backbone of the resin;
- The multimodal ligand approach, where both groups are connected via a scaffold/linker/spacer arm, resulting in a specific stoichiometric ratio and a well-defined three-dimensional structure;
- The responsive materials, which allow inducing chemical or physical changes on the primary interactions according to the conditions (e.g. temperature, pH, salt type and concentration.

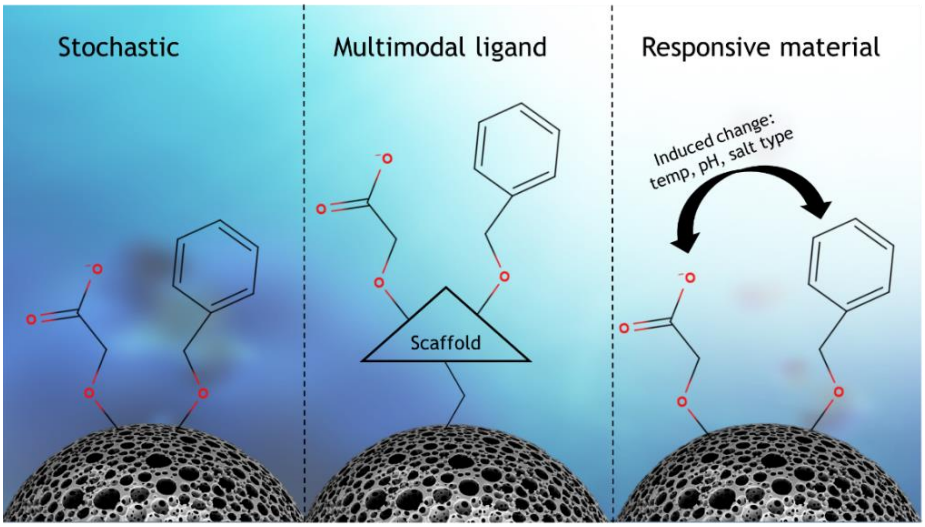

Figure 4 - Schematics examples of a multimodal medium or column based on the three types of preparation methods. Adapted from [28].

1.2.6. Biospecific interaction / Affinity chromatography (BIC / AC)

Affinity chromatography is based on the interaction between molecules that have a natural biospecificity to each other. As stationary phase is common the use of natural or synthetic ligands that are equal or very similar to those present in biological organisms. This interaction can be extremely specific, making it too difficult the desorption of the target protein from the column and sometimes requiring extreme pH conditions for elution[32].

One of the most elucidating examples of AC is the protein A chromatography used in purification of monoclonal antibodies (mAbs). Thanks to its high dynamic binding capacity, use at high flow rates, and selectivity towards IgG-type antibodies (in many cases yield >99% purity starting from the cell culture supernatant), Protein A chromatography has become one of the most important unit operations for antibody capture. Yet, it is also known to be a very expensive process, that need the use of subsequent polishing chromatographic steps[33]. Thus, the need for cost-effective processes seems to start outpacing Protein A capture step as the industry standard. Research tends to develop steps non-based in Protein A ligands, such as traditional interaction chromatography or emergent modalities like multimodal chromatography (MMC) to order to mitigate these costs. One of the objectives passes through pre-purify the cell culture harvest in order to reduce the burden over the protein A chromatography step, increasing the resin lifetime[32].

The aim of polishing steps is reducing the host cell protein levels, host DNA, leached Protein A that remains after the capture step (protease activity), and aggregates. Depending on the nature of impurities, at least two chromatographic steps are typically employed in the polishing step, anion or cation exchange chromatography, and hydrophobic interaction chromatography. In addition, to load the sample solution to IEX, depending on the previous processes, sample may require ionic strength reduction, which increases significantly the volume of the feedstock, making it unrealistic to use at the manufacturing scale. Therefore, in order to overcome this drawback, companies are currently developing new type of ligands that can provide polishing in one single step, this new type of chromatography is known as salt tolerant chromatography[34].

1.2.7. Salt tolerant chromatography (STC)

Salt tolerant chromatography (STC) or salt tolerant interaction chromatography (STIC) is described in the literature as an IEX subtype but with higher binding capacity at higher conductivities (up to 30 $mS.cm^{-1}$), over a wide range of pH[35]. As previously mentioned, the interest in this branch arose not only due to the unrealistic feedstock generated by the dilutions steps, but also because of the high separation efficiencies under high conductivities. STC explore the combination of electrostatic interactions, hydrogen bonds, and van der Waals interactions, to achieve selective separations and high resolutions of complex mixtures with very similar molecular properties, improving the productivity by reducing buffer costs and processing time[36].

In 2002, Kim and co-workers was one of the first groups to report the ability of weak anionic ligands to sustain the adsorption of biomolecules at high salt concentrations. They attached poly-allylamines into cellulose beads and observed that these established a strong interactions with BSA, this was explained by the dense distribution of charges instead of the random and sparse distribution present in DEAE-cellulose beads[37,38]. In the following year, Johansson and co-workers[39] studied several prototypes of multi-modal ligands suitable for the capture of negatively charged proteins from high conductivity mobile phases. They found that the most promising salt-tolerant anion-exchange ligands were the polyamines, which have 20–30 times higher breakthrough capacities, when compared with Q-Sepharose, for BSA at mobile phases with conductivities of 28mS.cm^{-1}. The ability of polyamines to establish electrostatic interactions with primary amine groups and hydrogen bonding with the ligand backbone was one of the explanations given for salt tolerance. Lately, in order to optimize the design of these new ligands, Riordan in 2009[36], evaluated different structural derivatives of the concluding that in addition to the use of polyamines, the ligand structure, net charge and ligand density are also fundamental factors.

1.2.7.1. Molecular structure of STC ligand

As previously mentioned, Johansson et al. in 2003, carried out screening experiments with several structures of non-aromatic and aromatic ligands in order to obtain multimodal interactions[39]. They found that alkyl chains attached with primary amines, secondary amines and guanidinium groups with a large delocalized charge (*Table 2*), allow higher binding capacities at higher conductivities when compares with tertiary and quaternary amine ligands. Nowadays, it is known that polyamines have strong interaction with a large number of biomolecules, such as DNA, α-synuclein, mAbs, serum proteins (BSA, HAS, parvalbumin, β-lactoglobulin), among others[40–48], mainly due to the combination of electrostatic interactions and hydrogen bonding, in polyamines an increased number of hydrogen atoms are available to participate in hydrogen bonding[36]. This explanation is consistent with the fact that strong anion exchangers based on the Q ligand (no available hydrogens) consistently fail to show any salt tolerance.

Moreover, *Riordan, et al., 2009* hypothesized that salt tolerance effect was due to the decreased concentration of counter-ions in the diffuse double layer of polyamine ligands[36]. At higher salt concentrations, protein-ligand electrostatic interactions are weakened due to charge shielding by counter-ions, making adsorption energetically unfavorable[49]. Therefore, only the promotions secondary interactions like hydrogen bonding, could increase the magnitude of total interaction energy, making adsorption possible under conditions where electrostatics alone would not[36].

Johansson's[39] work also allowed to conclude, that the proximity between hydrogen donor groups and anion-exchange groups provided by polyamines, seemed to be essential for the

ligand to function at high salt concentrations. To optimize these ligands, design of experiments (DoE) technics can be used to optimize the primary and secondary amines ratio, the distance between them, and the length of the carbon chain. The working pH and temperature[35], are also very important to get mixed-interactions essential to obtain high retention times at high conductivities[50].

Table 2 - Structures of some promising non-aromatic salt tolerant anion-exchange ligands[39].

Salt tolerant anion-exchange ligands	Molecular structure
1,3-Diamino-2-propanol	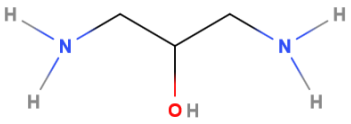
Tris(2-Aminoethyl) amine (TAEA)	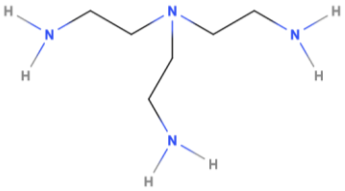
1-Amino-4-guanidobutane (AGM)	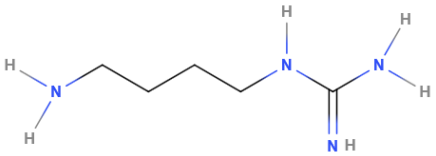
1,2-Diaminoethane	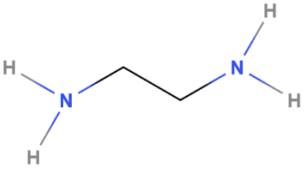
Bis(3-Aminopropyl) amine	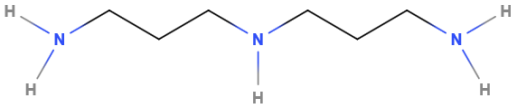
1,3-Diaminopropane	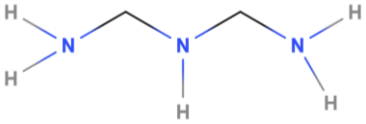

Tris(Hydroxymethyl) aminoethane

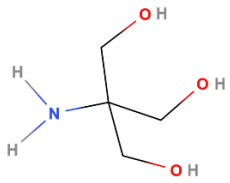

Pentaethylenhexamine

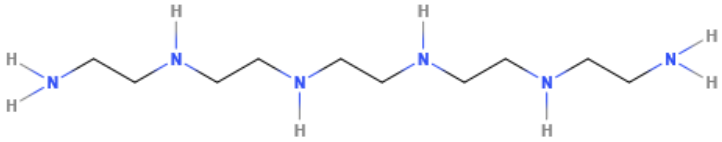

Polyhexamethylene biguanide (PHMB)

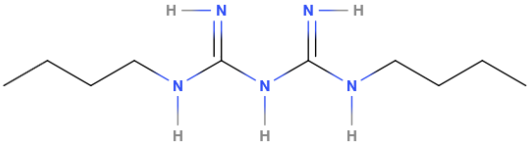

Polyethylenermine (PEI)

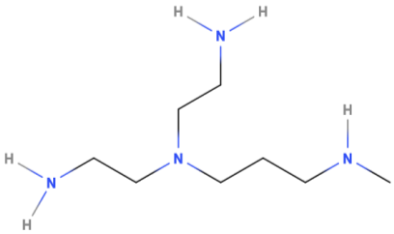

1.2.7.2. Net charge of STC ligand

The net charge is characterized by the number of positive/negative charges per ligand molecule. Riordan, et al., 2009 refers to the work developed by Roth, 1996[51] and Ståhlberg in 1999[52], to explain how the net charge influences the ability for the polyamines to have a higher salt tolerance. Both, Roth and Ståhlberg, developed studies about retention models of proteins onto ion-exchange supports and postulate, using concepts taken from colloid theory, that the magnitude of the free energy of interaction between oppositely charged bodies increases with the increase of the charge density. Thus, transferring these ideas to understand the influence of net charge in salt tolerance chromatography, the higher net charge of STC ligands, when compared with IEX supports, more favorable adsorption and consequently, a higher concentration of salt is needed to disrupt the interaction.

1.2.7.3. Ligand density and Pore size

Ligand density and pore size ware considered a secondary factor in salt tolerance justification. Having a high ligand density *per si* cannot provide salt tolerance, however, some authors affirm that can have an important influence in binding capacity and protein conformation on

surfaces[13,53-55]. It was observed experimentally by *Riordan, et al., 2009* that using a ligand structure favorable for salt tolerance (high net charge and available hydrogens), the increase in ligand density increased the salt tolerance of protein-support interaction and consequently intensified binding capacity. Thus, the combination of these factors may decrease the probability of desorption and increased the total binding strength, yielding a stronger interaction that is less likely to be disrupted by salt.

On the other hand, the results of Yuan's work with DEAE resins (not salt tolerant), show that increasing the ligand density, mass transport of proteins into the pores might be slowed down, resulting from the decrease of diffusion coefficients (De)[54,56]. Furthermore, Kim and colleges in 2002 found that resins with small pores could not be grafted with large polyallylamine molecules due to steric hindrance. This fact compromises the resins functionalization, hence the use of resins or membranes with macropores.

Although the increase of surface area by reducing the pore diameter usually gives greater adsorption capacities, large proteins such as albumin and IgG (3.6 and 5.5 nm radius respectively) may undergo steric hindrance on the surface of small pores, increasing the limitation caused by diffusivity[57]. Contrary, larger pores provide an easy accessibility for large polyallylamine molecules and proteins or dimeric forms that are important to be separated. Further, the pore diffusion limitation is reduced or even eliminated in macroporous absorbers, once convection becomes the dominant transport mechanism as illustrated in *Figure 5* and *Figure 6*[54].

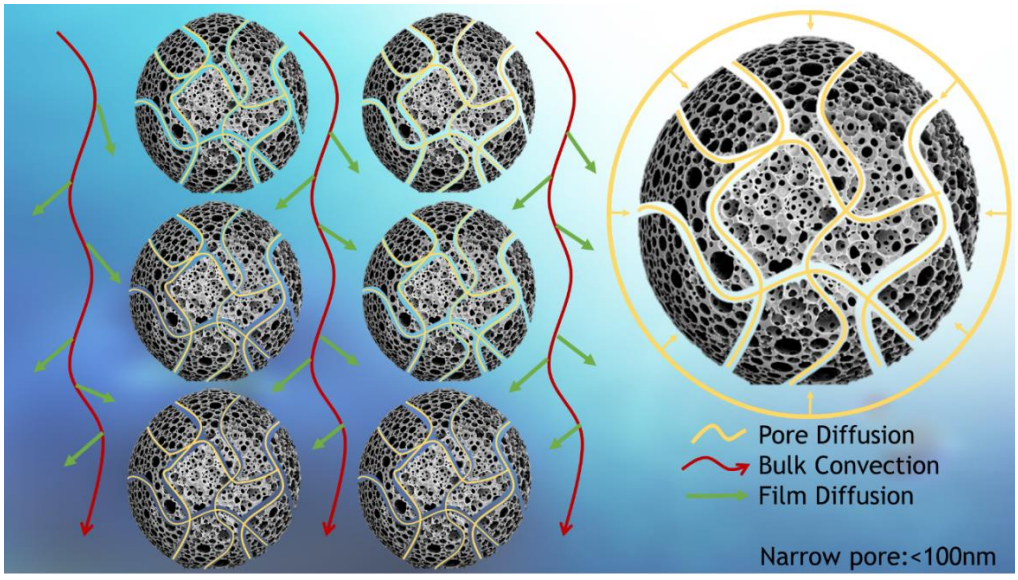

Figure 5 - Transport mechanism of packed-bed chromatography with small pores. The yellow curves show the slow pore diffusion process inside the resin channels, which is the limiting step of protein binding for packed-bed chromatography[58].

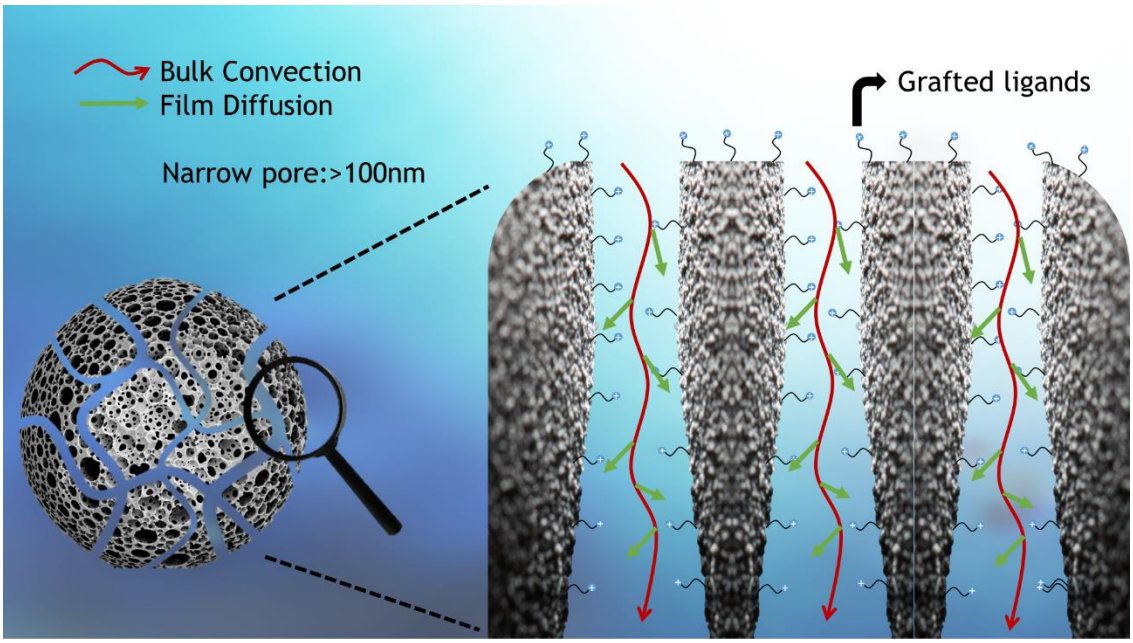

Figure 6 - Transport mechanism of packed-bed chromatography with macroporous resins. The pore diffusion process is basically eliminated due to the macroporous structure[58].

1.3. The adsorption mechanism of biomolecules on chromatographic supports.

The adsorption mechanism of molecules in liquid-solid chromatography may be considered as a dynamic equilibrium where adsorption and desorption events are continually happen between the proteins, or ions and water molecules, and the chromatography support[20]. When the protein or mixture reaches the support, the equilibrium conditions are disturbed, leading to the displacement of solvent molecules/ions by the protein molecules, followed by a competition for the adsorptive sites. Under dynamic conditions, i.e., when the mobile phase is flowing through the column, the equilibrium is reestablished under the influenced of dispersive factors, contrary to what happens under static conditions where the column has a theoretical infinite efficiency[3].

Currently, the understanding of the adsorption phenomena has become the key for the research and development of chromatographic supports and for the design of new purification methods. *Figure 7* is a schematic representation of the complex processes taking place inside a chromatographic column and the vast role of parameters that can influence the protein's adsorption phenomena[59].

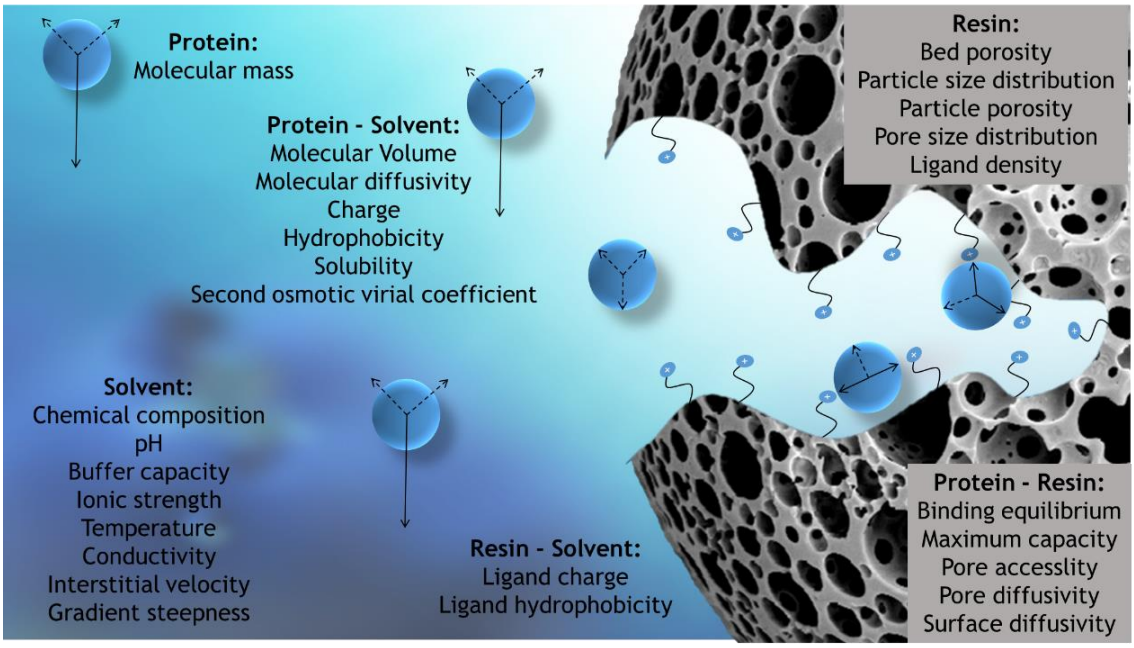

Figure 7 - Schematic representation of the parameters commonly used to describe protein molecular properties, resin properties, and their interactions inside a chromatographic column. Arrows indicate mass-transfer effects: solid arrows convection, dashed arrows diffusion, and the length of each arrow is qualitatively related to the magnitude of the effect[59].

A wide range of techniques are already used to study the adsorption phenomena, for example, atomic force microscopy[60], nuclear magnetic resonance[29], Fourier transform infrared spectroscopy[61], X-ray crystallography[62], surface plasmon resonance[60], ellipsometry[60], hydrogen-deuterium isotope exchange[13], confocal laser scanning microscopy[63], differential scanning calorimetry[61], isothermal titration calorimetry[64] and flow microcalorimetry[47,49,65–73]. However, none of these techniques, except flow microcalorimetry, processes *in situ*, and without making any kind of molecules modification, making it possible to obtain data of some adsorption events involved on the biomolecule adsorption process. Chromatographic adsorption can be divided into a sequence of subprocesses as described by Yamamoto, (2001)[74]; Hearn, (2002)[75] and Yu, (2015)[13].

These researchers made several thermodynamic fundamental studies for the protein adsorption onto ion exchange and hydrophobic interaction supports. They concluded that the binding process of biomolecules at a liquid-solid interface can be divided at least, into five subprocesses:

1. Dehydration or/and removal of the protein electrical double layer (EDL);
2. Dehydration or/and removal of the ligands electrical double layer (EDL);
3. The interaction between protein and ligands;
4. The structural rearrangement of the protein upon adsorption;
5. Rearrangement of the excluded water or/and ion molecules in bulk solution.

1. Dehydration or removal of the protein electrical double layer (EDL). The electrical double layer (EDL) is a phenomenon on the surface of any charged object when it is exposed to a fluid with free ions[76]. Hearn in 2002[75], describe that this charged object form two parallel layers of ions, called Stern layer, that comprises the ions adsorbed directly onto the protein and, a second layer, that is composed of ions attracted to the surface via a Coulombic force, electrically screened by the first layer (*Figure 8*). Therefore, prior to adsorption, water molecules or/and ions that surround the protein must be partially excluded to create available sites to establish the protein-support interaction. It was observed that dehydration/de-counter-ion step is an energy consuming process in which enthalpy of adsorption increases. However, the increase in the degree of freedom of counter-ions causes an entropy gain, compensating this unfavorable enthalpic increase.

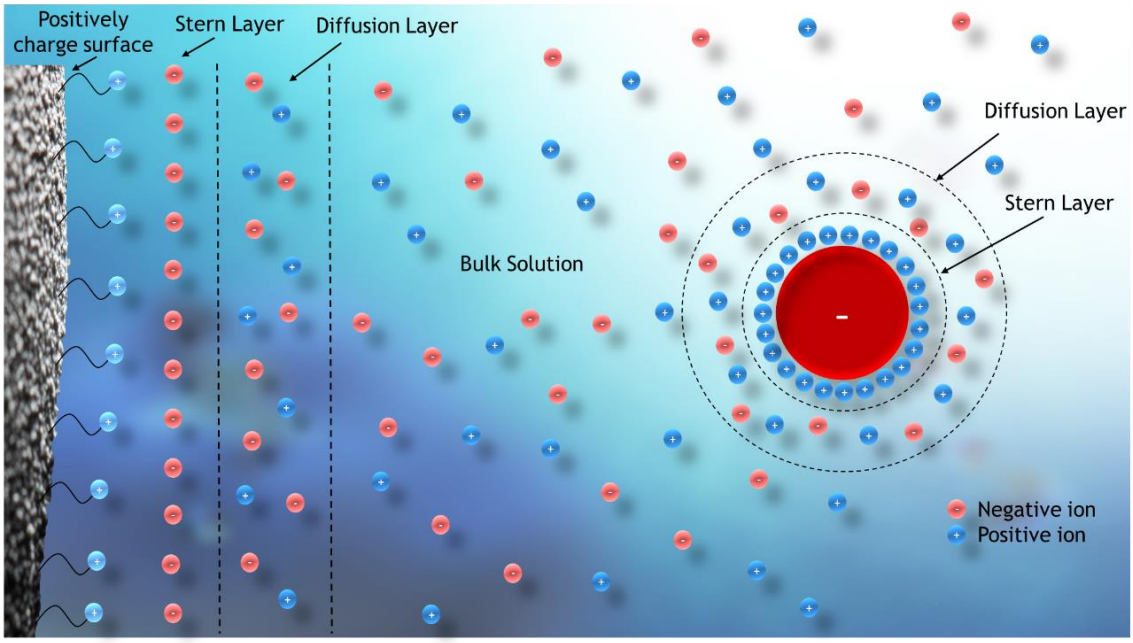

Figure 8 - Electrical double layer scheme of a negatively charged molecule and a positive ligand. Negative and positive ions are represented in red and blue, respectively [75].

2. Dehydration or removing ligands EDL. Ion exchange supports also hold an electrical double layer, which depends on its electrostatic charge, ligand functional groups and hydrophobicity. So, water molecules or/and ions must be displaced for adsorption occur.

3. The interaction between protein and ligands. Depending on the experimental conditions, nonspecific interactions such as van der Waals forces, hydrogen bonding, and hydrophobic effects may occur between the protein and an ion exchanger support[69]. However, the electrostatic interactions are usually the factor that has a more pronounced contribution to the adsorption spontaneity because it is the most energetic interaction of the class of non-covalent interactions. These forces are usually accompanied by enthalpy release and entropy loss, giving this subprocess an important role in the determining the magnitude of the total adsorption enthalpy[75].

4. The structural rearrangement of the protein upon adsorption. It is now generally accepted that many proteins undergo conformational changes upon adsorption to a solid interface[60,61,77-79]. In the adsorbed state, protein residues are involved in non-native interactions with the solid surface interface[75], thus, the surface–protein contact area induces a gain in free energy and hence proteins tend to maximize their footprint through a conformational re-organization[13]. These structural changes may cause the establishment of secondary adsorption sites mainly in proteins that are considered "soft", like BSA. Other surface phenomena review by *Yan Sun et al., 2015*[13], with the perspective to optimize the ligand chemistry, ligand density and ligand distribution, is the transport behavior of proteins on the chromatographic surfaces. They suggested that beyond the orientation and the conformational transitions, proteins may also suffer intraparticle mass transfer as well as surface diffusion mechanisms as illustrated in *Figure 9*.

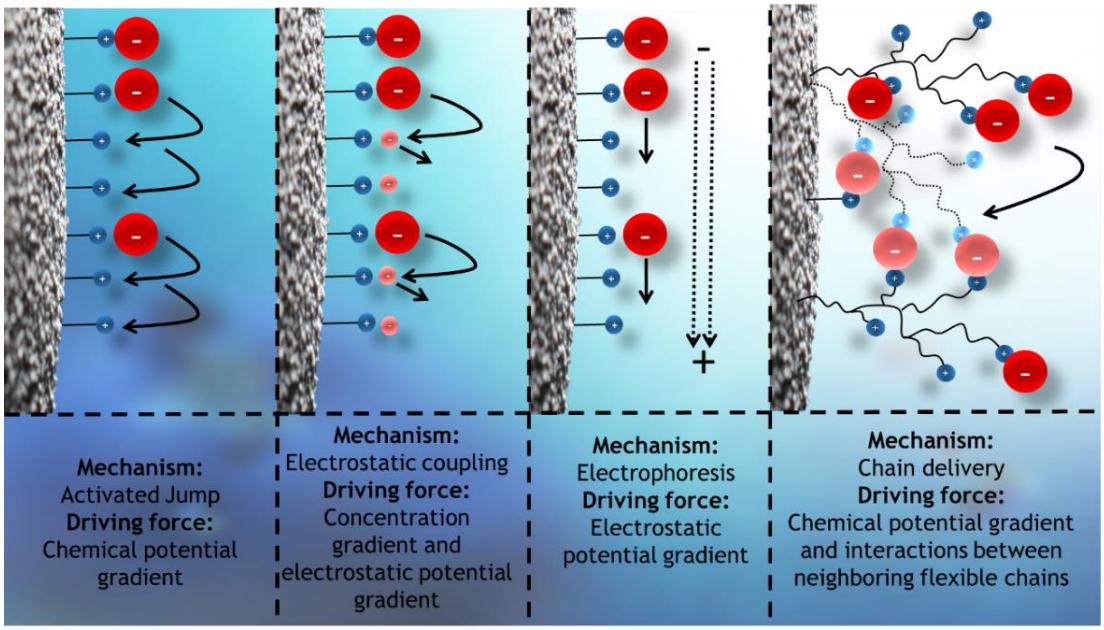

Figure 9 - Schematic diagram for surface transport mechanisms.

5. Rearrangement of the excluded water or ion molecules in bulk solution. After the protein-support equilibrium is reached, some of the previously displaced water molecules and ions 're-solvate', leading to changes in the state of the hydration of the protein and the sorbent. However, the energetic contribution of this subprocess is considered insignificant being sometimes despised[74].

1.4.Specific interaction forces between proteins and ligands

As explained before, protein adsorption at chromatographic surfaces involves various non-covalent intermolecular interactions that may include hydrogen bond, hydrophobic effect, electrostatic interaction and van der Waals forces[80,81].

1.4.1. Hydrogen bond

The idea that a single hydrogen atom could interact simultaneously with two other atoms was proposed in 1920 by Latimer and Rodebush[82], referring that hydrogen atom is special because it is the only that forms covalent sigma bonds with electronegative atoms like N, O and S, and uses the inner shell (1S) electron(s) in that covalent bond. When the electronegative bonding partner pulls the bonding electrons away from hydrogen, the hydrogen nucleus (a proton) becomes unshielded on the backside (distal from the bonding partner). The unshielded face of the proton is exposed, providing the simultaneous attachment by two electronegative atoms[83].

When the bonding partner are highly electronegativity, strong hydrogen bonds are established between charged donors and acceptors (20-40 kcal/mol)[84], nearly as strong as covalent bonds. However, in biological systems the most common are formed by N and O, establishing energy levels in the order of 3-12 kcal.mol^{-1} [83]. Although rare, weak hydrogen bonds of 1-5 kcal/mol can also be formed with C as the proton donor. Several studies have illustrated that with increased polarization due to adjacent atoms, aliphatic compounds are capable of forming weak hydrogen bonds no stronger than conventional dipole-dipole interactions and sometimes refer as a Van der Waals interactions[85]. *Nan Li at al. 2016*, also demonstrate that nonspecific hydrogen bonding combined with electrostatic interaction plays a key role in strong adsorption of protein at surfaces, however, highly dependent of ionic strength and temperature[86].

1.4.2. Hydrophobic effect

Hydrophobic effect is the principal driving force present in HIC and RFC. Hydrophobic moieties of proteins bind to water more weakly than water itself. Thus, the water hydrogen bonds are reoriented tangentially to the surface of hydrophobic moieties to minimize the disruption of the hydrogen bonded 3D network of water molecules, leading to a structured water solvation shell around the nonpolar surface. Generally, this leads to significant losses in translational and rotational entropy of water molecules that is not compensated for an enthalpy gain, making the process unfavorable in terms of the free energy of the system[87].

As the temperature is raised, this low-entropy water is no longer favored and cause the redistribution of the ordered water molecules around apolar moieties back into the bulk solution[88]. The interaction between hydrophobic moieties will establish a lower surface area exposed to water, and consequently, a lower state of free energy. The reduction in the Gibbs energy can be explained by the gain of entropy caused by released water molecules from the

surface of the protein or the solid phase[89]. Besides the temperature, the adsorption of proteins in HIC it is also promoted by polar kosmotropes (antichaotropic salts). As explained in chapter 1.2.3., these salts stabilize and structure of water-water interaction and enhance the salting out of protein from an aqueous solution[89].

1.4.3. Van der Waals interaction

Van der Waals interactions are described as a set of forces induced by dipolar interactions and dispersive forces between uncharged molecules. Due to the fact that they are relatively weak attractive forces with a short range distance (around 0.2 nm), are often considered the major contribution to the hydrophobic interaction[90]. However, the term "van der Waals interaction" is not well-defined and does not decompose the interactions in a physically meaningful way. As described further, the set of forces that are part of the van der walls interactions can be subdivided into: Dipole-dipole interactions (Keesom Interactions), Dipole-induced dipole interactions (Debye Interactions) and Fluctuating Dipoles (Dispersive interactions or London Forces)[91].

The Keesom interaction can only occur between two polar molecules that possess permanent dipole moments. The attractive or repulsive behavior between dipole-dipole depends on the orientations of the dipoles that tend to orient favorably in liquids. However, even if there is no permanent dipole moment, it is possible to induce a dipole moment when one molecule with a permanent dipole repels another molecule's electrons and cause mutual attraction (Debye interaction). To this phenomenon is called polarization and the magnitude of the dipole moment induced is a measure of the polarizability of the molecular species. Nevertheless, London Forces are the dominant contribution of van der Waals interactions. They are caused by random fluctuations of electron density in an electron cloud. An atom with many electrons will have a greater associated London force than an atom with fewer electrons. When electron density fluctuates, the dipole moments of the molecules that are located nearby to each other oscillate in synchrony[92].

1.4.4. Electrostatic interaction

In 1787, Charles-Augustin de Coulomb published a paper explaining the mechanism of the torsion balance[93]. These measurements allow him to accurately measure very weak electric forces and establish the mathematic relationship between two charges and the respective distance between them.

$$F_e = K_e \frac{q_1 q_2}{r^2} \quad (1)$$

Where F_e is the electric force, $K_e = 8{,}9875 * 10^9 N.m^2/C^2$ the Coulomb constant, r the distance between charges and q_i is the charge of the object i. Since the charges q_i can be either positive or negative, Coulomb's law implies that the resultant force can be either attractive or repulsive. In an aqueous environment, these charged species are surrounded by counter-ions, which, forms the so-called electrical double layer. When a protein molecule adsorb to the sorbent surface, an overlap of the electrical double layers cause the redistribution of ions, resulting in a negative free energy change of the system that is a favorable thermodynamic event[81].

To measure the "strength" of electrostatic interactions, the Dutch physical chemist Peter Debye, based on Poisson–Boltzmann theory, formulated the following equation that correlate the distribution of oppositely charged ions around a central ion as a function of the distances and, the effect on the decay of the electrical potential, called Debye-Hückel theory[94].

$$\lambda_D = \sqrt{\frac{\varepsilon_r \varepsilon_0 RT}{2F^2 I}} \qquad (2)$$

Where ε_r is the relative permittivity, ε_0 is the dielectric constant of vacuum, F is Faraday's constant, and I is the ionic strength. Permittivity is the material's ability to resist to an electric field, so, materials with higher permittivity have charges that are more easily displaced. Thus, the more easily they are displaced, the greater its ability to store electric energy, so the greater the charge of a ligand the greater it is the Debye length. On the other hand, by increasing the ionic strength present in the medium, lesser will be the Debye length and consequently weaker will be the interaction[95].

1.5.The role of mechanistic modeling in liquid chromatography

As previously discussed, the financial effort in biopharmaceutical purification requires the development of optimal and efficient chromatography processes. This issue is even more urgent with respect to the concept of Quality by Design, launched by the US Food and Drug Administration, which requires additional attention to process robustness and reproducibility matters. To overcome this problem, the empiric response surface modeling (RSM) can be complemented with the screenings for optimal factors given by the design of experiments (DoE). However, in parallel with the DoE-RSM-approach, strategies based on mechanistic modeling rise due to increased time efficiency of algorithms.[59] Additionally, batch experiments based on developments of the Langmuir theory and retention studies associated with theoretical models, may also successfully elucidate biomolecule adsorption onto a chromatography resin[96]. In addition, the application of retention studies likewise proved to be useful for optimization, scale up, design space characterization, as well as robustness and sensitivity analysis[59].

1.5.1. Langmuir theory

One the first reported models used to describe the molecules adsorption equilibrium is the Langmuir theory developed in 1918[97]. Langmuir established this model for the adsorption of gases onto metal surfaces but, even today, is still being widely used because of its simplicity and wide applicability. Langmuir isotherm model considers that the equilibrium results from a dynamic reversible interaction between an adsorbate and an adsorbent. However, this model undertakes that the adsorbate have homogeneous adsorption sites and, each adsorption site bind only an individual solute molecule[98]. Furthermore, the model excludes the possibility of interaction between solutes on the surface to alter their adsorption behavior, thus cannot predict the formation of multilayers, aggregates and steric rearrangements of the solute or the support ligands.

Despite that, this model is being used as a starting point for adsorption mechanisms studies. The model assumes a stoichiometric association of an adsorbate molecule, P, with a surface-bound ligand, L:

$$L + P \underset{k_d}{\overset{k_a}{\rightleftharpoons}} L.P \qquad (3)$$

where k_a ($L.mol^{-1}.s^{-1}$) and k_d (s^{-1}) are the rates for adsorption and desorption, respectively. The rate of protein adsorption on the surface (in units of $moles.s^{-1}$) can be expressed as being proportional to the concentration of the protein (C) ($mol.l^{-1}$ (M)) in solution and, to the number of vacant sites for adsorption (Q-q). Where Q ($mol.m^{-2}$) is the amount of solute adsorbed at surface saturation when all the binding sites are filled, and q ($mol.m^{-2}$) is amount of solute adsorbed on the surface for a given solution concentration (C). Thus, the change in the amount of solute adsorbed on a surface per unit area over time can be expressed as:

$$\frac{\partial q}{\partial t} = k_a C(Q - q) - k_d q \quad (4)$$

where t is time (s). Under dynamic equilibrium conditions:

$$\frac{\partial q}{\partial t} = 0 \quad (5)$$

In this case, combining *Equations 4 and 5* yields:

$$k_d q = k_a C(Q - q), \text{ or } K_{eq} = \frac{k_a}{k_d} = \frac{q}{C(Q-q)} \qquad (6)$$

which can be further rearranged to:

$$q = \frac{QC}{C + K_{eq}^{-1}} \qquad (7)$$

where K_{eq} (l.mol^{-1}) is the adsorption equilibrium constant for the Langmuir adsorption process and values of Q and K_{eq} can be determined by fitting *Equation (7)* to an isotherm plot of *q versus C* as illustrate in *Figure 10*.

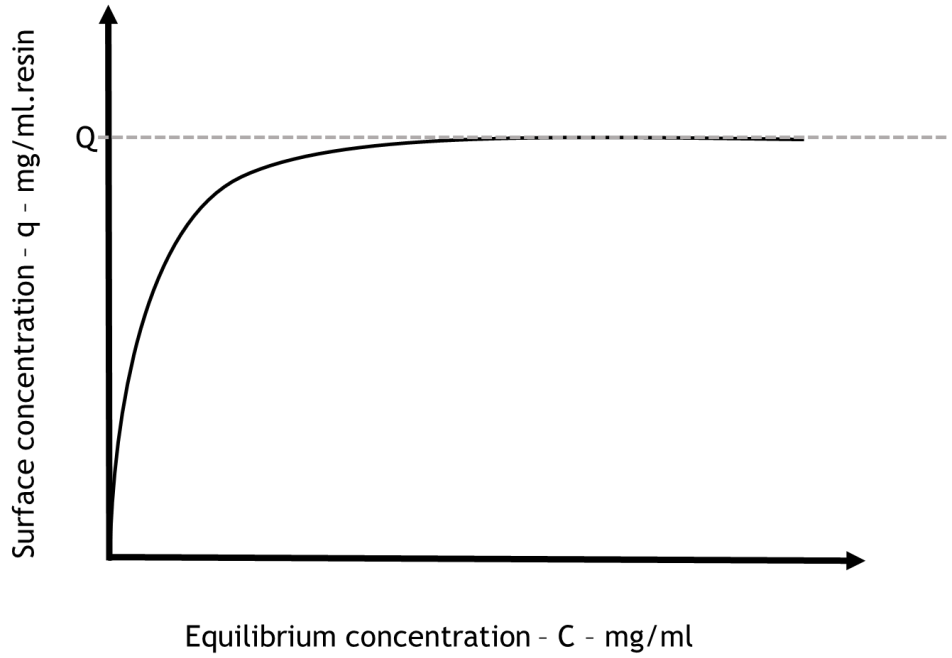

Figure 10 - Example of an adsorption equilibrium isotherm obtained by plotting surface concentration of a given molecule versus the concentration obtained after the equilibrium. The dashed line represents the maximum capacity of the isotherm.

1.5.2. Stoichiometric displacement model (SDM)

In order to overcome the drawbacks of Langmuir theory, *Kopaciewicz et al.*[99] developed in 1983 the stoichiometric displacement (SD) model based on chromatography retention studies. They postulated that in the case of polyelectrolytes adsorption onto ion exchangers, the number of charged sites involved in binding might be greater or less than the net charge of the protein, due to the protein steric rearrangement. Therefore, the underlying assumption is that protein adsorption occurs via the stoichiometric exchange with counter-ions leading to a redefinition of equilibrium *Equation (3)* by *Equation (8)*

$$P.I_p + zI_L \rightleftharpoons P_L + z.aI_{mp} + z.bI_p \qquad (8)$$

where P and P_L are the protein on mobile phase and attached to the ligand, respectively. I_p represents the counter-ions accompanying the protein, I_L the ions bounded to the stationary phase and I_{mp} the ions released to the mobile phase (*Figure 11*).

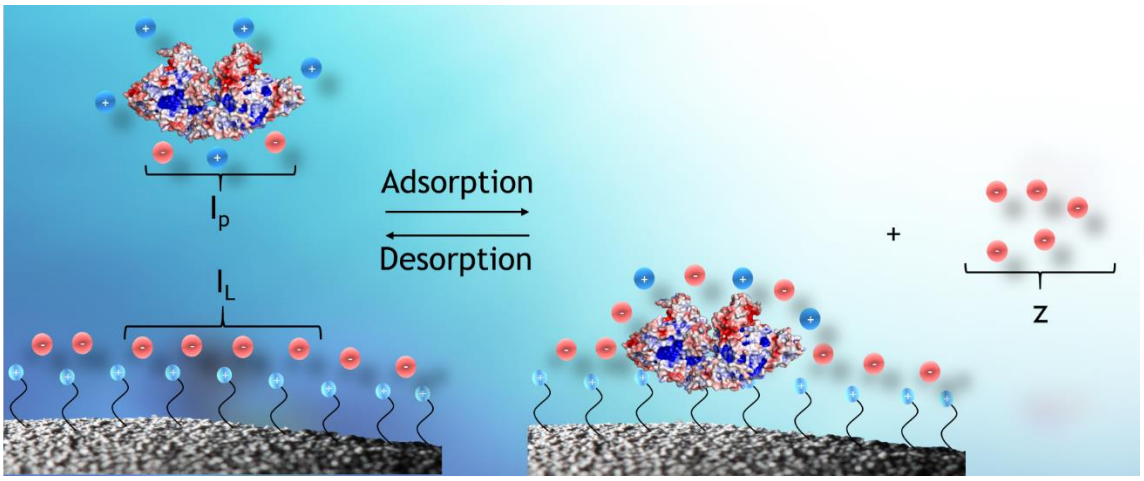

Figure 11 - Schematic representation of stoichiometric displacement model.

Moreover, the SDM also takes into account factors like the equilibrium constant (K_e), the initial ligand concentration ($[L]_0$) and the fraction of the surface available for binding ($1-f$)[100]. Nevertheless, in chromatographically meaningful terms, the (K_e) must be related to the chromatographic distribution coefficient (K_i), resulting in the following Equation:

$$K_i = K_e \frac{([L]_0)^z}{(a)^z(b)^z(I_{mp})^z(I_p)^z} * (1-f) \qquad (9)$$

However, when operated with very low protein concentrations, ($1-f$), K_e, $([L]_0)^z$, $(a)^z$ and $(b)^z$ may be incorporated into a single constant (K_y), reducing the *Equation (9)* to a simpler expression:

$$K_i = \frac{K_y}{[(I_{mp}).(I_p)]^z} \qquad (10)$$

Furthermore, in IEXC is common to express the solute retention in terms of the capacity factor k',

$$k' = \frac{K_i.A}{V_m} \qquad (11)$$

Where A designate the available surface area in $m^2.g^{-1}$ and V_m the mobile phase volume. Combining the *Equation (10) and (11)*, and incorporating K_y, A, and V_m, into a new constant, K_z, result in an expression that relates the retention of solute to the displacing agent concentration of the mobile phase and, the apparent number of contact between the biomolecule and the ion-exchange adsorbent, referred as the *effective charge* or *binding charge (z)*.

$$k' = \frac{K_z}{[(I_{mp}).(I_p)]^z} \qquad (12)$$

When a monovalent salt like sodium chloride is used as a displacing agent, it is assumed that (I_{mp}) equals (I_p), reducing the *Equation (12)* to:

$$k' = \frac{K_z}{[NaCl]^{2z}} \qquad (13)$$

By linearizing *Equation (13)* it is obtained:

$$\log k' = 2z \log\left(\frac{1}{[NaCl]}\right) + \log K_z \quad (13)$$

where *2z* is the slope and, *log* K_z the intercept of a plot of *log k'* versus *log (1/[NaCl])*.

1.5.3. Steric Mass Action model (SMA)

In 1991, *Cysewski et al.*[101] replicated the experiments proceeded by *Kopaciewicz et al., 1983*[99]*; Rounds and Regnier, 1984*[100]*;* and *Drager and Regnier, 1986*[102]; demonstrating that the SDM successfully accounts for the variation of solute retention with mobile phase salt concentration under linear conditions. However, when extended to nonlinear conditions, the results shown that the isotherm derived from the law of mass-action is unable to properly describe the isotherm *plateau*. In the previous year, *Velayudhan et al.*[103]*,* during the work done in his dissertation about nonlinear chromatography, suggested that macromolecules, by virtue of their size, cover more binding sites than those dictated by their characteristic charge. Predicting that mainly in nonlinear ion-exchange systems, the steric shielding of stationary phase binding sites plays a major role in the adsorption behavior. However, it was only in 1992 that Brooks and Cramer[104] introduced an important refinement of the SD model, called the *steric mass action model*. The key assumption of SMA model is that because of the large footprint of the protein molecule, protein binding not only involves z-ligands through a counter-ion exchange process as in the SD model, but also results in the shielding or steric hindrance of a number (σ) of these ligands, as can be seen in *Figure 12*[105].

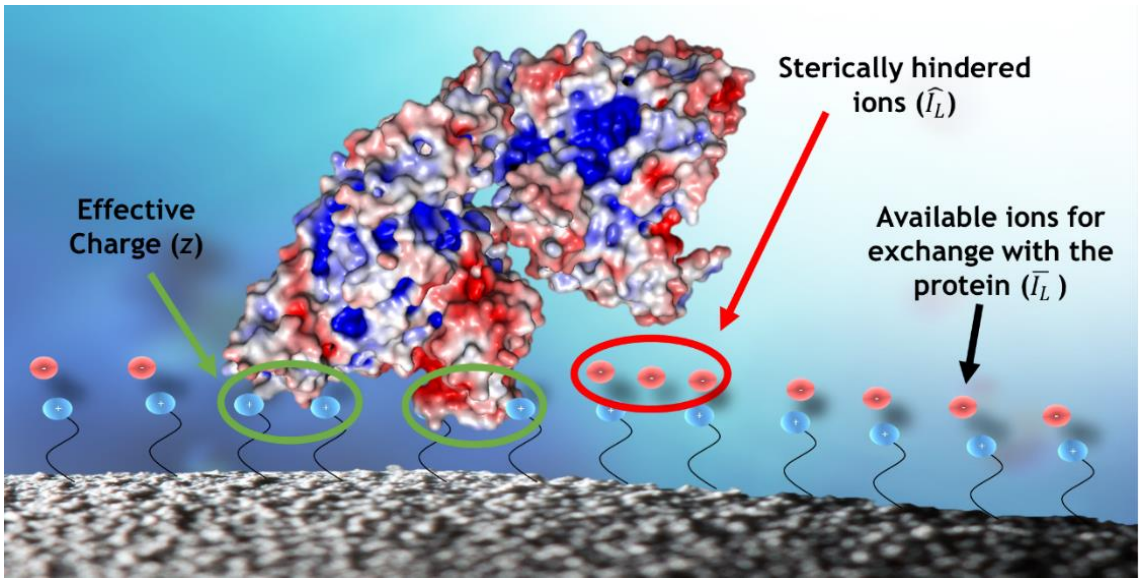

Figure 12 - Schematic drawing of the effects of steric hindrance on protein binding to the surface of an anion exchanger.

Starting from the same equilibrium equation described in SDM, they subdivided the ions bounded to the stationary phase (I_L) in two categories, those who are available for exchange with the protein ($\overline{I_L}$) and those who are sterically hindered ($\widehat{I_L}$), unavailable for exchange with the protein. So, the hindered ions are described by the follow equation:

$$\widehat{I_L} = \sigma_p . P_L \qquad (14)$$

Where σ_p represent the steric factor. Therefore, the stoichiometric exchange of the protein and exchangeable salt counter ions was readapted to:

$$P_{mp} + z.\overline{I_L} \rightleftharpoons P_L + z.I_{mp} \qquad (15)$$

Where the z_p represent the ratio of the protein and counter-ion characteristic charges for an *n*-valent salt. Thus, the equilibrium constant is defined by:

$$K_e = \left(\frac{P_L}{P_{mp}}\right)\left(\frac{I_{mp}}{\overline{I_L}}\right)^z \qquad (16)$$

After the adsorption of protein occurs, the total concentration of salt on the stationary phase, I_L, is given by the following expression.

$$I_L = \overline{I_L} + \sigma_s . P_L \quad (17)$$

So, for the stationary phase have electroneutrality, requires:

$$\Lambda \equiv \overline{I_L} + (\sigma_p + z)\, P_L \qquad (18)$$

Where Λ is the ionic capacity. Combining the *Equation (18)* on the equilibrium equation constant it is found that:

$$K_e = \left(\frac{P_L}{P_{mp}}\right)\left(\frac{I_{mp}}{\Lambda-(\sigma_p+z)P_L}\right)^z \quad (19)$$

When the protein concentration in mobile phase is very low ($P_{mp} \to 0, P_L \approx 0$) the isotherm reduces to:

$$\lim_{P_{mp}\to 0} P_L = \left(\frac{\Lambda}{I_{mp}}\right)^z . P_{mp} \quad (20)$$

As expected on Ion Exchange supports, the initial slope of isotherm decreases exponentially as the mobile phase salt concentration coefficient increases. However, when the protein concentration in mobile phase tends to infinity ($P_{mp} \to \infty, \overline{I_L} \approx 0$) the $P_L = P_L^{max}$, and the steric factor becomes significant as described in *Equation (21):*

$$\lim_{P_{mp}\to \infty} P_L = \frac{\Lambda}{\sigma_p + z} = P_L^{max} \ (21)$$

Where, in contrast to Langmuir isotherm, the maximum capacity of SMA isotherm (P_L^{max}), is independent of mobile phase salt concentration.[106] The sum of the characteristic charge and the steric factor provides a direct relationship between the bed capacity and the saturation capacity of the protein. The steric factor, which requires information from the nonlinear portion of the isotherm, can be determined from breakthrough experiments. Where, the breakthrough volume, V_B, of a front can be related to the column phase ratio (β) and the mobile and stationary phase concentrations of protein, by the following expression.

$$V_B = V_0 \left(1 + \beta . \frac{P_L}{P_{mp}}\right) \quad (22)$$

Where the V_0 represents the dead volume (the breakthrough volume of an unretained solute). Substituting the term, $\left(\frac{P_L}{P_{mp}}\right)$ in the equilibrium *Equation (19)* yields the following expression:

$$K_e = \frac{1}{\beta}\left(\frac{V_B}{V_0} - 1\right)\left(\frac{I_{mp}}{\Lambda - (\sigma_p + z)\frac{P_{mp}}{\beta}\left(\frac{V_B}{V_0} - 1\right)}\right)^z \quad (23)$$

Solving for the steric factor, yields:

$$\sigma_p = \frac{\beta}{P_{mp}\left(\frac{V_B}{V_0} - 1\right)}\left(\Lambda - I_{mp}\left(\frac{\left(\frac{V_B}{V_0} - 1\right)}{\beta . K_e}\right)^{\frac{1}{z}}\right) - z \ (24)$$

However, when is used highly charged polymer as displacers, is commonly obtained *square* isotherms under low mobile phase salt conditions. Under these conditions, the assumption of complete saturation of the bed is reasonable; therefore, the concentration of adsorbed solute (P_L) can be assumed to equal to the saturation capacity (P_L^{max}), enabling the steric factor to be directly calculated by the following equation[104,106]:

$$\sigma_p = \frac{\Lambda}{P_L^{max}} - z \quad (25)$$

1.5.4. Yamamoto´s approach

Isocratic runs are rapid and accurate methods, however, these pulse response experiments are only valid for the protein concentration used in the experiment[107]. Thus, in 1983, Yamamoto[108] developed a mathematic model to predict relationships between the elution characteristics and the operating conditions of proteins on ion exchange columns. His theoretical assumptions are based on the continuous-flow plate theory initially proposed by Martin and Synge in 1941[109], which claims that the distribution coefficient is dependent of ionic strength and protein concentration, so the number of plates should vary with time. However, considering a time-dependent number of plates increases significantly the complexity of mathematical expressions, so, the author includes longitudinal dispersion and gel phase diffusion to assume that the number of plates is constant and relate that number derived from a mass balance model[110]. In this way, Yamamoto developed a simplistic model that require only two parameters: the distribution coefficient, which can be experimentally measured by batch experiments or by frontal analysis, and the number of theoretical plates.

Initially the model assumes that the relative peak position ($\theta_R = V_e/V_0$) is varying with the slope of a linear gradient (g).

$$g = \frac{I_{max} - I_0}{V_G} \qquad (26)$$

Where V_e, V_0 and V_G represent the peak elution volume, the void volume of the column and the slope in ml, respectively. While I_{max} and I_0 represent the final and the initial salt concentration of the elution buffer. Yamamoto also found the following empirical equation by normalizing the slope of linear gradient with respect to the gel volume of the column (GH):

$$GH = \frac{{I_R}^{(B+1)} - {I_0}^{(B+1)}}{A(B+1)} \qquad (27)$$

Where I_R is the salt concentration at the peak retention time (or volume), A includes the equilibrium coefficient, B is the number of binding sites (effective charges) involved in electrostatic interaction, G is slope of a linear gradient normalized with respect to the void volume of the column ($G = g.V_0$) and H is the ratio between gel volume and void volume

$$H = \frac{V_t - V_0}{V_0} = \frac{1-\varepsilon}{\varepsilon} \qquad (28)$$

Where V_t is the column volume and ε is the porosity. Comparing the term ${I_0}^{(B+1)}$ with ${I_R}^{(B+1)}$, it is observed that the initial salt concentration of the elution buffer is negligibly small, so that *Equation (27)* can be simplified to

$$GH = \frac{{I_R}^{(B+1)}}{A(B+1)} \qquad (29)$$

By linearizing *Equation (29)* it is obtained:

$$\ln(GH) = (B+1).\ln(I_R) - \ln(A(B+1)) \qquad (30)$$

Where from the slope of GH - I_R curve we can get the number of effective charges involved in the interaction.

1.5.5. Preferential interaction analysis

Later, in mid-1996, Perkins and co-workers[111] developed a correlation between adsorption and the release of water and counter ions on the adsorptive process for large molecules. This model was initially designed to hydrophobic interaction chromatography, however, in its genesis no assumptions regarding the adsorption mechanism were made, allowing its application to different types of chromatography: hydrophobic interaction, ion exchange or reversed phase[65,96]. As an alternative to the solvophobic theory, Perkins provided a thermodynamic independent model to relate the effect of salt on the observed equilibrium constant from the change in the distribution of salt ions and water molecules, based on the *preferential interaction analysis*. This analysis had previously been used to explain the effect of solutes on a variety of assembly processes, including protein stabilization, precipitation, aggregation, ligand binding and adsorption[111].

The theoretical principles of Perkins analyses are based on the work developed by Eisenberg (1976)[112], which postulated that the distribution of a protein between the solvent and solute molecules is characterized by a measurable quantity known as the preferential interaction coefficient:

$$\Gamma_{32}^{m} = \left(\frac{\partial m_3}{\partial m_2}\right)_{T,\mu_1,\mu_3} \qquad (31)$$

Where the subscripts 1,2 and 3 refer to the solvent, the protein, and the solute respectively and *m* the molality. Years later, Timesheff (1993)[113] and Anderson (1995)[114], apply two-domain models which divide the solution in two different regions, one that is unaffected by the presence of the protein (non-electrolytic) and another local region where the preferential accumulation or exclusion of solutes is noted (electrolytic). Therefore, the coefficient for non-electrolytic species can be expressed by:

$$\Gamma_{32}^{m} = v_3 - \frac{m_3}{m_1}.v_1 \qquad (32)$$

Where v_1 and v_3 represent the moles of solvent and solute respectively, in the vicinity of the protein *per* mole of protein. It is important to note that, if a solute is preferentially accumulated near a protein, relative to its concentration in bulk, Γ_{32}^{m} is positive. Negative values of Γ_{32}^{m} indicate preferential exclusion of solute (preferential solvation). For the

(uncommon) quasi-ideal situation in which the solute and solvent are in effect randomly mixed, the local and bulk solute concentrations are identical, so that $\Gamma_{32}^{m} = 0$.

The analogous equation for the electrolytic species gives:

$$\Gamma_{+.2}^{m} + \Gamma_{-.2}^{m} = (v_{+} + v_{-}) - \frac{n.m_3}{m_1} v_1 \qquad (33)$$

Where n is the number of ions associated with the electrolyte, and + and – is the cations and anions.

Applying these concepts in the protein adsorption equilibrium equation:

$$pP + lL = plPL \qquad (34)$$

where P in the protein, L the ligand adsorption site and PL is the protein-ligand complex, the logarithm of the observed equilibrium constant is defined by:

$$lnK_{obs}^{m} = pl\ln(m_{PL}) - p\ln(m_P) - l\ln(m_L) \qquad (35)$$

Through the manipulation of partial stoichiometric, the variation of the equilibrium constant with the concentration of a nonelectrolyte or with the mean ionic activity ($a_{\pm}$) of an electrolyte, is given by the stoichiometric weighted sum of the preferential interaction coefficients:

Nonelectrolyte:

$$SK_{obs} = \left[\frac{\partial \ln(K_{obs})}{\partial \ln(m_3)}\right]_{T,P,EQ} \qquad (36)$$

Electrolyte:

$$SK_{obs} = \left[\frac{\partial \ln(K_{obs})}{\partial \ln(a_{\pm})}\right]_{T,P,EQ} \qquad (37)$$

Combining the *Equation (36) and (37)* by the *Equation (32) and (33)* yields:

Nonelectrolyte:

$$SK_{obs} = \left[\frac{\partial \ln(K_{obs})}{\partial \ln(m_3)}\right]_{T,P,EQ} = \Delta v_3 - \frac{m_3}{m_1}.\Delta v_1 \qquad (39)$$

Electrolyte:

$$SK_{obs} = \left[\frac{\partial \ln(K_{obs})}{\partial \ln(a_{\pm})}\right]_{T,P,EQ} = (\Delta v_{+} + \Delta v_{-}) - \frac{n.m_3}{m_1}\Delta v_1 \qquad (40)$$

In linear conditions, the equilibrium constant and fluid properties are independent of protein concentration, so, the capacity factor is equal to the observed equilibrium constant divided by the phase ratio. However, when the phase ratio it is not affected by the composition of mobile phase, the observed variation in the retention factor is dictated only by the salt concentration. Rewriting the *Equation (40)* in terms of the capacity factor and incorporating the variation in the mean ionic activity with the molal salt concentration gives:

$$\left[\frac{\partial \ln(k')}{\partial \ln(m_3)}\right]_{T,P,EQ} = \frac{(\Delta v_{+} + \Delta v_{-})}{g} - \frac{n.\Delta v_1}{m_1.g} m_3 \qquad (41)$$

where

$$g = \left(\frac{\partial \ln(m_3)}{\partial \ln(a_{\pm})}\right)_{T,P} \qquad (42)$$

When electrostatic forces govern the adsorption, the $(\Delta v_{+} + \Delta v_{-})$ become the dominant term of the equation and, ions and water stoichiometries become independent of the salt concentration. Resulting in the following expression:

$$\ln(k') = \frac{(\Delta v_{+} + \Delta v_{-})}{g}.\ln(m_3) - \frac{n.\Delta v_1}{m_1.g} m_3 + c \qquad (43)$$

where c is the integration constant, $(\Delta v_{+} + \Delta v_{-})$ the change of the binding of ions and Δv_i the number of water molecules released.

1.6. Thermodynamic study of biomolecules adsorption

As previously mentioned in subchapter 1.5., in the last 50 years the technological development allows us to obtain a huge amount of structural data for biological molecules and their complexes. However, none of these techniques processes *in situ* and/or without modifying the native structure of studied molecules, thus, *per si*, cannot completely characterize the complex adsorption mechanisms of biomolecules in liquid chromatography. Therefore, to gain further understanding, it is necessary to combine three-dimensional structure with the underlying thermodynamics and the kinetics of the process. This approach is necessary because any effort to modulate the adsorption process, for example in therapeutics, is grounded on a sufficiently detailed understanding of the molecular events that take place. The commonly used methods to obtain information about thermodynamic quantities associated with liquid chromatographic adsorption are van't Hoff plots analysis and microcalorimetric measurements[64].

The base theory of thermodynamic is that for a process spontaneously occur, at constant pressure and temperature, the change in standard Gibbs free energy (ΔG°) of the system must be negative as shown by *Equation (44)*[115];

$$\Delta G^0 = \Delta \mathrm{H}^0 - \mathrm{T}\Delta \mathrm{S}^0 < 0 \quad (44)$$

where ΔH° is the standard enthalpy change and ΔS° is the standard entropy change. When ΔH°<0 means that there is heat released by the system (Exothermic event), while endothermic events (ΔH°>0) require heat transfer into the system. The equilibrium binding affinity constant (K) can also be related to the standard Gibbs free energy change (ΔG°) for a specific protein-solid phase as:

$$\Delta G^0 = \mathrm{RT}\ \ln(K) \quad (45)$$

where *R* is the gas constant (8,314462 $J.K^{-1}.mol^{-1}$) and *T* is the absolute temperature in Kelvin.

In 1884, Jacobus van 't Hoff published in his book *"Études de Dynamique chimique"*[116] an indirect method to measure thermodynamic quantities associated with the chemical equilibrium. Years later, his work was applied to the thermodynamic study of molecules adsorption in liquid chromatography, using the following van't Hoff linear expression:

$$\ln(k') = \frac{-\Delta \mathrm{H}^0}{R}\left(\frac{1}{T}\right) + \frac{\Delta \mathrm{S}^0}{R} \quad (46)$$

Where the $\Delta \mathrm{H}^0 = -R * slope$ and $\Delta \mathrm{S}^0 = R * YY\ intersecion$. Although the model allows us to obtain an overview of proteins-support interaction driving forces, this experimental approach is often faulty since the enthalpy may not be temperature independent. Horvath and co-workers in 1996 postulated that some complex molecules as proteins may not change the retention time linearly with temperature[68,88,117]. Thus, they develop a correction of this model taking into account the dependence of the standard-state enthalpy change of adsorption on temperature, resulting in the following equation:

$$\ln(k') = \frac{\Delta \mathrm{C}_P^0}{R}\left(\frac{T_H}{T} - \ln\left(\frac{T_S}{T}\right) - 1\right) + \ln(\beta) \quad (47)$$

where $\Delta \mathrm{C}_P^0$ is the standard state heat capacity change; T_H and T_S are the reference temperatures at which $\Delta \mathrm{H}^0$ and $\Delta \mathrm{S}^0$ are zero; and β is the phase ratio.

It is important to note that the subprocesses of adsorption described in chapter 1.5. are responsible for thermodynamic changes in a chromatographic system. However, the fact that these events are interconnected and highly related makes it extremely difficult to individualize their thermodynamic contribution to the system by the van't Hoff plots analysis. Also, many studies have demonstrate the inherent superiority of the calorimetric methods when compared to van 't Hoff analysis for obtaining enthalpy values[64]. Notwithstanding, microcalorimetry

enthalpy measurements being more reliable, they require more demanding experimental operation procedures and skillful interpretation. Calorimeters are instruments that directly and quantitatively measure the heat of an interaction. Whilst chemists have used them since the 18th century, it has only in the last four decades that electronics, materials design and temperature sensing technology have advanced to the point where calorimeters have enough sensitive to allow the meaningful study of biological molecules and their interactions. Nowadays, three different but complementary calorimetric techniques can be used for thermodynamic studies: Differential scanning calorimetry (DSC), used to protein unfolding or nucleic acid melting studies[61,118], Isothermal titration calorimetry (ITC) and Flow microcalorimetry (FMC) to examine the binding interaction of ligand–macromolecule or macromolecule–macromolecule[61,111]. In this work, we present a brief overview of FMC because it was the calorimetric technique used for the development of thermodynamic studies.

1.6.1. Flow Microcalorimetry

FMC is a powerful and unique technique because unlike other calorimetry techniques, that operate under static (or closed-system) conditions, the measurements are obtained from a flowing fluid stream, simulating the adsorption process of biomolecules onto a packed-bed chromatographic system at the micro-scale. The technique was invented in 1958 by Groszek[120], who applied the FMC to estimate surface areas of minerals. However, it was only in the beginning of the seventies that Microscal® develops the first commercial FMC. Since then, the technique has been widely used to the understanding of the driving forces, mechanisms, and kinetics involved in liquid-solid interfaces[65–67,71,72,96,121–127]. However, only in the beginning of this century it starts to be applied to biomolecules, it is described in literature that FMC has been used with different types of biomolecules and chromatography supports, i. e. hydrophobic interaction chromatography[69], ion exchange chromatography[70], affinity chromatography[127] and with several types of proteins[65,67,71], pDNA[73] and virus like particles (experiences in progress by our research group).

As shown in *Figure 13*, the FMC cell or column is located in the interior of the apparatus, in order to minimize heat flow from the cell to the surrounding. The microcalorimeter cell has a total volume of 171 µl (where the adsorbent is packed) that is interfaced with two highly sensitive thermistor sensors that are responsible for measuring very small power changes (10^{-7} W). These energy changes are converted to heats of adsorption using a calibration factor determined experimentally with a specific outlet provided by the supplier. After the thermistor measurements, the effluent passes through a conductivimeter and an UV detector, which allows the biomolecules output control. At the end, the effluent can be collected and analyzed by other techniques.

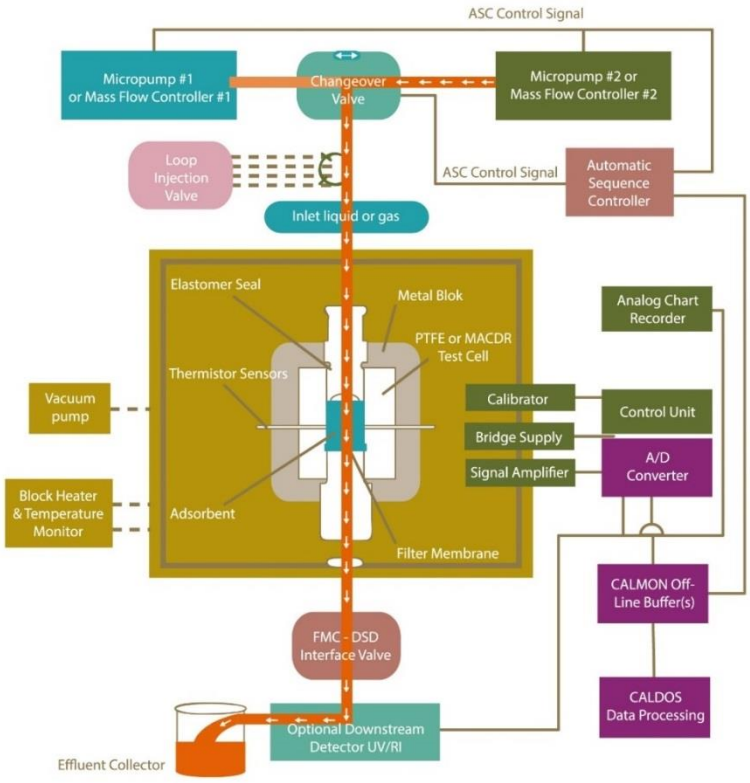

Figure 13 - Flow microcalorimeter representative scheme.

The output obtain from the thermistors is a graph like the represented in *Figure 14*, which may be called a thermogram. In essence, is a plot of heat in $\mu J.s^{-1}$ *versus* time in seconds, which allows to quantify the magnitude and chronology of thermal events during and after the biomolecule-adsorbent interaction. The thermogram may be shaped by negative or positive peaks, representing the endothermic and exothermic events, respectively. Due to the reference system used, the exothermic peak, which represents a negative enthalpy, show a positive peak because when the studied system release energy, the thermistors sense a heat increase. Consequently, when the studied system gain energy (endothermic peak), the thermistors sense a heat decrease and a negative peak will appear.

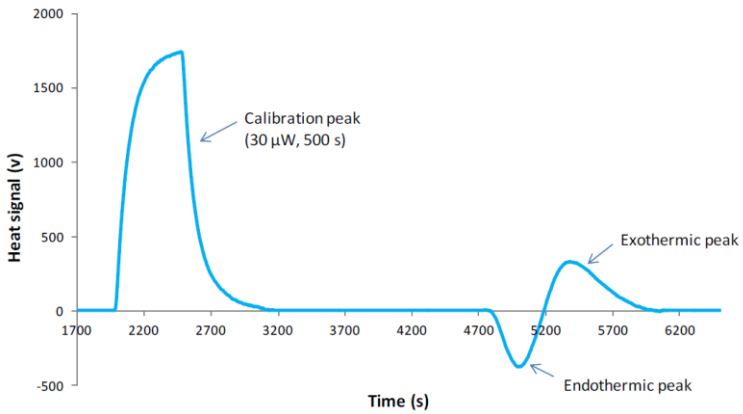

Figure 14 - Example of the FMC thermogram.

As previously referred, the adsorption events are highly interconnected; therefore, the use of high flow rates (like the chromatographic systems) makes it impossible to differentiate the adsorptive events obtained in thermograms. Because of this, low working flows rates (between 0.6-6 $ml.h^{-1}$) are used to obtain good peaks resolution and to avoid problems associated with system pressure. Even so, it is common to observe an overlap of peaks, representing that different adsorption event occur simultaneously. To differentiate them, it is used a mathematic program to deconvolute the overlapped peaks. Although these limitations cause time-consuming experiments, flow microcalorimetry still is one of the only methods that allow the measurement of heat exchange under fluid stream flowing conditions, reproducing the conditions during a chromatographic process for any range of product concentration.

Chapter II. Aims of study

As mentioned, it is well recognized that ion-exchange chromatography is a powerful technique for the separation and purification of biomolecules on a large process scale. However, when starting with high conductivity feedstocks (≥15mS.cm^{-1}), additional steps are required before loading, such as dilution and/or diafilteration, which increases process time and costs. Thus, it is imperative, for economic reasons, to design chromatography ligands that are capable to make a direct processing of biological feedstocks or intermediate fractions without these extra steps.

The chromatography support used in this work, Toyopearl NH2-750F, is one good example of technology improvement. This resin can maintain high DBC at conductivities greater than 30mS.cm^{-1}, making it ideal for protein initial capture step or even for polishing steps (antibody aggregates removal), overcoming the drawback of the conventional methods. However, this new chromatographic support is considerably more complex than the conventional ones, and suitable models to explain the adsorption process do not exist. Consequently, the prediction of separation behavior is still unreliable, creating an impediment in the design and implementation of scaled-up units.

Considering all this information, this work aims to elucidate how the salt concentration, pH and protein surface concentration affect the adsorption mechanism of BSA, as a model protein, onto the salt tolerant anion exchange support, Toyopearl NH2-750F.

To do that, it was used a Flow Microcalorimetric system, because it has proven its ability to provide an improved understanding of the driving forces, mechanisms and kinetics involved in the interaction process of biomolecules during their adsorption onto several chromatographic systems. The ability to perform enthalpy measurement *in situ*, makes FMC not only, a unique technique to comprehend the adsorption force, but also the subsequent events that occur after the entire molecule being in contact with the support. Furthermore, as complementary studies to the thermodynamic tests, retention studies couple to semi-empirical models like, Stoichiometric Displacement model, the Steric Mass Action model, Yamamoto's approach and Preferential Interaction analysis were performed because they also have previously show great utility in the interpretation of thermograms and in the understanding of the observed adsorption events.

Chapter III. Materials and methods

3.1.Materials, Apparatus and Software

BSA was chosen as the probe protein. It was purchased from Sigma-Aldrich, St. Louis, Missouri, USA and used without further purification. BSA is a globular ellipsoid (140 × 40 × 40 Å), with a molecular mass of 66 500 Da, and an isoelectric point (pI) of 4.7[128]. The salt tolerant anion exchange support, Toyopearl NH2-750F was kindly offered by TOSOH Bioscience (Germany) (pK_a=8.5)[50].

Retention chromatographic data was obtained using an ÄKTA Pure system from GE Healthcare (Uppsala, Sweden). Data was collected and analyzed by UNICORN software from GE Healthcare (Uppsala, Sweden).

All the BSA samples were quantified with xMarK TM Microplate spectrophotometer from Bio-rad Life Science Research (California, USA).

TableCurve 2D v5.01 (Systat Software Inc.) was used to curve-fit the adsorption isotherm measurements and the preferential interaction analyzes measurements.

Thermodynamic studies were performed using a Flow Microcalorimeter FMC 4 Vi from Microscal Ltd (London, UK). Data was collected and analyzed with CALDOS4 software from Microscal Ltd (London, UK). Further analysis was done through peak deconvolution using PEAKFIT software package (version 4.12, Seasolve Software Inc., San Jose, USA).

3.2.Adsorption isotherm measurements

Adsorption isotherms experiments were performed in 12-well plates previously tested to verify if adsorption of proteins into plate walls occur and, if there is a release of molecules that may interferences with the determination of BSA concentration. A known concentration of BSA (Sigma-Aldrich, St. Louis, Missouri, USA) was prepared in two distinct equilibrium buffers, 20 mM Tris-HCl (Nzytech, Portugal) at pH 8.0 and 20mM Bis-tris (Sigma-Aldrich, USA) at pH 6.0. In each of the pH employed were tested three concentrations of NaCl (Panreac, Barcelona, Spain), 150 mM, 300 mM and one in the absence of salt. The deionized distilled water used in solutions preparation was obtained by the Milli-Q ADV (Millipore, Madrid, Spain) and all the used salts had an analytical grade. The salt tolerant anion exchange resin, *TOYOPEARL NH2-750F* kindly offered by TOSOH Bioscience (Tokyo, Japan), underwent two washing steps, one with deionized water and other with the equilibrium buffer solution.

Firstly, 1 ml of dilutions of BSA solution was transferred into the 12-well plates together with 10 µl of the solid phase suspension (1:2). The 12-well plates were then sealed with parafilm

and placed on an orbital shaker at 21.5ºC and 230 rpm during more than 16h to ensure that the equilibrium is reached. While the adsorption equilibrium was reached, the BSA initial solution was left at room temperature to posteriorly measure the initial concentration and realize the mass balance. Previous experiments demonstrate that the values of BSA concentration do not suffer any significant difference between leaving it at 21.5°C or at room temperature for 1 day. (*Appendix-Figure 22)*

After reaching the equilibrium, the slurry was transferred to eppendorf tubes and left to settle down by gravity for a few minutes depending on the resin density. The supernatant was separated from the solid-phase with a syringe, and then filtered with a 0.22 µm pore low protein binding syringe filter (Millex-GV, Merck KGaA, Germany). To measure the initial and equilibrium concentration, samples were aliquoted into 96-well UV transparent plates (Thermo Scientific, Portugal) and absorbance measured at 280 nm with a UV microplate spectrophotometer.

To analyze the data, surface concentration - q (mg BSA.ml^{-1} resin) was plotted against equilibrium concentration – C (mg BSA.ml^{-1}) with the curve-fit made by Table Curve 2D v5.01.

3.3.Retention chromatographic data

3.3.1. Isocratic Runs

The experiments were performed on a fully automated liquid chromatography system (ÄKTA Pure system from GE Healthcare (Uppsala, Sweden)) and temperature was controlled by a bath from Amersham Bioscience (Uppsala, Sweden) with the Multi-Temp III system. This setup circulates constant temperature water into the column thermostatic jacket.

A XK16 empty chromatographic column (GE Healthcare, Uppsala, Sweden) was packed with 1 ml of Toyopearl NH2-750F. Before each assay, the system was equilibrated with at least 10 column volumes of the respective buffer (20 mM Tris-HCl at pH 8.0 and 20 mM Bis-tris at pH 6.0) with 1.00, 1.10, 1.25, 1.40 and 1.50 M NaCl (Sigma–Aldrich, Steinheim, Germany) at flow-rate of 1 ml.min^{-1} and at a selected temperature. Retention times (t_r), measured under isocratic conditions, were obtained by injecting 20 µl of 20 mg.ml^{-1} BSA. The elution profile was determined by continuous measurements of the absorbance at 280 nm. Following the elution, the column was washed with the same injection buffer but in the presence of 2 M NaCl. This buffer was also used to determine the elution time for an 'inert' tracer (t_0) by injecting, at the same flow rate, the same quantity and concentration of BSA. Two replicated studies were done for each elution profile and the retention factor, k', was determined directly from the chromatogram as:

$$k' = \frac{t_r - t_0}{t_r} \qquad (48)$$

3.3.2. Linear gradients

Similar to Isocratic elution studies, the experiments were performed on an ÄKTA Pure system at constant temperature. However, the retention times (t_r) was measured under a linear gradient of 0 M to 1.5 M NaCl with five different gradient slopes twice repeated. Buffer solutions were Bis-tris 20 mM and Tris-HCl 20 mM for pH 6.0 and pH 8.0, respectively, and volumetric flow-rate was 1.0 ml/min. Following the elution of the loaded sample (20 mg BSA.ml^{-1} with a 20 µl injection loop) the column was washed with the same injection buffer but in the presence of 2 M NaCl.

The conductivity (mS.cm^{-1}) at UV maximum of the peak (I_R) was measured for the different gradient slopes and plotted against normalized gradient, *GH*. The calibration curves between the conductivity and the NaCl concentration in the buffer solution were prepared for the determination of I_R. (*Appendix-Figure 23*)

From the linearization of GH-IR curve, the number of binding sites (effective charges) involved in the electrostatic interaction, B value, were determined according with the following equation.

$$GH = \frac{{I_R}^{(B+1)}}{(A[B+1])} \quad (49)$$

The parameter A includes the equilibrium coefficient. $GH=g(V_t - V_o)$, $G=g.V_o$, H is the volumetric phase ratio = $(1 - \varepsilon)/\varepsilon$, ε is the column void fraction $=V_o/V_t$, and $g=(I_f - I_0)/V_g$ is the gradient slope of the salt (I_f, final salt concentration; I_0, initial salt concentration; V_g, gradient volume). V_t is the total column bed volume, V_o is the column void (interstitial space) volume.

3.4. Zeta Potential measurements

For each measurement, different volumes of the stationary phase (20; 30; 40; 50; 75; 100 µl) suspended in 2 ml buffer solution (20 mM Tis-HCL pH 8.0 and 20 mM Bis-tris pH 6.0) and left overnight to allow full swelling and equilibration. The zeta potential measurements were done immediately after removing the suspension from ultrasonic bath for 10 min. Before each measurement the stability of the suspension was automatically tested by Zetasizer and, in case of satisfactory suspension, automatically calculated by Zetasizer from electrophoretic mobility µ using the Smoluchowski's formula:

$$\mu = \frac{\varepsilon_r \varepsilon_0 \zeta}{\eta} \quad (50)$$

where η is the viscosity of the solution, ε_r is its relative permittivity of the medium, and ε_0 is the absolute permittivity of vacuum ($8.85 * 10^{-12}\ C^2N^{-1}M^{-2}$) and ζ the zeta potential of the resin. The zeta potential measurements were repeated three times for each sample and only the results reported as "good" by the equipment were taken into consideration.

3.5.Flow Microcalorimetry (FMC)

The real-time enthalpy measurements of BSA adsorption onto *Toyopearl NH2-750F* packed bed was performed with a flow microcalorimeter (Microscal FMC 4 Vi, Microscal Limited, UK).

FMC cell (or column) has a volumetric capacity of 171 µl, which is packed with the resin previously washed with the respective buffer. The equilibrium step was conducted by passing the equilibration buffer through the cell at a constant flow rate (1.5 $ml.h^{-1}$) overnight at 23 ºC ± 0,3, using precision syringe pumps (Harvard Apparatus, UK). Two buffers were tested in this work, 20 mM Tris-HCl at pH 6.0 and 20 mM Tris-HCl at pH 8.0, each with three concentrations of NaCl (no salt, 150 mM, and 300 mM).

After reaching the equilibrium, the 100 µl loop was filled with BSA dissolved in the respective buffer and injected into the column. To evaluate the surface concentration (mg $BSA.ml^{-1}$ support), the flow through and the injected sample were read with a UV spectrophotometer (XMark, Bio-rad, Portugal) at 280 nm.

Between each injection, a cleaning-in-place (CIP) with a 0.5 M NaOH solution (José Manuel Gomes dos Santos Lda., Odivelas, Portugal) was done to ensure the removal of strongly bound impurities or irreversibly adsorbed product. After the CIP, a washing step with ultrapure water was performed, followed by an equilibrium step with the respective buffer, overnight with a flow rate of 1.5 $ml.h^{-1}$.

The enthalpy changes caused by the adsorption of the sample onto the adsorbent was measured by two thermistors interfaced in the FMC column. The thermistors are highly sensitive to heat changes in the order of 10^{-7} W and were calibrated by a specific outlet (calibrator). This outlet releases an energy pulse of 3 µW during 100 seconds with the cell loaded with resin, corresponding to 0.3 mJ. The calibration factor obtained was later used to convert digitals to a heat signal (mJ).

The acquisition, storing and data processing was made by CALDOS 4 software (Microscal, Limited, UK). Peak deconvolution and peak area calculation were performed with PeakFit 4.12 software (Seasolve Software Inc., USA) using asymmetric Gaussian peaks and Residuals method with a Savitsky-Golay type smoothing. Finally, the heat of adsorption was calculated from the area of the deconvoluted peaks and normalized by the amount of protein injected and adsorbed.

Chapter IV. Results and Discussion

4.1. Adsorption isotherms data

The adsorption isotherms experimentally obtained at pH 6.0 and pH 8.0 for BSA onto *Toyopearl NH2-750F*, are reported in *Figure 15* and *Figure 16*, respectively. Through the analysis of the isotherm profile, it can be seen that the adsorption capacity follow a linear trend at lower equilibrium concentrations followed by a plateau region at both pH (a type I Langmuir isotherm profile)[97]. However, taking a closer look to *Figure 16*, at pH 8.0 without salt and with 50mM of NaCl, the isotherm plateau is followed by a region of increasing capacity, which may indicate the formation of multiple layers or a reorganization of the adsorbed protein to accommodate more molecules[49,70,98].

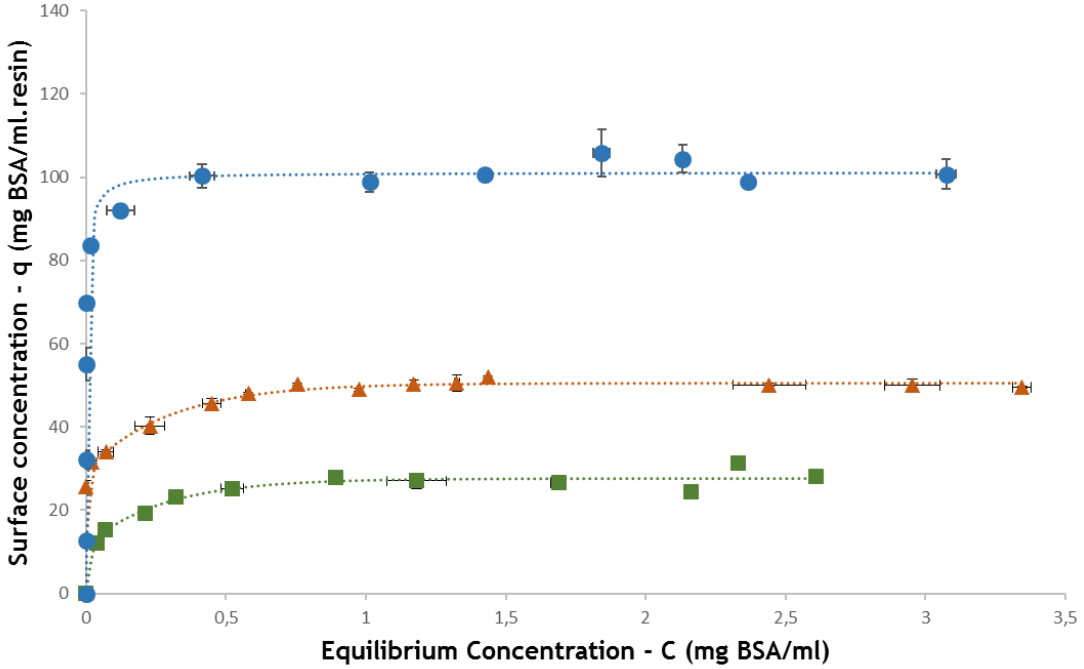

Figure 15 - Equilibrium binding isotherms for bovine serum albumin adsorption onto Toyopearl NH2-750F at Bis-tris pH 6.0 and 295 K. (●) 0.0 mM NaCl, (▲) 150 mM NaCl (■) 300 mM NaCl.

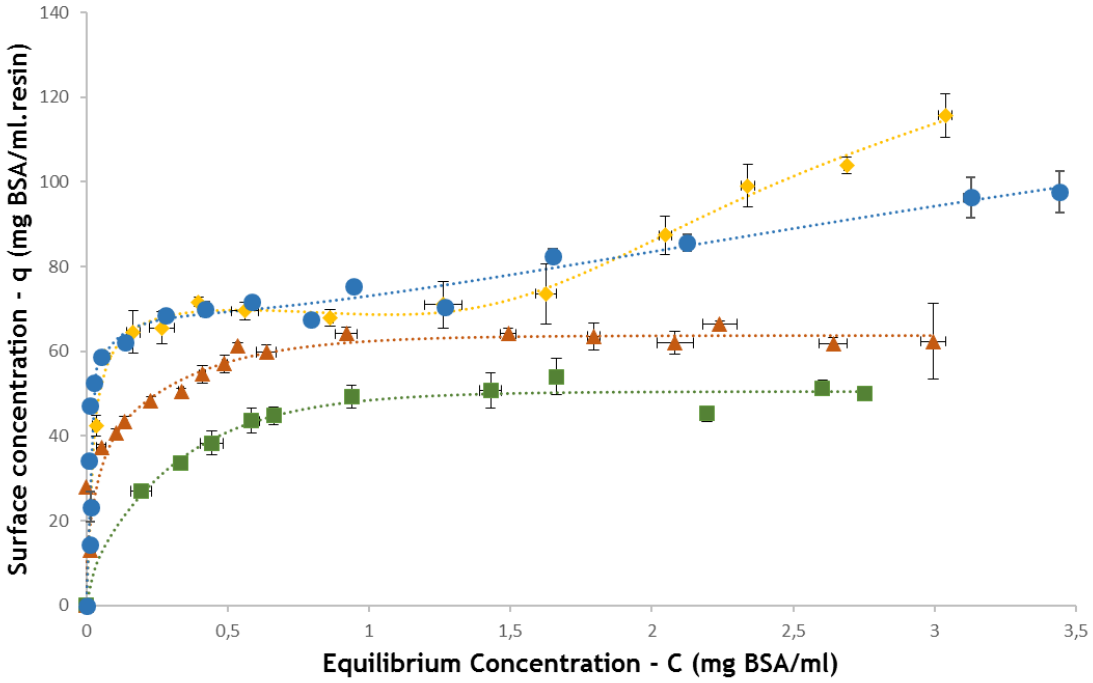

Figure 16 - Equilibrium binding isotherms for bovine serum albumin adsorption onto Toyopearl NH2-750F at Tris-HCl pH 8.0 and 295 K. (●) 0.0 mM NaCl, (◆) 50 mM NaCl, (▲) 150 mM NaCl (■) 300 mM NaCl.

Looking now for the effect of salt concentration on the adsorption maximum capacity, it can be seen that with the increase of salt concentration, the maximum capacity of isotherm decreases. Salt is expected to shield the electrostatic interaction between the protein and the surface, thereby reducing the q_{max} and K_a[129]. This trend is also consistent with other empirical[74,130] semiempirical[104] descriptions of protein ion-exchange equilibrium based on the stoichiometric exchange model. However, the decrease of q_{max} with the increase of salt concentration in the salt-tolerant resin *Toyopearl NH2-750F* is much less significant when compared *with Toyopearl GigaCap Q-650M* and *Toyoperal DEAE-650M*, observed in Pousada's work [130]. These results demonstrate that the use of primary and secondary amine based ligands provide more efficient interactions in the presence of salt when compared to quaternary amine ligands.

We can also compare the effect of salt concentration between both studied pHs. The results show that with the increase of salt concentration, the maximum capacity of isotherm decreases more sharply at pH 6.0 than at pH 8.0, demonstrating that at pH 8.0 the interactions established between the protein and the ligand are more salt-tolerant. These results are coherent with those found in documents supplied by Tosoh Bioscience®[50], which indicate that at higher pH the *NH2-750F* support shows to have higher salt tolerant properties. However, at pH 6.0 in the absence of salt, the resin has a higher capacity compared to pH 8.0, that can possibly be explained by the higher effective charge of polyamine ligand (pK_a 8.5), or even by the adsorbed BSA footprint on the support surface (further discussion will be presented on the next sections).

4.2.Stoichiometric displacement model

As outlined in the introduction, the retention behavior of proteins on ion exchange surfaces can be successfully correlated with the apparent number of contacts between the biomolecule and the ion-exchange adsorbent (z), using the SDM method. However, some authors demonstrate that this model can be applied not only to ion exchange resins but also to mixed mode supports[131]. In our case, the z value is determined by measuring the retention of BSA onto the salt-tolerant support *Toyopearl NH2-750F* that present different kinds of interactions[43]. The application of the SDM to our data is illustrated in *Table 3*.

Table 3 - Apparent number of contacts with SDM, z as function of temperature from the adsorption of BSA onto Toyopearl NH2-750F using as modulator NaCl at pH 6.0 and 8.0.

pH	Temperature (K)	R	Slope	z
6	288.15	0.9942	2.1492	1.08
	298.15	0.9972	2.0631	1.03
	308.15	0.9942	2.5291	1.27
8	288.15	0.9995	3.7528	1.88
	298.15	0.9952	3.5795	1.79
	308.15	0.9976	3.924	1.96

The obtained z values demonstrated to be highly dependent on pH, showing that at higher pH (more salt-tolerant) the number of protein-ligand binding points also increases. These results are similar to those demonstrated by Rounds and Regnier in 1983[100]. Regnier retained four different proteins (β-lactoglobulin A, conalbumin, ovalbumin and soybean trypsin inhibitor) with a quaternary ammonium ligand and observed that the z value consistently increased with the increase of pH. The magnitude of the z values obtained in our work, suggests a straight relation with the protein charge, because as far from the protein isoelectric point we work, more charged is the protein and higher we expect to be the observed z value.

However, it cannot be forgotten that the apparent number of contacts between the protein and the support cannot only be explained by the proteins net charge alone, but also the ligand net charge should be considered. The quaternary ammonium resin used in Regnier's work is a strong anion exchanger, hence can sustain the net charge over a high range of pH. On the other hand, the *Toyopearl NH2-750F* is considered a weak anion exchanger, so the net charge is significantly reduced with the increase of pH. Thus, the increase of z value at pH 8.0 should be

explained by the presence of other type of interactions. The fact that not all the ligand amines are protonated, leaves free hydrogen atoms that are available to establish hydrogen bonding[2] simultaneously with the electrostatic interactions.

Furthermore, the structural nature of the protein molecule itself should be considered. The BSA molecule increase the molecular volume at pH 8.0, starting a transition state between the normal conformation (N) to basic (B). This isomerization is supposed to be a structural fluctuation, a loosening of the molecule structure with loss of rigidity, particularly affecting the N-terminal region[128]. It has been reported that many ligands and drugs bind to albumin depending on the state of N-B equilibrium, playing a physiological role as ligand transporter to the liver[132,133]. The surface exposure of flexible random coil and the loss of heart-shape, increases the hydrodynamic volume and as consequence produces a greater footprint on the ligand surface[128,134] that can be a factor that facilitates the establishment of hydrogen bounds simultaneously with electrostatic interactions, this could be also an explanation for the higher value of z observed.

The influence of temperature on the z parameter can also be observed in *Table 3*. z presents the highest value at 308 K, which is an indication of BSA structural changes, as expected for a flexible and malleable protein.

4.3.Yamamoto's approach

In this approach, the number of binding sites, *B* (effective charge) are determined according to *GH-IR* curve using several linear gradients. The values for the fitted parameters at different pHs are listed in *Table 4*. Unlike the isocratic runs, the linear gradients allowed to obtain *B* values for monomers and other oligomeric forms of BSA. It is known that BSA may be present in different oligomeric forms. Chromatograms in Appendix-Figure 24 denote a more significant presence of this forms at pH 6.0 than at pH 8.0, similar results were observed by Babcock in 2013[135]. Studies carried out by Barbosa[77] have also shown the coexistence of dimers and monomers in solution at pH 5.4, and a predominance of monomers at more basic pHs. The proximity to the protein's isoelectric point may be the explanation for this phenomenon. A lesser repulsion caused by similar charges may enable protein-protein interactions promoting the formation of the oligomeric forms.

B values are higher at pH 8.0 for the monomeric forms, showing the same tendency observed with the results obtained by the SDM. However, there is a large discrepancy between the numerical values (z values obtained by the SDM and the B values obtained by the Yamamoto's approach). This may be explained by the difference in the base principles of each applied model. Nevertheless, the evolution of the B value with pH show the same tendency as the z value obtained by the SMD.

Table 4 - Apparent number of binding sites with Yamamoto's approach, B from the adsorption of BSA onto Toyopearl NH2-750F using as modulator NaCl at pH 6.0 and 8.0.

pH	Oligomer forms	R	Slope	B
6	Monomer	0.9958	7.7227	7.7
	Dimer	0.9981	15.213	15.2
	Aggregates	0.977	7.7454	7.8
8	Monomer	0.9909	10.873	10.9

The *B* values for dimer and aggregates were only obtained at pH 6.0 where a good chromatographic resolution was achieved (*Appendix*-Figure 24). At pH 8.0 it was possible to separate the BSA monomeric form from the oligomers, however the low resolution between oligomeric species did not allow the I_R values attainment (*Appendix-Figure 24)*. At pH 6.0 the results were consistent with the ones shown by Yamamoto in 2015[35], the dimeric forms of BSA have higher *B* values when compared with monomers. Also at this pH, aggregates demonstrate to have a similar *B* value as the monomeric form, which may be explained by steric hindrance. BSA dimer is small enough to adopt a surface organization that allows it to establish multiple binding points as opposed to the aggregates, where the steric hindrance becomes a weight factor. These concept, that larger molecules may suffer a more steric hindrance on surface is well founded by Brook and Cramer that developed the steric mass action model[104].

4.4.Steric Mass Action Model

As shown in sub-chapter 1.5.3., the steric factor σ_p is commonly determined by *Equation (24)*, however, the high number of unknowns factors that require empirical values, make its application a time-consuming protocol that requires a variety of chemical reagents. Unfortunately, the reagents needed to develop this protocol did not arrive in time. Nevertheless, as mentioned in sub-chapter 1.5.3., under certain conditions, *Equation (25)* may be used. In absence of salt the adsorption isotherms at both studied pHs, show a *square* isotherm profile, therefore, *Equation (25)* was applied to calculate the steric factor. Results are presented in *Table 5*.

Table 5 - SMA parameters from the adsorption of BSA onto Toyopearl NH2-750F at pH 6.0 and 8.0.

pH	Ion Capacity (Λ) (mmol.l^{-1})	z	P_L^{max} (mg BSA.ml^{-1}.resin)	P_L^{max} (mmol BSA.l^{-1}.resin)	σ_p
6	100	1.03	100	1.51	65.43
8	100	1.79	72	1.08	90.52

The maximum capacity values (P_L^{max}) were taken directly from the adsorption isotherm data, the effective charge of protein-ligand interaction (z) was calculated from the SDM and the Toyopearl NH2-750F ionic capacity (Λ) was obtained from the supplier [43] (Tosoh Bioscience®). The calculated steric factors are in the same order of magnitude as the ones obtained by Shi et al.[136], who studied the evolution of BSA steric factor in a wide range of pH using the DEAE ligand.

Our results showed that at pH 6.0, the σ_p is significantly lesser than at pH 8.0, which may be explained by the increase of the molecular volume of BSA, as stated in SDM discussion. This result is also coherent with the higher isotherm maximum capacity obtained at pH 6.0 in the absence of salt. Is intuitive to think that a larger footprint on support surface, due to the loss of protein rigidity, allows the establishment of multiple adsorption sites but also may hinder some ligand binding sites, leading to a decrease in the maximum capacity. However, in the present work, the interest of this model application is to understand how the steric factor changes in the presence of high ionic strengths, this will be done in a future work and with the application of *Equation (24)*.

4.5.Preferential interaction analysis

Using the model developed by *Perkins et al.* [111], the number of water molecules (Δv_1) and salt ions ($\Delta v_+ + \Delta v_-$) accompanying the adsorption of BSA onto *Toyopearl NH2-750F* were determined. The retention factor was correlated with sodium chloride molality (*Equation (43*)), using a non-linear least squares regression analysis with Table Curve 2D employing the Marquardt–Levenberg method (the data used to calculate *g* can be found in *Appendix-Figure 25)*. The results shown in *Table 6*, demonstrate that the number of ions and water molecules released are in the same order of magnitude as the ones obtained by *Pinto et al.* for BSA adsorption onto a polyethylenimine ligand[124].

Comparing our studied conditions (*Table 6*), we can see that at pH 8.0 the number of water molecules and salt ions removed from the protein and ligand are highest when compared to the

values obtained at pH 6.0. One possible explanation is that the electrical double layer thickness surrounding the protein's surface is greater at pH 8.0 due to the higher effective charge causing a long-range ordering of water dipoles and ions. Thus, it seems reasonable to suggest that a higher volume of interphase water and ions needs to be displaced for the adsorption occurs. Another possible explanation may be related with the number of binding sites established between the protein-ligand. As shown with SDM and Yamamoto's approach, at pH 8.0 more binding points are stablished, so is intuitive to think, according to the adsorption events reported in chapter 1.5, that more salt ions and water molecules are displaced as more binding sites are established.

Table 6 - Estimate of water molecules and salt ions released from adsorption of BSA onto Toyopearl NH2-750F using as modulator NaCl at pH 6.0 and 8.0.

pH	Temperature (K)	$n(\Delta v_1)/(m_1/g)$ (Kg.mol^{-1})	$-(\Delta v_+ + \Delta v_-)/g$ (mol.mol^{-1})	R	Δv_1 (mol.mol^{-1})	$(\Delta v_+ + \Delta v_-)$ (mol.mol^{-1})
6	298.15	4.1908	8.7735	0.9979	126.40	9.52
8	298.15	7.7285	15.8283	0.9965	233.10	17.19

4.6.Zeta Potential measurements of STC

The zeta potential of *Toyopearl NH2-750F* were measured using two different electrolytes solutions: 20 mM Tris-HCl at pH 8.0 and 20 mM Bis-tris at pH 6.0. To identify the optimum resin concentration to measure the zeta potential, five/six resin concentration were tested and the results are presented in *Table 7*.

Table 7 - Zeta potential measurement at different Toyopearl NH2-750F concentrations and with two different pH.

	pH	[Resin] (µl resin/ml buffer)						
		0	10	15	20	25	37.5	50
Zeta potential (mV)	6.0	-4,4±0,8	17.8±1.5	---	18.6±1.0	30.1±0.5	41.5±0.2	40.7±0.4
	8.0	-9.5±1.0	8.5±0.6	10.1±1.3	14.4±1.2	18.3±1.4	28.8±2.1	30.9±2.6

It is observed that, at both pH, zeta potential values have a linear growth up to the concentration of 25 µl resin.ml^{-1} buffer, reaching a plateau at 37.5 µl resin.ml^{-1} buffer. The value of the plateau was considered the actual value and, as expected, demonstrated to be lower at pH 8.0 due to the proximity to the pK_a (8.5) described by the supplier[50].

4.7. Microcalorimetric data

FMC studies were performed to better understand the adsorption mechanism of BSA onto the salt tolerant support *Toyopearl NH2-750F*. In this work, experiments were conducted under different pHs (6.0 and 8.0), salt concentrations (0; 150 and 300 mM NaCl) and three different concentrations of injected protein (20.0; 40.0 and 60.0 $mg.ml^{-1}$), maintaining constant the injection loop of 100 µl. The different pHs were chosen considering the *Toyopearl NH2-750F* pK_a (pK_a=8.5) and BSA isoelectric point (pI≈4.7). Results can be found at *Table 8, Figures 17,18 19 and 20.*

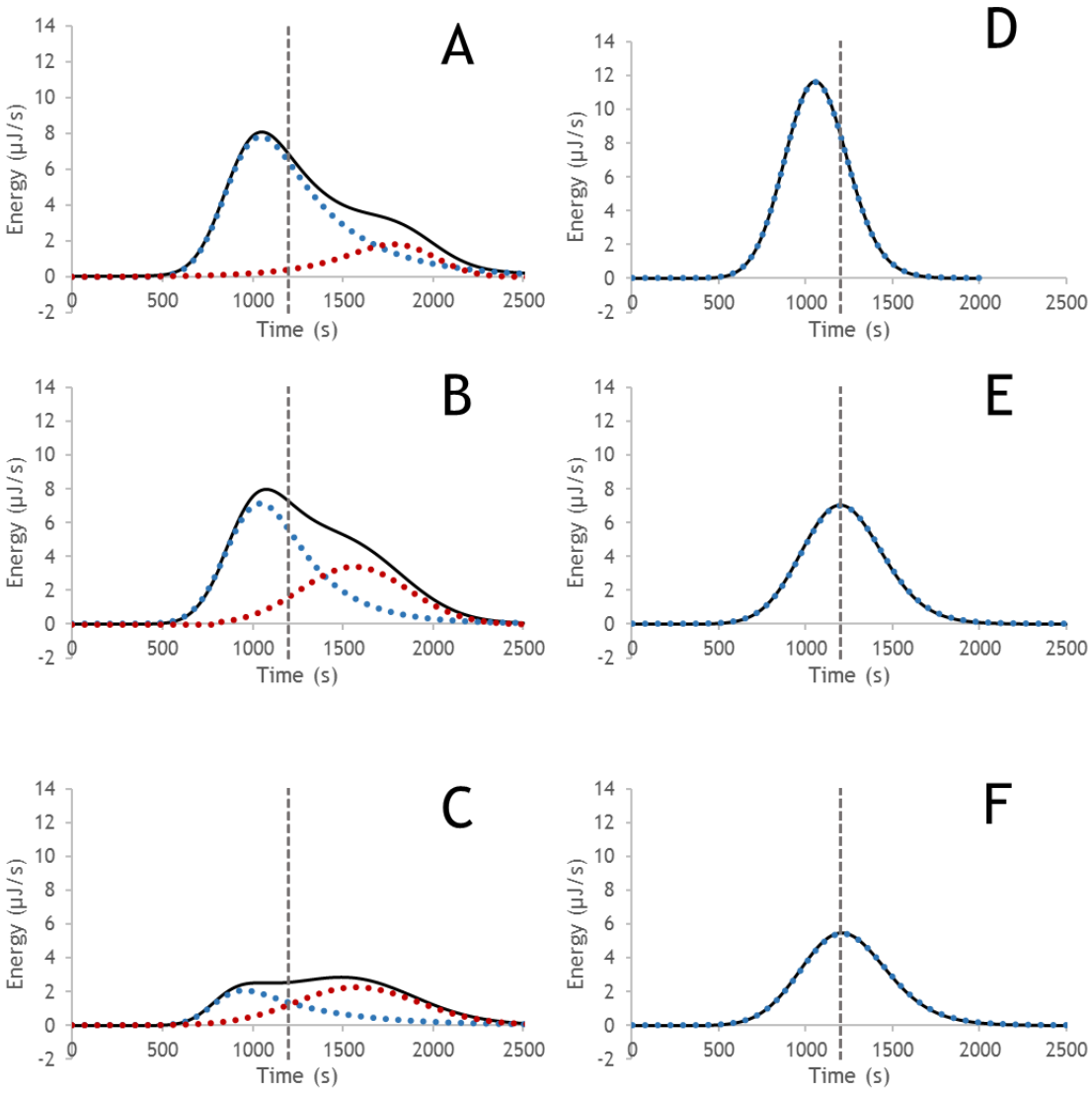

Figure 17 - PeakFit de-convolution of thermograms obtained for BSA adsorption onto Toyopearl NH2-750F at two different pHs, in absence and in presence of 150 mM and 300mM NaCl. Injection loop: 100 µl. BSA concentration: 20 $mg.ml^{-1}$. Mobile phase flow-rate: 1.5 $ml.h^{-1}$. (A) 20 mM Bis-tris, pH 6.0, (B) 20 mM Bis-tris, 150 mM NaCl, pH 6.0, (C) 20 mM Bis-tris, 300 mM NaCl, pH 6.0, (D) 20 mM Tris-HCl, pH 8.0, (E) 20 mM Tris-HCl, 150 mM NaCl, pH 8.0, (F) 20 mM Tris-HCl, 300 mM NaCl, pH 8.0. Curves showed are for total peak fit (black line) and peaks resulting from de-convolution (first exothermic peaks - blue dotted lines, second exothermic peaks - red dotted lines). Vertical dashed lines represent the time where the protein-containing plug of solution is replaced with protein-free mobile phase.

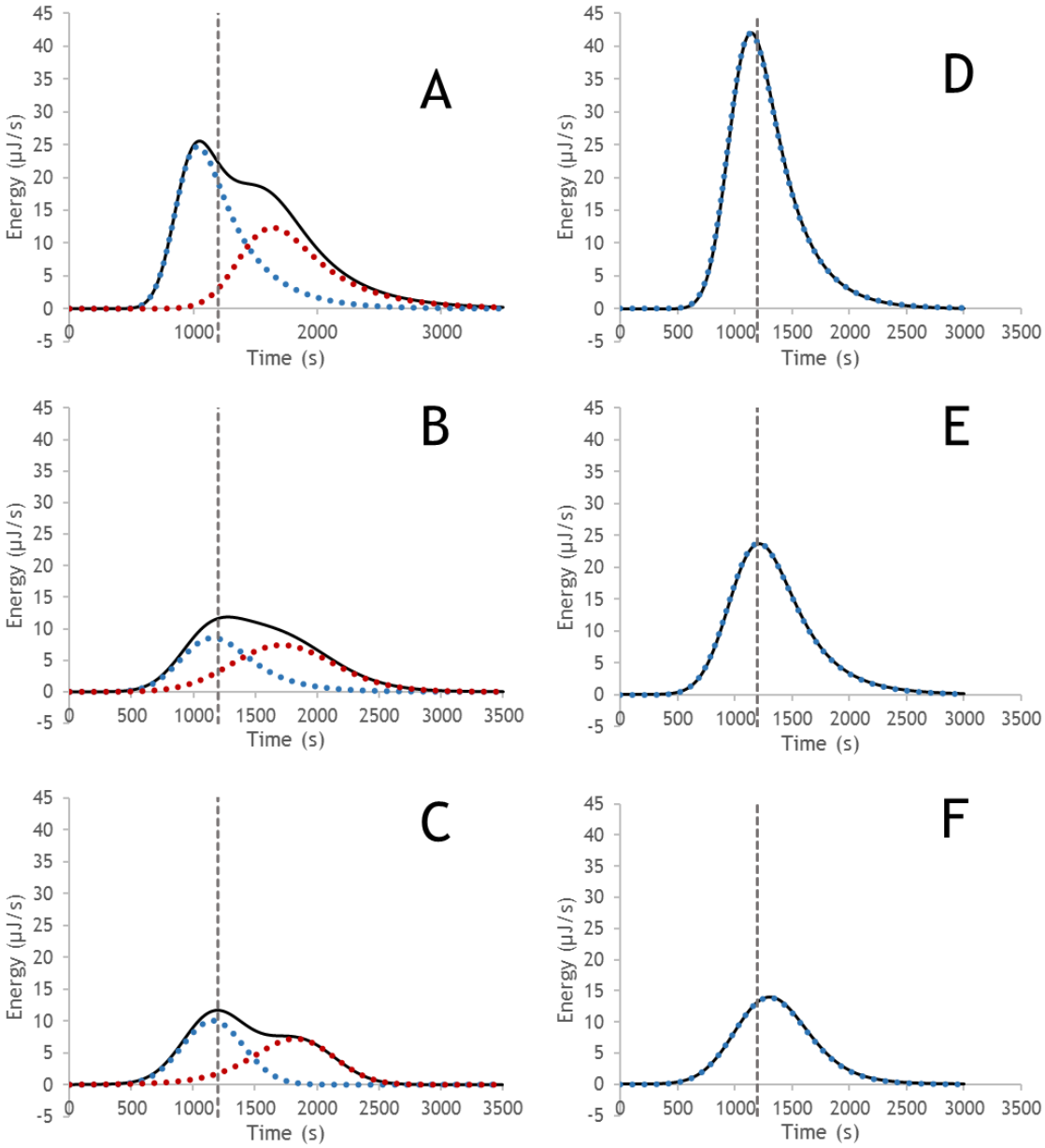

Figure 18 - PeakFit de-convolution of thermograms obtained for BSA adsorption onto Toyopearl NH2-750F at two different pHs, in absence and in presence of 150 mM and 300mM NaCl. Injection loop: 100 µl. BSA concentration: 40 mg.ml^{-1}. Mobile phase flow-rate: 1.5 ml.h^{-1}. (A) 20 mM Bis-tris, pH 6.0, (B) 20 mM Bis-tris, 150 mM NaCl, pH 6.0, (C) 20 mM Bis-tris, 300 mM NaCl, pH 6.0, (D) 20 mM Tris-HCl, pH 8.0, (E) 20 mM Tris-HCl, 150 mM NaCl, pH 8.0, (F) 20 mM Tris-HCl, 300 mM NaCl, pH 8.0. Curves showed are for total peak fit (black line) and peaks resulting from de-convolution (first exothermic peaks - blue dotted lines, second exothermic peaks - red dotted lines). Vertical dashed lines represent the time where the protein-containing plug of solution is replaced with protein-free mobile phase.

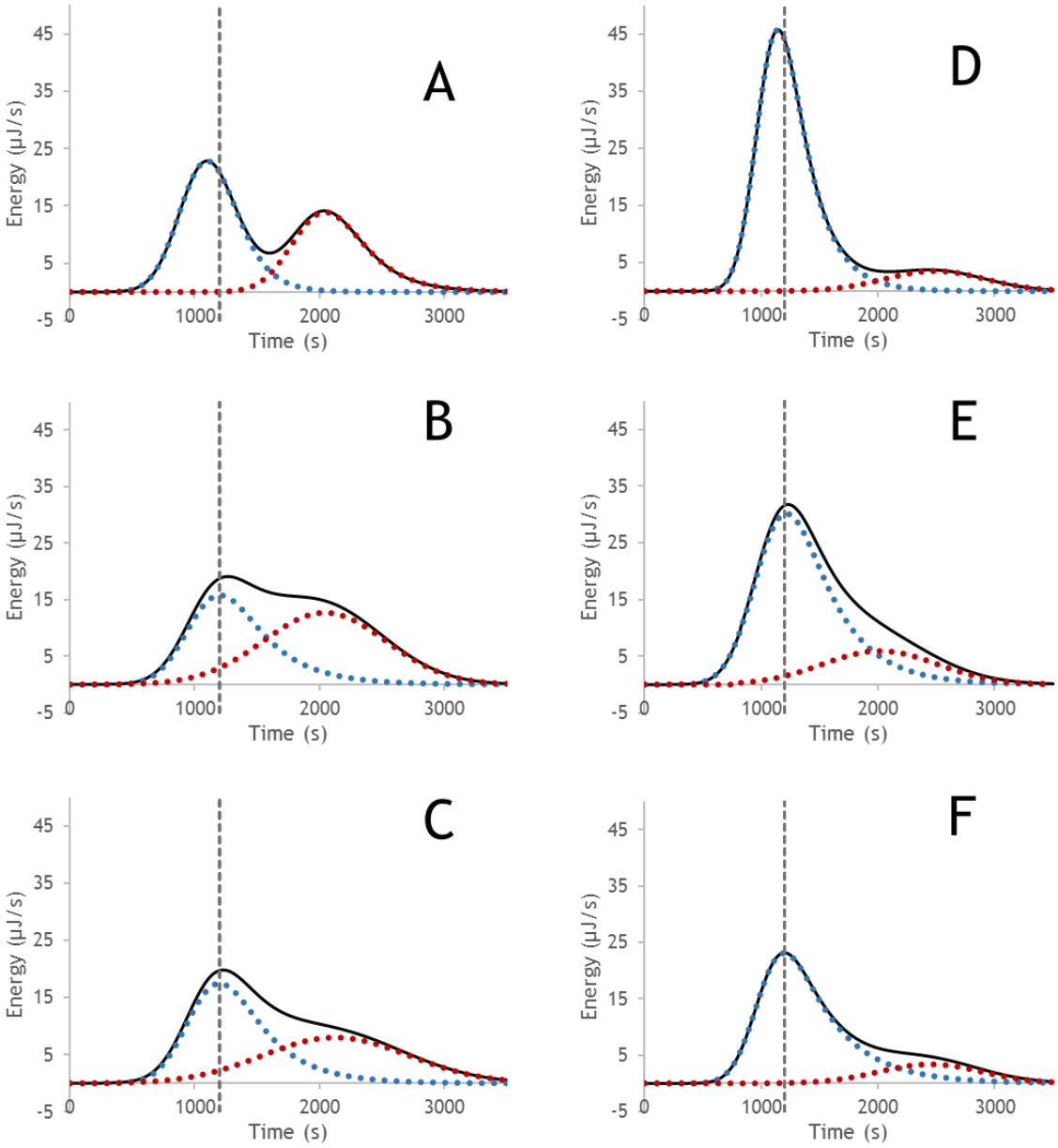

Figure 19 - PeakFit de-convolution of thermograms obtained for BSA adsorption onto Toyopearl NH2-750F at two different pHs, in absence and in presence of 150 mM and 300mM NaCl. Injection loop: 100 µl. BSA concentration: 60 mg.ml^{-1}. Mobile phase flow-rate: 1.5 ml.h^{-1}. (A) 20 mM Bis-tris, pH 6.0, (B) 20 mM Bis-tris, 150 mM NaCl, pH 6.0, (C) 20 mM Bis-tris, 300 mM NaCl, pH 6.0, (D) 20 mM Tris-HCl, pH 8.0, (E) 20 mM Tris-HCl, 150 mM NaCl, pH 8.0, (F) 20 mM Tris-HCl, 300 mM NaCl, pH 8.0. Curves showed are for total peak fit (black line) and peaks resulting from de-convolution (first exothermic peaks - blue dotted lines, second exothermic peaks - red dotted lines). Vertical dashed lines represent the time where the protein-containing plug of solution is replaced with protein-free mobile phase.

Table 8 - Heat of adsorption for BSA onto Toyopearl NH2-750F resin considering a sample loop and adsorbent volumes of 100 µl and 171 µl, respectively. All experiments were performed using a flow-rate of 1.5 ml/h^{-1}. Enthalpies were determined from the de-convoluted thermograms by PeakFit software. Results are displayed as mean ± STDV.

Buffer	pH	Injected concentration (mg.ml^{-1})	Injected mass (mg)	[NaCl] mM	Surface concentration (mg BSA.ml^{-1}.resin)	Flowthrough %	Exothermic I Normalized by the injected mass ΔH_I (mJ.mg^{-1} BSA)	Exothermic II Normalized by the adsorbed mass ΔH_{II} (mJ.mg^{-1} BSA)	ΔH_{Total} (mJ.mg^{-1} BSA)
Bis-tris	6	20	1.92	0	11.25	0	-2.44 ±0.25	-0.63±0.00	-3,07±0.25
			2.20	150	12.78	0	-2.19±0.05	-1.37±0.08	-3,56±0.13
			1.98	300	9.90	15	-0.77±0.06	-1.26±0.10	-2,03±0.16
		40	4.06	0	23.35	2	-3.80±0.06	-2.80±0.08	-6,6±0.14
			4.36	150	18.88	26	-1.48±0.00	-2.33±0.11	-3,81±0.11
			4.13	300	9.69	60	-1.59±0.09	-3.61±0.26	-5,2±0.35
		60	6.07	0	35.07	1	-2.13±0.09	-1.81±0.08	-3,94±0.17
			6.10	150	21.02	41	-2.18±0.10	-4.53±0.23	-6,71±0.33
			5.64	300	10.96	67	-2.35±0.23	-7.23±1.37	-9,58±1.6
Tris-HCl	8	20	2.12	0	12.38	0	-2.49±0.01	0.00	-2,49±0.01
			1.99	150	11.60	0	-2.19±0.07	0.00	-2,19±0.07
			1.85	300	10.81	0	-1.86±0.00	0.00	-1,86±0.00
		40	4.19	0	24.49	0	-6.16±0.19	0.00	-6,16±0.19
			4.27	150	24.96	0	-4.40±0.04	0.00	-4,4±0.04
			4.11	300	14.89	38	-2.55±0.22	0.00	-2,55±0.22
		60	5.78	0	33.81	0	-4.13±0.15	-0.50±0.14	-4,63±0.29
			6.14	150	22.46	37	-3.72±0.03	-1.68±0.21	-5,4±0.24
			5.68	300	13.80	59	-3.56±0.08	-1.80±0.02	-5,36±0.1

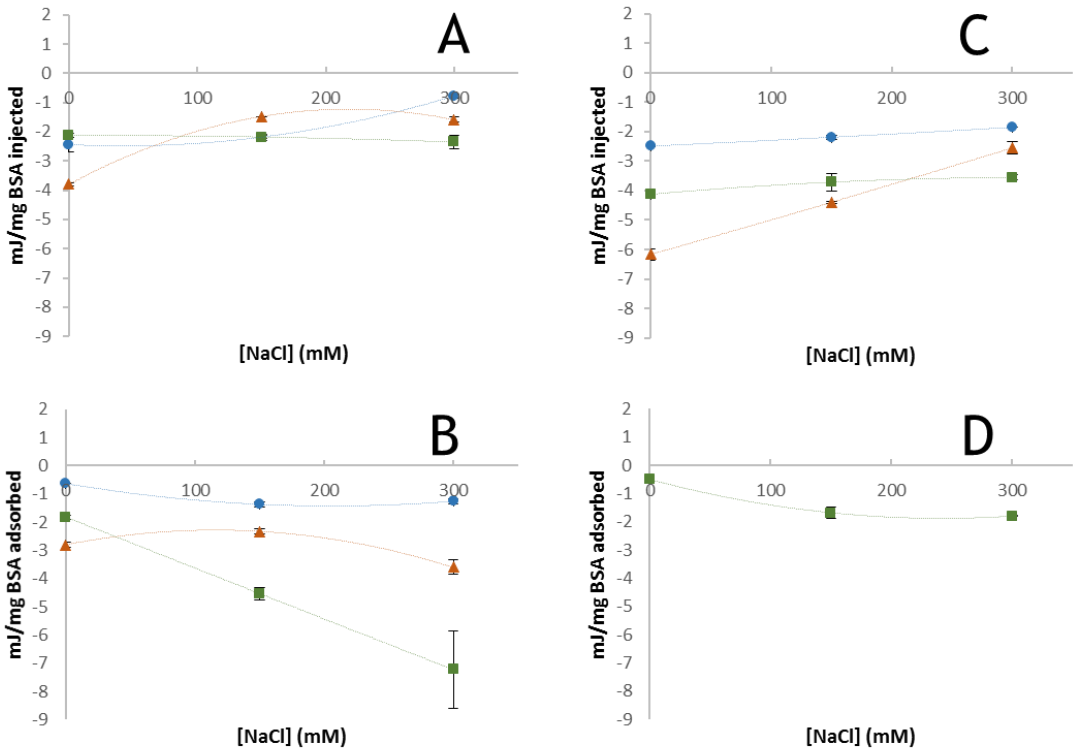

Figure 20 - Energy for BSA adsorption onto Toyopearl NH2-750F as function of NaCl concentration. (A) Enthalpy of first exothermic peak normalized by the injected mass of BSA at 20 mM Bis-tris pH 6.0; (B) Enthalpy of second exothermic peak normalized by the adsorbed mass of BSA at 20 mM Bis-tris pH 6.0; (C) Enthalpy of first exothermic peak normalized by the injected mass of BSA at 20 mM Tris-HCl pH 8.0; Enthalpy of second exothermic peak normalized by the adsorbed mass of BSA at 20 mM Tris-HCl pH 8.0. (●) 20 mg.ml^{-1} of injected BSA; (▲) 40 mg.ml^{-1} of injected BSA; (■) 60 mg.ml^{-1} of injected BSA.

As expected for ion-exchange interactions, net enthalpy of adsorption showed that BSA adsorption onto the salt-tolerant resin is enthalpically driven ($\Delta H_{total}<0$) (*Table 8*). According to Ross et al.[137], electrostatic interactions have negative ΔH_{Total}, therefore, are considered to be one of the largest contributors to total enthalpy magnitude of the adsorption process. However, this does not mean that protein adsorption in IEXC is solely driven by enthalpic contributions, as observed by prior studies[70,75,138].

Distinct peaks were observed in the thermograms for every condition tested (*Figures 17, 18 and 19*), suggesting the presence of different events during adsorption. These events result in heat signals that occur simultaneously, overlapped or in sequence depending on the conditions. In order to more clearly evaluate the magnitude and chronology of thermal events during adsorption, peak deconvolution was performed using PeakFit Software as already done by previous authors[67,73].

For a good interpretation of the heat signals, in *Table 9* are presented the processes believed to be responsible for enthalpy changes during adsorption in a chromatographic system.

Table 9 - Summary of events responsible for enthalpy changes during adsorption in a chromatographic system[75].

Process	ΔH
1- Dehydration and removal of the protein and ligand electrical double layer [75]	Positive
2- Van der Waals interactions	Negative
3- Hydrogen bonding	Negative
4- Electrostatic interaction[137]	Negative
5- Protein conformational changes	Positive
6- Reorientation and rotation in IEX solid phase	Positive
7- Repulsive forces	Positive
8- Secondary adsorption	Negative
9- Surface transport mechanisms	Negative

As a starting point, it is important to observe the thermograms previously obtained by our research group, which compares BSA adsorption onto three anion exchange supports (*Figure 21*). Note that the profile of BSA adsorption thermograms is characterized by an initial endothermic event followed by an exothermic one. Considering the mechanism proposed by Yamamoto and co-workers[74] mentioned in the first chapter, Cardoso[1] hypothesized that the first endothermic event was due to sub-process 1. and 6., described in *Table* 9, and the exothermic event due to the 4., 8. and 9., depending if occurs before or after the protein-containing solution (called *protein plug*) being replaced by protein-free mobile phase.

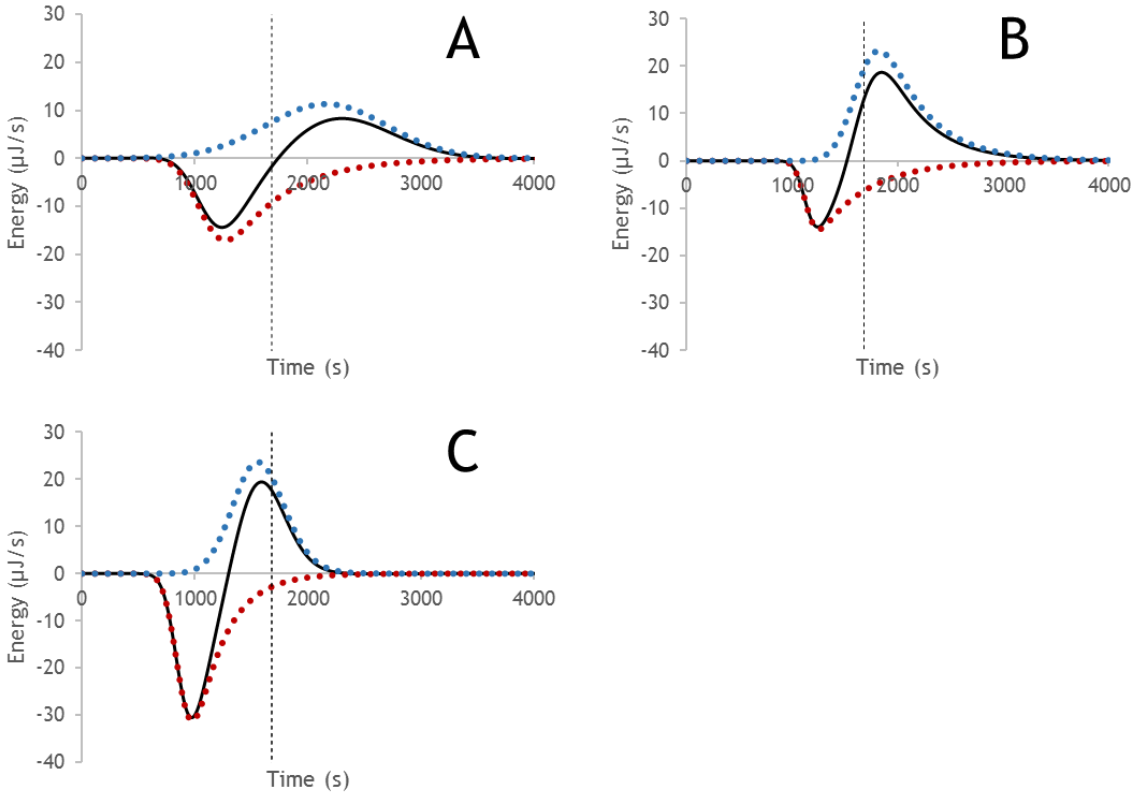

Figure 21- PeakFit de-convolution of thermograms obtained for BSA adsorption onto (A) TSKgel SuperQ 5PW; (B) Toyopearl GigaCap Q-650M; (C) Toyopearl DEAE-650mM at pH 9.0, in absence of salt. Injection loop: 240 µl. BSA concentration: 40 mg.ml^{-1}. Mobile phase flow-rate: 1.5 ml.h^{-1}. Curves showed are for total peak fit (black line) and peaks resulting from de-convolution (exothermic peak - blue dotted lines, endothermic peak - red dotted lines). Vertical dashed lines represent the time where the protein-containing plug of solution is replaced with protein-free mobile phase[1].

Nevertheless, the thermograms obtained for the salt-tolerant anion-exchange support revealed a different profile (*Figure 17, 18 and 19*). In *Figure 17* are represented the thermograms resulting from the conditions where no flowthrough was observed, with the exception of the result at pH 6.0 in presence of 300mM salt, which shows a flowthrough < 15% (*Figure 17C*). In a first instance observation, it is clear that the initial endothermic event observed on the thermograms from BSA adsorption onto the anion exchange supports (*Figure 21*) is not present on the thermograms for the salt tolerant anion exchanger (*Figure 17*). This leads us to believe that the energy release associated with the protein-ligand interaction is much higher than the energy required for removing the protein and ligands electrical double layer.

Furthermore, pH and salt presence clearly modulates the mechanisms involved in the adsorption process under study. From pH 6.0 (*Figure 17A; 17B; 17C*) to pH 8.0 (*Figure 17D; 17E; 17F*) the second overlapped exothermic peak disappears. Since the second exothermic peak, at pH 6.0, occurs after *protein plug* and no flowthrough was observed, the second exothermic peak is not the result of multi-layer formation[70]. Thus, this event could be related with secondary adsorption of BSA molecules as observed by *Katiyar et. al, 2010*[67] or even with surface transport phenomena[13]. After the primary adsorption, the BSA molecule, as a *soft*

protein, may reorganize itself creating new available binding sites on the protein surface, which can result in a posterior interaction with the chromatographic support. Additionally, polyamines are flexible hydrocarbon chains[139], thus, as described by *Yu et, al. 2015*[13], flexible polymers may promote chain delivery phenomena, which consists in the delivery of an adsorbed molecule from a flexible grafted chain to a close enough neighbouring chain.

On the other hand, the single exothermic peak observed at pH 8.0, leads to believe that the adsorption of BSA acquire a highly stable interaction with the support surface, hindering the possibility to undergo posterior secondary adsorption events. Moreover, thermodynamic studies with affinity chromatographic supports, which are currently being developed in our group, also revealed the presence of single exothermic events. It is described that affinity chromatography usually involves multiple specific interactions[32], strengthening the idea that at pH 8.0, this specificity stabilizes the adsorbed protein on the support surface. As previously referred, at pH 8.0, not all the amines are protonated, so the possibility to establish electrostatic interaction combined with hydrogen bonding may be the explanation for specificity. Additionally, the flexible structure of BSA at pH 8.0 may also contribute to its stabilization on the surface.

It is also possible to observe that in presence of salt, the exothermic peak maximum is delayed *(Figure 17*). One possible explanation is the decrease of the distribution coefficient. *Jungbauer et, al.* in 1996[107], postulate that in ion-exchange chromatography, the distribution coefficient is strongly influenced by the protein and salt concentration, being reduced with their increase. This results in slower movement of BSA through the bed, explaining the shift of the timing for exothermic peak at higher salt concentrations.

Observing the influence of pH on adsorption energy, we can conclude that the heat of the first exothermic event is significantly higher at pH 8.0 compared to pH 6.0, mainly at high injected concentrations (*Table 8* and *Figure 20)*. These results are consistent with those observed in the retention studies, where it was concluded that at pH 8.0, there is a higher number of binding points established at pH 6.0.

In presence of salt, considerable changes on thermograms profile were also detected. At pH 8.0 with no flowthough (*Table 8 and* Figure 20), is observed a decrease of about 12 % and 25 % in the net heat of adsorption when is added 150 mM and 300 mM NaCl, respectively. This tendency is similar, but more marked for the first exothermic event obtained at pH 6.0, where a decrease of about 11 % and 68 % in presence of respectively 150 mM and 300 mM NaCl is observed. This more marked decrease of energy in the present of salt at pH 6.0 is coherent with the idea that all ligand amines are protonated (showing a more electrostatic profile). The energy decrease behavior is probably due to the salt shielding effect towards BSA and polyamine ligands, that weakens the electrostatic attractive forces, which led to a decrease of the heat signal[74,127]. On the other hand, the stablishing of hydrogen bonding combined with electrostatic interactions at pH 8.0, decrease the salt screening effect, resulting in a more salt tolerant

profile. Additionally, at pH 6.0, the second exothermic peak increases in presence of salt. The results lead us to believe that as weaker is the initial adsorption (due to the increasing of salt concentration); greater will be the amount of BSA molecules that suffer reorganization on the surface.

To understand the influence of protein surface concentrations onto the adsorption mechanism, under the same conditions of pH and NaCl concentration, were also loaded higher BSA concentrations to the column. As showed in *Table 8*, when the injected protein concentration is raised from 20 $mg.ml^{-1}$ to 40 $mg.ml^{-1}$ and 60 $mg.ml^{-1}$, we left the linear zone of the isotherm and began to obtain significant percentages of flowthrough in presence of salt. In previous FMC thermodynamic studies[49,68,121,124] enthalpy values were normalized for the protein surface concentration. Once enthalpy is an extensive property, to characterize a process, should be transformed in an intensive property that is independent of the amount of substance in the sample. However, recently it was detected that even when 100 % of the injected protein comes out of the column (100 % flowthought) an energetic contribution is observed, as can be seen from thermograms in *Appendix-Figure 26*. Thus, care should be taken how normalization is made. Based on the previous interpretation of thermogram peaks the energy events that occur before the protein plug were normalized for the total amount of BSA injected, and the events occurring after the protein plug were normalized by the protein adsorbed mass, because only the protein that remain on the support could suffer surface reorganization.

For the 40 $mg.ml^{-1}$ of injected protein (*Figure 18)*, were observed similar thermogram profiles to those obtained with 20 $mg.ml^{-1}$ *(Figure 17)*. The first exothermic peak at pH 6.0 and the single exothermic peak at pH 8.0, decreases with increasing salt concentration and the second exothermic event at pH 6.0 increase with increasing of salt concentration. Moreover, also here the delay in the first peak became more noticeable at both pHs with the increase of salt concentration and between protein injection concentration. Peak maximum delay is higher at 40 $mg.ml^{-1}$ of injected protein when compared with 20 $mg.ml^{-1}$ supporting the idea of protein distribution coefficient influence[67,107].

On the other hand, the results obtained for 60 $mg.ml^{-1}$ of injected protein demonstrated some peak profile changes. In the absence of salt at pH 6.0, the two exothermic peaks that were previously overlapped, start to show a sequential profile (*Figure 19A*). A possible explanation is the small number of available ligands to establish secondary interaction with the protein. This hindrance to establishing new interactions, even after the protein has already undergone reorganizations, is reflected in the timing at which the second peak appears. In addition, it is possible that there is a masked endothermic event between the two exothermic peaks (*Figure 19A*). It is well argued by some authors[67,140] that structure rearrangements of proteins are from

endothermic nature, so before the second exothermic event occur it is possible that this sub process has a significant influence that cause a delay of the second exothermic event.

Likewise, for 60 $mg.ml^{-1}$ of injected protein at pH 8.0, a new exothermic event appears as observed in *Figure 19D;19E;19F*, however, the second exothermic peak is overlapped with the first in the presence of salt and sequential in absent of salt. This profile change lead us to believe that when a great amount of proteins reaches the support at the same time, not all BSA molecules can acquire the multiple interaction previously described (electrostatic and hydrogen bonding). This hindrance leads the molecules that had a poor adsorption to initiate surface reorganizations and subsequent secondary adsorption as observed at pH 6.0. Once more, in the present of salt, the energy of the first exothermic event decreases and the energy of the second exothermic event increases.

Chapter V. Conclusion and Future work

This dissertation had the objective of studying the adsorption mechanisms underlying salt-tolerant chromatography. To achieve this, different complementary studies were performed with the aim of understanding the influence of factors such as pH and salt concentration on the adsorption mechanism of BSA onto the salt-tolerant Toyopearl NH2-750F. Being the focus of this work, flow microcalorimetry displayed once more the capability of a valuable insight on the overall adsorption process. Furthermore, retention studies also prove to be an important tool to help the interpretation of the thermodynamic data.

The results obtained by flow microcalorimetry demonstrated that the driving forces of the adsorption process on salt tolerant supports are different from the ones present when using traditional ionic supports such as Toyopearl DEAE 650M, Toyopearl GigaCap Q-650M and TSKgel SuperQ 5PW. As previously demonstrated by our research group for traditional IEX supports thermograms include an initial endothermic event, related to the desolvation process, followed by an exothermic event associated with the interaction between the protein and the support. In the case of the analyzed salt-tolerant support, at pH 8.0 a single exothermic peak is observed conversely to pH 6.0 where two exothermic events are present. Under this condition the second event, occurs after the protein being completely replaced by the buffer solution inside the column. This timing of the second exothermic event, leads us to believe that it is due to secondary adsorption of the protein caused by its reorganization on the surface.

Additionally, it has also been concluded that at pH 6.0 in the presence of salt, the energy associated with this second event increases, unlike the first exothermic event, where the increase of salt causes a decrease in the energy released. Salt has the property of shielding the electrostatic interactions and weaken the adsorption, so it is intuitive to think that the higher is the salt concentration in the mobile phase, the weaker will be the initial interaction of the protein-support (decrease of the first exothermic peak), and greater the contributions of secondary adsorption events. However, at pH 8.0 it is not observed this second event, indicating that the protein acquires a preferential interaction on the support surface. This preferential interaction at pH 8.0 may be related to the establishment of hydrogen bonding in addition to the electrostatic interactions. At pH 8.0 not all the ligand amines are protonated, being available to establish hydrogen bonding that require a specific conformation of protein-ligand interaction (a single exothermic peak).

The models came to reinforce these hypothesis, at pH 8.0, BSA has a higher footprint on ligand (Steric mass action), establishing a greater number of protein-support interaction points (SD and Yamamoto model), and consequently, a greater removal of water molecules and ions of surface (Perkins analysis). This indicates that the protein adopts a specific and highly stable adsorption (hydrogen bonding and electrostatic interactions), which makes it difficult to be

disrupt by salt; hence, a higher salt tolerance at pH 8.0 than pH 6.0 was observed (adsorption isotherms).

Finally, in the injections at pH 8.0, but close to the saturation limit of the column, the thermogram present a second exothermic event similar to those obtained at pH 6.0. These results reinforce the idea that the surface BSA footprint is bigger at pH 8.0. Because of the large number of BSA molecules are flowing into the support at the same time, competition for the binding sites becomes very significant and not all molecules can adopt a preferential adsorption interaction, being then subject to suffer phenomena similar to those described at pH 6.0.

All these results confirm that, for a more consistent understanding of adsorption mechanisms, the use of flow microcalorimetry has a great interest in the systematic study of the different chromatographic supports. In addition, the modeling together with molecular structure studies have proved to be important tools for elucidating the complex process of protein adsorption. Theoretical, semi-empirical and computational simulations related to the adsorption mechanism, especially of molecules with high molecular weight, are starting to account these enthalpy events with the ultimate goal of developing not only faster and more efficient chromatographic supports, but also to simplify and reduce the costs associated with the biotechnological production of biomolecules with a pharmaceutical interest.

For future work, further experiments should be conducted with the studied salt-tolerant support but this time, with other molecules of pharmaceutical interest like virus-like particles or monoclonal antibodies. In addition, due to the dispersion of information regarding retention studies in the literature, it would be very interesting to carry out retention studies with two biomolecules, e.g. BSA and mAb, on various commercial chromatographic supports, to systematize and compare their differences.

References

1. Cardoso, J. Master's Thesis: Understanding ion exchange chromatography adsorption mechanisms under different conditions. (University of Beira Interior, 2016).
2. Blagbrough, I. S., Metwally, A. A. & Geall, A. J. in *Polyamines: Methods and Protocols, Methods in Molecular Biology* **720,** 493–503 (Springer Science, 2011).
3. Carta, G. & Jungbauer, A. *Protein Chromatography Process Development and Scale-Up*. (WILEY-VCH, 2010).
4. Golan, D., Armstrong, E. & Armstrong, A. *Principles of pharmacology*. (Wolters Klluwer, 2015).
5. CDER/CBER & FDA. *Quality Considerations in Demonstrating Biosimilarity of a Therapeutic Protein Product to a Reference Product*. *Guidance for Industry* (2015).
6. Leader, B., Baca, Q. J. & Golan, D. E. Protein therapeutics: a summary and pharmacological classification. *Nat. Rev. Drug Discov.* **7,** 21–39 (2008).
7. Reichert, J. M. Trends in Development And Approval Times For New Therapeutics In The United States. *Nat. Rev. Drug Discov.* **2,** 695–702 (2003).
8. Ecker, D. M., Jones, S. D. & Levine, H. L. The Therapeutic Monoclonal Antibody Market. *MAbs* **7,** 37–41 (2015).
9. Reichert, J. M., Rosensweig, C. J., Faden, L. B. & Dewitz, M. C. Monoclonal antibody successes in the clinic. *Nat. Biotechnol.* **23,** 1073–1078 (2005).
10. Komar, A. A. The Art of Gene Redesign and Recombinant Protein Production : Approaches and Perspectives. *Top. Med. Chem.* **21,** 161–177 (2016).
11. Alberts, B. *et al. Molecular Biology of the Cell. Garland Science* **6,** (2014).
12. Campbell, M. K. & Farrell, S. O. Biochemistry. (2013).
13. Yu, L., Zhang, L. & Sun, Y. Protein behavior at surfaces : Orientation , conformational transitions and transport. *J. Chromatogr. A* **1382,** 118–134 (2015).
14. Ballmoos, C., Wiedenmann, A. & Dimroth, P. Essentials for ATP synthesis by F1F0 ATP synthases. *Annu. Rev. Biochem.* **78,** 649–672 (2009).
15. Kastner, M. *Protein liquid chromatography*. (Elsevier B.V., 2000).
16. Champagne, J., Balluet, G., Gantier, R. & Toueille, M. 'Salt tolerant' anion exchange chromatography for direct capture of an acidic protein from CHO cell culture. *Protein Expr. Purif.* **89,** 117–123 (2013).
17. Palomares, L., Estrada-Mondaca, S. & Ramírez, O. in *Recombinant Gene Expression* **267,** 15–51 (2004).

18. Jayapal, K., Wlaschin, K., Hu, W. & Yap, G. Recombinant protein therapeutics from CHO cells-20 years and counting. *Chem. Eng. Prog.* **103,** 40–47 (2007).

19. Żerek, B. & Rózga, P. Recombinant Protein Therapeutics – The future is here. *Laborant* **4,** 34–37 (2012).

20. Sun, Y., Shi, Q., Zhang, L., Zhao, G. & Liu, F. in *Comprehensive Biotechnology* **1,** 665–679 (Elsevier B.V., 2011).

21. Li, J., Han, W. & Yu, Y. in *Protein Engineering - Technology and Application* 33–60 (InTech, 2013).

22. Jungbauer, A. Chromatographic media for bioseparation. *J. Chromatogr. A* **1065,** 3–12 (2005).

23. GE Healthcare. *Hydrophobic Interaction and Reversed Phase Chromatography: Principles and Methods*. (GE HealtCare Handbooks, 2012).

24. Müller, B. E. Properties and Characterization of High Capacity Resins for Biochromatography. *Chem. Eng. Technol.* **28,** 1295–1305 (2005).

25. Lenhoff, A. M. Protein adsorption and transport in polymer-functionalized ion-exchangers. *J. Chromatogr. A* **1218,** 8748–8759 (2011).

26. Majorek, K. A. *et al*. Structural and immunologic characterization of bovine, horse, and rabbit serum albumins. *Mol. Immunol.* **52,** 174–182 (2012).

27. Protein Purification by Ion-Exchange Chromatography. Available at: http://www.reachdevices.com/Protein/ProteinPurification.html. (Accessed: 23rd September 2017)

28. GE Healthcare. *Multimodal Chromatography Handbook*. (GE HealtCare Handbooks, 2014).

29. Keen, W., Freed, A. S., Holstein, M. A., Mccallum, S. A. & Cramer, S. M. Evaluation of protein adsorption and preferred binding regions in multimodal chromatography using NMR. **107,** 16811–16816 (2010).

30. Pinto, I. F., Aires-Barros, M. R. & Azevedo, A. M. Multimodal chromatography: debottlenecking the downstream processing of monoclonal antibodies. *Pharm. Bioprocess.* **3,** 263–279 (2015).

31. Zhao, G., Dong, X. Y. & Sun, Y. Ligands for mixed-mode protein chromatography: Principles, characteristics and design. *J. Biotechnol.* **144,** 3–11 (2009).

32. Roque, A. C. A., Silva, C. S. O. & Taipa, M. Â. Affinity-based methodologies and ligands for antibody purification: Advances and perspectives. *J. Chromatogr. A* **1160,** 44–55 (2007).

33. Hober, S., Nord, K. & Linhult, M. Protein A chromatography for antibody purification. *J.*

Chromatogr. B Anal. Technol. Biomed. Life Sci. **848,** 40–47 (2007).

34. Ambat, R. *et al.* Development of an acidic / neutral antibody flow-through polishing step using salt- tolerant anion exchange chromatography. **3,** 477–487 (2015).

35. Yoshimoto, N., Itoh, D., Isakari, Y., Podgornik, A. & Yamamoto, S. Salt tolerant chromatography provides salt tolerance and a better selectivity for protein monomer separations. *Biotechnol. J.* **10,** 1929–1934 (2015).

36. Riordan, W. *et al.* Design of salt-tolerant membrane adsorbers for viral clearance. *Biotechnol. Bioeng.* **103,** 920–929 (2009).

37. Kim, U. & Kuga, S. Ion-exchange separation of proteins by polyallylamine-grafted cellulose gel. *J. Chromatogr. A* **955,** 191–196 (2002).

38. Kim, U. & Kuga, S. Polyallylamine-grafted cellulose gel as high-capacity. *J. Chromatogr. A* **946,** 283–289 (2002).

39. Johansson, B. *et al.* Preparation and characterization of prototypes for multi-modal separation media aimed for capture of negatively charged biomolecules at high salt conditions. *J. Chromatogr. A* **1016,** 21–33 (2003).

40. Thomas, T. J., Thomas, T. & Carpentier, R. Polyamine Analogues Bind Human Serum Albumin. *Biomacromolecules* **8,** 3177–3183 (2007).

41. Chanphai, P., Thomas, T. J. & Tajmir-riahi, H. A. International Journal of Biological Macromolecules Conjugation of biogenic and synthetic polyamines with serum proteins : A comprehensive review. *Int. J. Biol. Macromol.* **92,** 515–522 (2016).

42. Liu, J., Wang, W., Wu, H., Gong, X. & Moriguchi, T. Polyamines function in stress tolerance : from synthesis to regulation. *Front. Plant Sci.* **6:827,** 1–10 (2015).

43. Vajda, J. *et al.* Mono- and polyprotic buffer systems in anion exchange chromatography of influenza virus particles. *J. Chromatogr. A* **1448,** 73–80 (2016).

44. Sudhakar, K., Erecinska, M. & Vanderkooi, J. M. Interaction of polyamines with the Ca2+ - binding protein parvalbumin. *Eur. j. Biochem.* **230,** 498–502 (1995).

45. Ouameur, A. *et al.* Effects of Organic and Inorganic Polyamine Cations on the Structure of Human. *Biopolymers* **73,** 503–509 (2004).

46. Fernández, C. *et al.* NMR of a-synuclein–polyamine complexes elucidates the mechanism and kinetics of induced aggregation. *EMBO J.* **23,** 2039–2046 (2004).

47. Kim, J. Investigation of the Interactions between Biomolecules and Mesoporous Inorganic Materials in Biomolecule Immobilization for Bioseparation and Biocatalysis. (University of Cincinnati, 2011).

48. Dubeau, S., Bourassa, P., Thomas, T. & Tajmir-Tiahi, H. Biogenic and Synthetic Polyamines Bind Bovine Serum Albumin. *Biomacromolecules.* **11,** 1507–1515 (2011).

49. Dias-cabral, A. C., Queiroz, J. A. & Pinto, N. G. Effect of salts and temperature on the adsorption of bovine serum albumin on polypropylene glycol-Sepharose under linear and overloaded chromatographic conditions. *J. Chromatogr. A* **1018,** 137–153 (2003).

50. Tosoh Bioscience. *Toyopearl NH2-750F-Salt Tolerant Anion exchange resin*. (2014).

51. Roth, C. M., Unger, K. K. & Lenhoff, A. M. Mechanistic model of retention in protein ion-exchange chromatography. *J. Chromatogr. A* **726,** 45–56 (1996).

52. Ståhlberg, J. Retention models for ions in chromatography. *J. Chromatogr. A* **855,** 3–55 (1999).

53. Wu, D. & Walters, R. R. Effects of stationary phase ligand density on high- performance ion-exchange chromatography of proteins. *J. Chromatogr.* **598,** 7–13 (1992).

54. Lu, H. L., Lin, D. Q., Zhu, M. M. & Yao, S. J. Effects of ligand density and pore size on the adsorption of bovine IgG with DEAE ion-exchange resins. *J. Sep. Sci.* **35,** 2131–2137 (2012).

55. Deitcher, R. W., Rome, J. E., Gildea, P. A., Connell, J. P. O. & Fernandez, E. J. A new thermodynamic model describes the effects of ligand density and type , salt concentration and protein species in hydrophobic interaction chromatography. *J. Chromatogr. A* **1217,** 199–208 (2010).

56. Yuan, W. & Sun, Y. Effect of ionic capacity on dynamic adsorption behavior of protein in ion-exchange electrochromatography. *Sep. Purif. Technol.* **68,** 109–113 (2009).

57. Riordan, W. T., Heilmann, S. M., Brorson, K., Seshadri, K. & Etzel, M. R. Salt tolerant membrane adsorbers for robust impurity clearance. *Biotechnol. Prog.* **25,** 1695–1702 (2009).

58. Liu, Z., Wickramasinghe, S. R. & Qian, X. Membrane chromatography for protein purifications from ligand design to functionalization. *Sep. Sci. Technol.* 1–21 (2016).

59. Hanke, A. T. & Ottens, M. Purifying biopharmaceuticals: Knowledge-based chromatographic process development. *Trends Biotechnol.* **32,** 210–220 (2014).

60. Roach, P., Farrar, D. & Perry, C. C. Interpretation of Protein Adsorption : Surface-Induced Conformational Changes. *J. Am. Chem. Soc.* **127,** 8168–8173 (2005).

61. Brandes, N., Welzel, P. B., Werner, C. & Kroh, L. W. Adsorption-induced conformational changes of proteins onto ceramic particles : Differential scanning calorimetry and FTIR analysis. **299,** 56–69 (2006).

62. Ramsden, J. Puzzles and Paradoxes in Protein Adsorption. *Chem. Soc. Rev.* 73–78 (1992).

63. Angelo, J. M., Cvetkovic, A., Gantier, R. & Lenhoff, A. M. Characterization of cross-linked cellulosic ion-exchange adsorbents : 2 . Protein sorption and transport. *J. Chromatogr. A* **1438,** 100–112 (2016).

64. Ladbury, John; Doyle, M. *Biocalorimetry 2 - Applications of calorimetry in the biological sciences*. (WILEY-VCH, 2004).

65. Pinto, N. G. albumin under overloaded conditions using flow microcalorimetry. **865,** 111–122 (1999).

66. Groszek, A. J. Flow adsorption microcalorimetry. *Thermochim. Acta* **312,** 133–143 (1998).

67. Katiyar, A., Thiel, S. W., Guliants, V. V & Pinto, N. G. Investigation of the mechanism of protein adsorption on ordered mesoporous silica using flow microcalorimetry. *J. Chromatogr. A* **1217,** 1583–1588 (2010).

68. Esquibel-KIng, M., Dias-Cabral, A., Queiroz, J. & Pinto, N. G. Study of hydrophobic interaction adsorption of bovine serum albumin under overloaded conditions using flow microcalorimetry. *J. Chromatogr. A* **865,** 111–122 (1999).

69. Korfhagen, J., Dias-Cabral, A. C. & Thrash, M. E. Nonspecific Effects of Ion Exchange and Hydrophobic Interaction Adsorption Processes. *Sep. Sci. Technol.* **45,** 2039–2050 (2010).

70. Silva, G. L., Marques, F. S., Thrash Jr, M. E. & Dias-cabral, A. C. Enthalpy contributions to adsorption of highly charged lysozyme onto a cation-exchanger under linear and overloaded conditions. *J. Chromatogr. A* **1352,** 46–54 (2014).

71. Kim, J., Desch, R. J., Thiel, S. W., Guliants, V. V & Pinto, N. G. Energetics of lysozyme adsorption on mesostructured cellular foam silica : Effect of salt concentration. *J. Chromatogr. A* **1218,** 6697–6704 (2011).

72. Phillips, J. M. & Pinto, N. G. Calorimetric investigation of the adsorption of nitrogen bases and nucleosides on a hydrophobic interaction sorbent. *J. Chromatogr. A* **1036,** 79–86 (2004).

73. Aguilar, P. A., Twarda, A., Sousa, F. & Dias-cabral, A. C. Thermodynamic study of the interaction between linear plasmid deoxyribonucleic acid and an anion exchange support under linear and overloaded conditions. *J. Chromatogr. A* **1372,** 166–173 (2014).

74. Lin, F., Chen, C., Chen, W. & Yamamoto, S. Microcalorimetric studies of the interaction mechanisms between proteins and Q-Sepharose at pH near the isoelectric point (pI) Effects of NaCl concentration , pH value , and temperature. *J. Chromatogr. A* **912,** 281–289 (2001).

75. Lin, F., Chen, W. & Hearn, M. T. W. Thermodynamic analysis of the interaction between proteins and solid surfaces : application to liquid chromatography. *J. Mol. Recognit.* **15,** 55–93 (2002).

76. Liang, Y., Hilal, N., Langston, P. & Starov, V. Interaction forces between colloidal particles in liquid: Theory and experiment. *Adv. Colloid Interface Sci.* **134-135,** 151–

166 (2007).

77. Barbosa, L. R. S., Ortore, M. G., Spinozzi, F., Mariani, P. & Bernstorff, S. The Importance of Protein-Protein Interactions on the pH-Induced Conformational Changes of Bovine Serum Albumin : A Small-Angle X-Ray Scattering Study. *Biophysj* **98,** 147–157 (2010).

78. Lafayette, W. Effect of Surface Hydrophobicity on the Conformational Changes of Adsorbed Fibrinogen. *J. Colloid Interface Sci.* **144,** 271–281 (1991).

79. Yu, M. *et al.* Microcalorimetric study of adsorption and disassembling of virus-like particles on anion exchange chromatography media. *J. Chromatogr. A* **1388,** 195–206 (2015).

80. Grushka, E. & Grinberg, N. *Advances in Chromatography*. (CRC Press, 2009).

81. Norde, W. Driving Forces for Protein Adsorption at Solid Surfaces. *Macromol. Symp.* **103,** 5–18 (1996).

82. Wendell M. Latimer, W. H. R. Polarity and Ionization From the Standpoint of the Lewis Theory of Valence. *J. Am. Chem. Soc.* **42,** 1419–1433 (1920).

83. Hubbard, R. E. & Kamran Haider, M. Hydrogen bonds in proteins : role and strength. *Encycl. Life Sci.* **1,** 1–6 (2001).

84. Emsley, J. Very strong hydrogen bonding. *Chem. Soc. Rev.* **9,** 91 (1980).

85. Horowitz, S. & Trievel, R. C. Carbon-oxygen hydrogen bonding in biological structure and function. *J. Biol. Chem.* **287,** 41576–41582 (2012).

86. Li, N., Xiao, J., Hai, X., Wang, K. & Dang, F. Key Role of Ionic Hydrogen Bonding in Nonspecific Protein Adsorption on a Hydrophobic Surface. *J. Phys. Chem. C* **120,** 19135–19141 (2016).

87. van Oss, C. J. Hydrophobicity of biosurfaces- origin , quantitative determination and interaction energies. *Colloids Surfaces B Biointerfaces* **5,** 91–110 (1995).

88. Haidacher, D., Vailaya, A. & Horvath, C. Temperature effects in hydrophobic interaction chromatography. *Proc. Natl. Acad. Sci. U. S. A.* **93,** 2290–2295 (1996).

89. Queiroz, J. A., Tomaz, C. T. & Cabral, J. M. S. Hydrophobic interaction chromatography of proteins. *J. Biotechnol.* **87,** 143–159 (2001).

90. Vailaya, A. Fundamentals of Reversed Phase Chromatography: Thermodynamic and Exothermodynamic Treatment. *J. Liq. Chromatogr. Relat. Technol.* **28,** 965–1054 (2005).

91. Ramalho, J. P. P., Gomes, J. R. B. & Illas, F. Accounting for van der Waals interactions between adsorbates and surfaces in density functional theory based calculations: selected examples. *RSC Adv.* **3,** 13085 (2013).

92. Israelachvili, J. N. & Ninham, B. W. Intermolecular forces-the long and short of it. *J.*

Colloid Interface Sci. **58,** 14–25 (1977).

93. Shech, E. & Hatleback, E. The Material Intricacies of Coulomb's 1785 Electric Torsion Balance Experiment. 1–33 (2014).

94. Bohinc, K. & Kralj-iglic, V. Thickness of electrical double layer. Effect of ion size. *Electrochim. Acta* **46,** 3033–3040 (2001).

95. Strathmann, H. *Ion-Exchange Membrane Separation Processes*. (Elsevier B.V., 2004).

96. Marques, F. S., Silva, G. L., Thrash Jr, M. E. & Dias-cabral, A. C. Lysozyme adsorption onto a cation-exchanger : Mechanism of interaction study based on the analysis of retention chromatographic data. *Colloids Surfaces B Biointerfaces* **122,** 801–807 (2014).

97. Langmuir, I. The adsorption of gases on plane surfaces of glass, mica and platinum. *Am. Chem. Soc.* **40,** 1361–1403 (1918).

98. Latour, R. A. The Langmuir isotherm : A commonly applied but misleading approach for the analysis of protein adsorption behavior. *J. Biomed. Mater. Res. A* **00A,** 1–10 (2014).

99. Kopaciewicz, W., Rounds, M. A., Fausnaugh, J. & Regnier, F. E. Retention model for high-performance ion-exchange chromatography. *J. Chromatogr. A* **266,** 3–21 (1983).

100. Rounds, M. A. & Regnier, F. E. Evaluation of a retention model for high-performance ion-exchange chromatography using two different displacing salts. *J. Chromatogr. A* **283,** 37–45 (1984).

101. Cysewski, P. *et al.* Multivalent ion-exchange model of biopolymer chromatography for mass overload conditions. *J. Chromatogr. A* **548,** 61–79 (1991).

102. Drager, R. R. & Regnier, F. E. Application of the stoichiometric displacement model of retention to anion-exchange chromatography of nucleic acids. *J. Chromatogr. A* **359,** 147–155 (1986).

103. Valayudhan, A. Modeling of Non-Linear Elution Chromatography for Preparative-Scale Separations. *AIChE Symp. Ser.* **88,** 1–9 (1990).

104. Brooks, C. A. & Cramer, S. M. Steric Mass-Action Ion Exchange : Displacement Profiles and Induced Salt Gradients. **38,** 1969–1978 (1992).

105. Geng, X. & Zebolsky, D. M. The Stoichiometric Displacement Model and Langmuir and Freundlich Adsorption. *J. Chem. Educ.* **79,** 3–6 (2002).

106. Osberghaus, A. *et al.* Determination of parameters for the steric mass action model-A comparison between two approaches. *J. Chromatogr. A* **1233,** 54–65 (2012).

107. Jungbauer, A. & Kaltenbrunner, O. Fundamental Questions in Optimizing Ion-Exchange Chromatography of Proteins Using Computer-Aided Process Design. **52,** 223–236 (1996).

108. Yamamoto, S., Nakanishi, K., Matsuno, R. & Kamikubo, T. Ion Exchange Chromatography of Proteins-Prediction of Elution Curves and Operating Conditions . I.Theoretical

Considerations. *Biotechnol. Bioeng.* **XXV,** 1465–1483 (1983).

109. Martin, a. J. P. & Synge, R. L. M. A new form of chromatogram employing two liquid phases. *Biochem. J.* **35,** 1358–1368 (1941).

110. Kubin, M. Beitrag zur theorie der chromatographie. *Collect. Czechoslov. Chem. Commun.* **30,** 1104–1118 (1965).

111. Perkins, T., Mak, D., Root, T. & Lightfoot, E. Protein Retention in HIC Modeling variation with buffer ionic strength and column hydrophobicity. *J. Chromatogr. A* **766,** 1–14 (1996).

112. Reisler, E., Haik, Y. & Eisenberg, H. Bovine serum albumin and aqueous guanidine hydrochloride solutions. Preferential and absolute interactions and comparison with other systems. *Biochemistry* **16,** 197–203 (1977).

113. Timasheff, S. N. The control of protein stability and association by weak interactions with water: How Do Solvents Affect These Processes ? *Annu. Rev.Biophys.Biomol.Struct* **22,** 67–97 (1993).

114. Record, M. T. & Anderson, C. F. Interpretation of preferential interaction coefficients of nonelectrolytes and of electrolyte ions in terms of a two-domain model. *Biophys. J.* **68,** 786–794 (1995).

115. Gibbs, J. A Method of Geometrical Representation of the Thermodynamic Properties of Substances by Means of Surfaces. *Trans. Connect. Acad. Arts Sci.* **II,** 382–404 (1873).

116. Van't Hoff, J. H. *Etudes de dynamique chimique*. (Amsterdam, Frederik Muller, 1884).

117. Vailaya, A. & Horva, C. Retention Thermodynamics in Hydrophobic Interaction Chromatography. *Ind. Eng. Chem. Res.* **35,** 2964–2981 (1996).

118. Chen, W. *et al.* Studies of the interaction mechanism between single strand and double-strand DNA with hydroxyapatite by microcalorimetry and isotherm measurements. *Colloids Surfaces A Physicochem. Eng. Asp.* **295,** 274–283 (2007).

119. Huang, H., Lin, F., Chen, W. & Ruaan, R. Isothermal Titration Microcalorimetric Studies of the Effect of Temperature on Hydrophobic Interaction between Proteins and Hydrophobic Adsorbents. *J. Colloid Interface Sci.* **229,** 600–606 (2000).

120. Groszek, A. J. A calorimeter for Determination of Heats of Wetting. *Nature* **182,** 1152–1153 (1958).

121. Raje, P. & Pinto, N. G. Importance of heat of adsorption in modeling protein equilibria for overloaded chromatography. *J. Chromatogr. A* **796,** 141–156 (1998).

122. Kim, J., Desch, R. J., Thiel, S. W., Guliants, V. V & Pinto, N. G. Energetics of protein adsorption on amine-functionalized mesostructured cellular foam silica. *J. Chromatogr. A* **1218,** 7796–7803 (2011).

123. Kim, J., Desch, R. J., Thiel, S. W., Guliants, V. V & Pinto, N. G. Microporous and Mesoporous Materials Energetics of biomolecule adsorption on mesostructured cellular foam silica. *Microporous Mesoporous Mater.* **170,** 95–104 (2013).

124. Thrash Jr., M. E. & Pinto, N. G. Characterization of enthalpic events in overloaded ion-exchange chromatography. *J. Chromatogr. A* **944,** 61–68 (2002).

125. Thrash Jr., M. E. & Pinto, N. G. Incorporating water-release and lateral protein interactions in modeling equilibrium adsorption for ion-exchange chromatography. *J. Chromatogr. A* **1126,** 304–310 (2006).

126. Thrash Jr., M. E. & Pinto, N. G. Flow microcalorimetric measurements for bovine serum albumin on reversed-phase and anion-exchange supports under overloaded conditions. *J. Chromatogr. A* **908,** 293–299 (2001).

127. Desch, R. J., Kim, J. & Thiel, S. W. Microporous and Mesoporous Materials Interactions between biomolecules and an iron-silica surface. *Microporous Mesoporous Mater.* **187,** 29–39 (2014).

128. Peters, T. in *All About Albumin* 9–75 (Elsevier B.V., 1995).

129. Bankston, T. E., Stone, M. C. & Carta, G. Theory and applications of refractive index-based optical microscopy to measure protein mass transfer in spherical adsorbent particles. *J. Chromatogr. A* **1188,** 242–254 (2008).

130. Pousada, P. Master's Thesis: Understanding Ion Exchange adsorption mechanisms under overloaded conditions. (University of Beira Interior, 2014).

131. Nfor, B. K. *et al.* High-throughput isotherm determination and thermodynamic modeling of protein adsorption on mixed mode adsorbents. *J. Chromatogr. A* **1217,** 6829–6850 (2010).

132. Dékány, I. Comprehensive study on the structure of the BSA from extended-to aged form in wide (2–12) pH range. *Int. J. Biol. Macromol.* **88,** 51–58 (2016).

133. Atmeh, R., Arafe, I. & Al-Khateeb, M. Albumin Aggregates : Hydrodynamic Shape and Physico-Chemical Properties. *Jordan J. Chem.* **2,** 169–182 (2014).

134. Fullerton, G. D., Kanal, K. M. & Cameron, I. L. Osmotically unresponsive water fraction on proteins : Non-ideal osmotic pressure of bovine serum albumin as a function of pH and salt concentration. *Cell Biol. Int.* **30,** 86–92 (2006).

135. Babcock, J. J. & Brancaleon, L. Bovine serum albumin oligomers in the E- and B-forms at low protein concentration and ionic strength. *Int. J. Biol. Macromol.* **53,** 42–53 (2013).

136. Shi, Q., Zhou, Y. & Sun, Y. Influence of pH and Ionic Strength on the Steric Mass Action Model Parameters around the Isoelectric Point of Protein. *Biotechnol. Prog.* **21,** 516–523 (2005).

137. Ross, P. D. & Subramanian, S. Thermodynamics of Protein Association Reactions : Forces Contributing to Stability. *Biochemistry* **20,** 3096–3102 (1981).

138. David, J. & Willson, C. Microcalorimetric characterization of the anion-exchange adsorption of recombinant cytochrome b5 and its surface-charge mutants. *J. Chromatogr. A* **715,** 81–93 (1995).

139. Potter, A. J. & Paton, J. C. Spermidine biosynthesis and transport modulate pneumococcal autolysis. *J. Bacteriol.* **196,** 3556–3561 (2014).

140. Norde, W. Energy and Entropy of Protein Adsorption. *J. Dispers. Sci. Technol.* **13(4),** 363–377 (1992).

Appendix

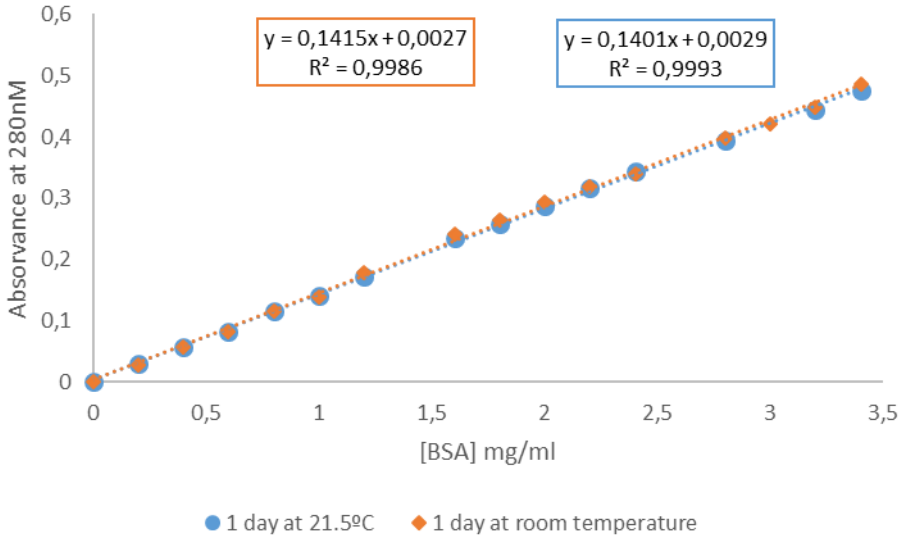

Figure 22- Tests performed to assess whether there are changes in BSA concentrations when left at room temperature and at 21.5˚C. The results demonstrate that there are no significant differences.

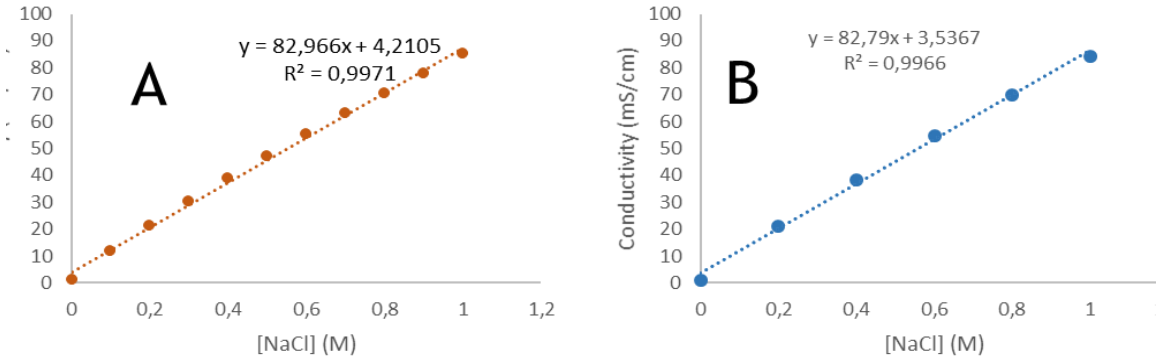

Figure 23- Calibration curve performed to calculate the NaCl concentration against a conductivity value, to subsequently, obtain the Ir values used in the Yamamoto model. (A) 20 mM Bis-tris pH 6.0; (B) 20 mM Tris-HCl pH8.0.

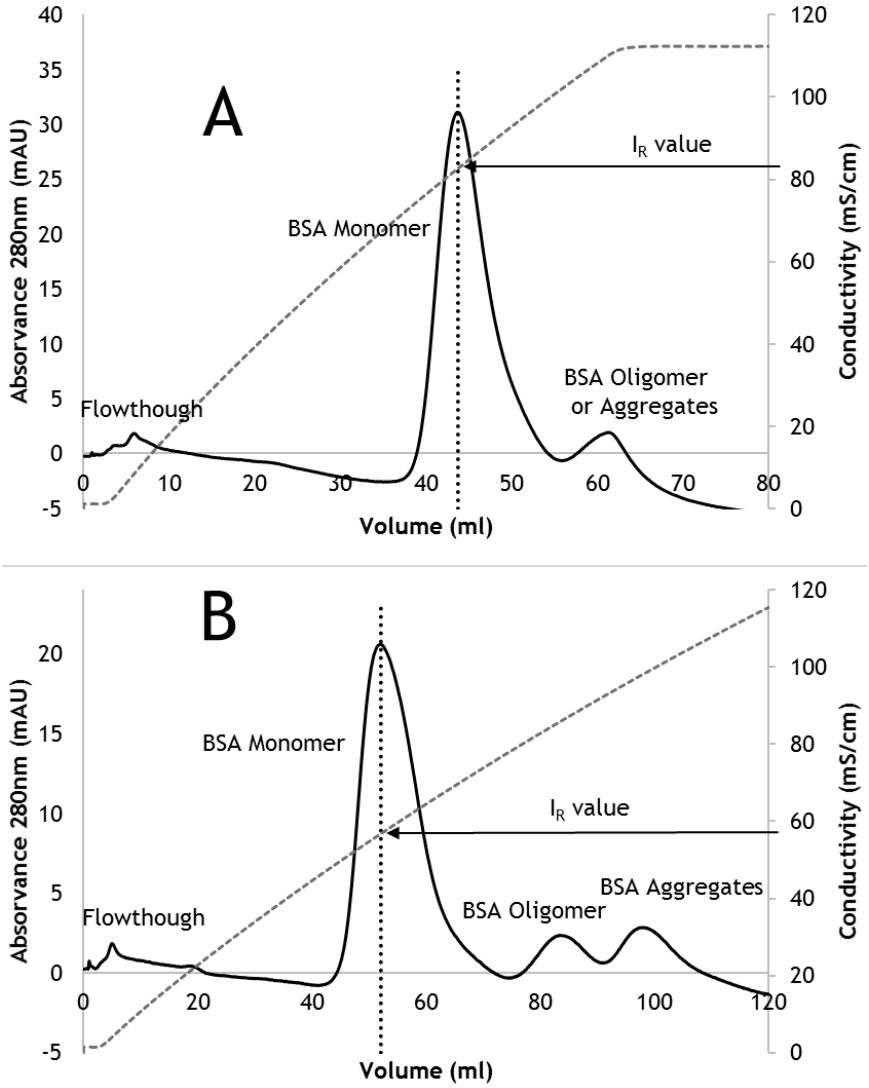

Figure 24 - Typical chromatograms obtained by injection of BSA 20 mg/ml onto Toyopearl NH2-750F with an injection loop of 20 µl and a flow rate of 1 ml.min^{-1}. (A) 20mM Tris-HCl pH 8.0 with a linear slope of 60 min; (B) 20 mM Bis-tris pH 6.0 with a linear slope of 120 min.

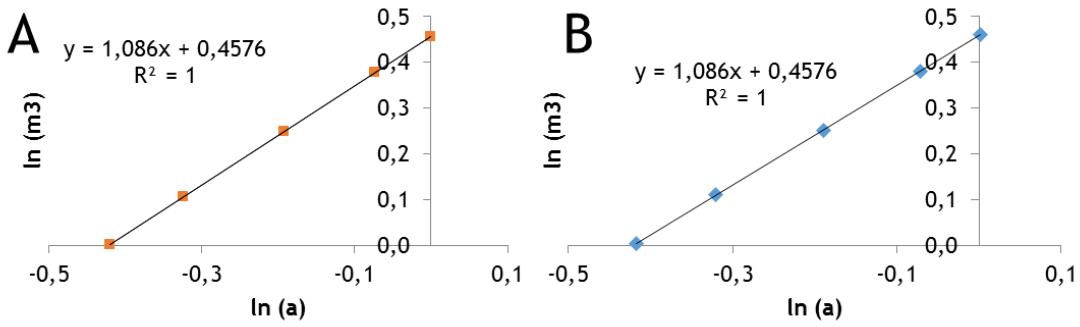

Figure 25- Natural logarithm of NaCl molality plotted against natural logarithm of the NaCl activity in order to obtain the slope that represents the g value used in preferential interaction analysis equation (43). (A) 20 mM Bis-tris pH 6.0; (B) 20 mM Tris-HCl pH 8.0.

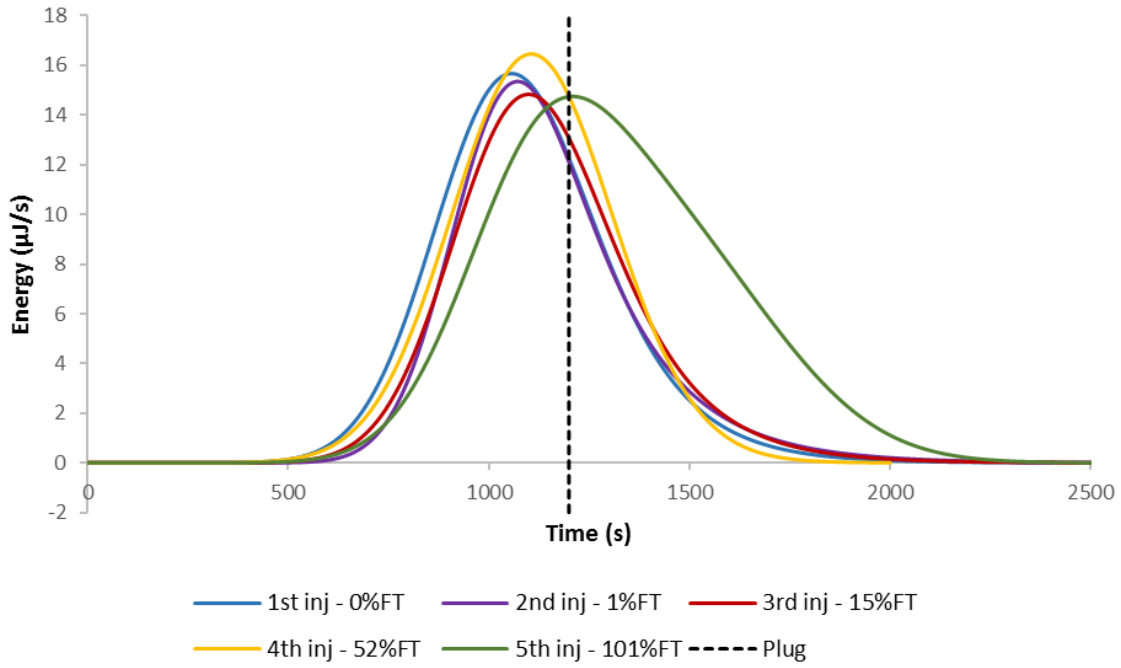

Figure 26- Thermograms obtained by sequential injections of 20 mg/ml BSA (20 mM Tris-HCl pH 8.0) onto Toyopearl NH2-750F with an injection loop of 100 µl. No elution step was performed between injections and the respective flowthrough are demonstrated on the image subtitle. These results allow to conclude that even when 100 % of the injected protein do not adsorb on the resin, there is a significant energy contribution of molecule-molecule interaction or ligand-molecule that has to be accounted when we proceed to the normalization of energy values.